Journal of South American Earth Sciences

Elemental composition and mineralogy of NW Venezuelan Guasare coals: Provenance study and role of illite in methane sorption capacity

--Manuscript Draft--

Manuscript Number:	SAMES-D-22-00416R2
Article Type:	Research Paper
Section/Category:	Economic geology, metallogenesis and hydrocarbon genesis and reservoirs
Keywords:	bituminous coal; Guasare Coalfield; elemental composition; Mineralogy; CBM; illite content
Corresponding Author:	Gonzalo Marquez, PhD University of Huelva: Universidad de Huelva Huelva, Huelva SPAIN
First Author:	Gonzalo Marquez, PhD
Order of Authors:	Gonzalo Marquez, PhD
	M. MARTÍNEZ, PhD
	G. CARRUYO, Dra
	C. BOENTE, PhD
	E. LORENZO, Dra
	R. TOCCO, MSc
Abstract:	A series of coal seams (groups 4 to 11) of Paleocene age in the Marcelina Formation have been open pit exploited in two mines (Paso Diablo and Mina Norte) in the Guasare Coalfield (NW Venezuela). An investigation has been conducted on the elemental composition, mineralogy, and coalbed methane (CBM) in Guasare coals. For this study, 46 core coal samples of 16 seams (groups 2 to 7) were collected from 16 exploratory boreholes that were drilled in both mines. It was also considered unpublished proximate-ultimate and gross calorific data of other 66 coals of 31 seams intersected in most of these wells. The coals under study showed low ash yields (3.4 wt. % on average) and were classified as high volatile bituminous A. Mean values of trace element and lanthanide (REE) contents in Marcelina coals generally indicate depletion compared to average values for world hard coals. The statistical evaluations indicate that elements (except Se) show inorganic affinity or intermediate association and mixed mode of occurrence. La/Sc, Th/Sc, La/Co, and Th/Cr ratios support a felsic or metamorphic felsic source for the mineral matter present in Marcelina coals. Most coal samples exhibited similar normalized REE patterns, showing light REE enriched, as well as negative Ce and Eu anomalies. The comparison of REE patterns to those of some nearby granitoids suggests that Marcelina coals received a supply of sediments from theses granitic source rocks. The mineralogical compositions of representative coal samples are notably similar, kaolinite and quartz were noted as the major mineral species in all coal seams. The measured gas volumes available for CBM production from Marcelina seams vary approximately between 5 and 11 cm3/g. Variation in the illite content has an appreciable positive effect on gas adsorption capacity of Guasare coals. Lastly, a numerical model of the gas generative potential of the coals in the Marcelina Formation was also developed.
Suggested Reviewers:	Katya Reategui, Dra. Associate Professor, Central University of Venezuela katya.reategui@ciens.ucv.ve Expertise in gas and petroleum geochemistry from the region of the study area.
	Javier Alejandre, Dr Full Professor, University of Seville falejan@us.es He is a very good specialist in mineralogy, particularly clays, in coals and other rocks
	Tatiana M. Juliao, Dra.

	Senior Researcher, Ecopetrol tatiana.juliao@ecopetrol.com.co She is an expert in coal geology and her Master´s thesis was about Guasare coals and their CBM resorces
	Cristina Rodrigues, Dra. Associate Professor, Fernando Pessoa University cfrodrig@gmail.com Expertise in coals and CBM
Opposed Reviewers:	
Response to Reviewers:	

Dear Dr. Frank Audemard:

I am submitting the last modified version of the manuscript entitled "**Elemental composition and mineralogy of NW Venezuelan Guasare coals: Provenance study and role of illite in methane sorption capacity**" for your considerations in order to be published in International Journal of South American Earth Sciences.

Attached you can find highlights, manuscript, figures, tables and appendices.

Yours sincerely,

Dr. Gonzalo Márquez

Dear Dr. F. Audemard:

All minor changes have been carried out in the last revised manuscript. Harvard (name-date) reference style was adequately followed.

Please, be aware of changes (**greenish colour**) in the text.

Enclosed you will find the text, figures and tables.

Yours sincerely, Dr. G. Marquez

Highlights

Element contents in Marcelina coals suggest depletion in relation to world hard coals

Guasare coals received a supply of sediments from nearby granitoids based on REE data

A numerical modeling of the gas generative potential of Guasare coals was developed

Measured methane sorption capacity of raw coal samples range between 5 and 12 cm^3/g

Variation in the illite content impacts on gas adsorption capacity of Guasare coals

Elemental composition and mineralogy of NW Venezuelan Guasare coals: Provenance study and role of illite in methane sorption capacity

G. MÁRQUEZ[a,*], M. MARTÍNEZ[b], G. CARRUYO[c], C. BOENTE[a], E. LORENZO[d] and R. TOCCO[e]

[a] Center for Research in Sustainable Chemistry (CIQSO), University of Huelva, 21006 Huelva, Spain
[b] Institute of Earth Sciences, Faculty of Sciences, Central University of Venezuela, Caracas 3895-1010A, Venezuela
[c] School of Chemical Engineering, Faculty of Engineering, University of Zulia, Maracaibo 4002-A, Venezuela
[d] School of Engineering Sciences, State University Santa Elena Peninsula, 240204 La Libertad, Ecuador
[d] Independent Petroleum Geochemistry Consultant, Madrid, 28410, Spain

Abstract: A series of coal seams (groups 4 to 11) of Paleocene age in the Marcelina Formation have been open pit exploited in two mines (Paso Diablo and Mina Norte) in the Guasare Coalfield (NW Venezuela). An investigation has been conducted on the elemental composition, mineralogy, and coalbed methane (CBM) in Guasare coals. For this study, 46 core coal samples of 16 seams (groups 2 to 7) were collected from 16 exploratory boreholes that were drilled in both mines. It was also considered unpublished proximate-ultimate and gross calorific data of other 66 coals of 31 seams intersected in most of these wells. The coals under study showed low ash yields (3.4 wt. % on average) and were classified as high volatile bituminous A. Mean values of trace element and lanthanide (REE) contents in Marcelina coals generally indicate depletion compared to average values for world hard coals. The statistical evaluations indicate that elements (except Se) show inorganic affinity or intermediate association and mixed mode of occurrence. La/Sc, Th/Sc, La/Co, and Th/Cr ratios support a felsic or metamorphic felsic source for the mineral matter present in Marcelina coals. Most coal samples exhibited similar normalized REE patterns, showing light REE enriched, as well as negative Ce and Eu anomalies. The comparison of REE patterns to those of some nearby granitoids suggests that Marcelina coals received a supply of sediments from theses granitic source rocks. The mineralogical compositions of representative coal samples are notably similar, kaolinite and quartz were noted as the major mineral species in all coal seams. The measured gas volumes available for CBM production from Marcelina seams vary approximately between 5 and 11 cm^3/g. Variation in the illite content has an appreciable positive effect on gas adsorption capacity of Guasare coals. Lastly, a numerical model of the gas generative potential of the coals in the Marcelina Formation was also developed.

Key-words: bituminous coal, Guasare Coalfield, elemental composition, mineralogy, CBM, illite content.

1. Introduction

Venezuela hosts potential resources of approximately ten billion metric tons of coal, 80 percent of them located in the Paleocene aged Guasare Coalfield (e.g., Carruyo, 2017). This basin stretches over a relatively small (55×5 km) geographical zone in the NW sector of Zulia State (Fig. 1a), 85 km northwest of the city of Maracaibo (Escobar et al., 1997). The Guasare Coalfield contains the majority (~1.6 billion tons) of the Venezuelan bituminous coal reserves and holds about 30 coal

seams in the Paleocene Marcelina Formation, with good lateral continuity and thicknesses ranging from 2 to 13 m (Quintero et al., 2011; Escobar et al., 2016). The Marcelina coal seams have been exploited in two mines (Paso Diablo and Mina Norte), operated by open-cast methods, since 1987 (Carruyo, 2017). The Paso Diablo mine and the nearby Mina Norte open-pit are located in the eastern flank of the Sierra de Perijá, between the Oca Fault northwards and the Totumo-Inciarte uplift southwards (Fig. 1b). According to Hackley and Martínez (2007), coal seams in both mines are classified into 11 groups (numbered from bottom to top; see Fig. 2) which, in turn, have been divided into seams so that the stratigraphically highest bed is assigned a Latin capital letter and each of the next lower seams are given letters farther down along the alphabet.

Figure 1

Figure 2

Previous geological studies have been conducted on the mineable and unmined Marcelina coal seams (e.g., Martínez et al., 1989; Juliao, 2010). The Guasare Coalfield has been studied in terms of coal-bed methane potential (Canónico, 2002; Tyler et al., 2006), petrography (Hackley and Martínez, 2007; Escobar et al., 2016), palynology (Pardo, 2004; Petersen et al., 2009), and organic geochemistry (Canónico et al., 2004; Quintero et al., 2011; Escobar et al., 2016). However, very few studies focused on the mineralogical and inorganic geochemical features of the coals in the basin (Morán, 1987; Hackley et al., 2005; Carruyo, 2017).

The minerals and concentrations of minor and trace elements are important for coal conversion and for evaluation of the paleo-depositional environment (Moore and Esmaeili, 2012; Dai et al., 2020a) by way of examples. Elements in coal appear to be in organic, inorganic and intimate organic associations (Dai et al, 2020b); while elemental concentrations are influenced by factors such as depositional environments of coal genesis, hydrothermal fluids, volcanic ash input, weathering or coalification processes (e.g., Dai et al., 2012). The element contents can also vary notably between

and even within coal seams (Yang et al., 2018). In this regard, mineralogy is useful in determining the modes of occurrence for trace elements. It is used in the correlation of coal seams, the identification of source areas, and the evaluation of environmental and health impacts during coal utilization (Ward, 2016). Statistical relationships between elements and ash yield are also frequently used to study their modes of occurrence (e.g., Qin et al., 2018; Dai et al., 2021).

Regarding the main source rocks at the time of peatification in the Guasare Coalfield, it was inferred that deltaic deposits of the Marcelina Formation were sourced from positive areas including the Guayana Shield (Parnaud et al., 1995). Also, Carruyo (2017) postulated that the source of minor, trace, and rare earth elements (REE) in Marcelina coals may have been partly sourced from granitoids such as the Late Triassic El Palmar Granite and El Carmen Granodiorite boulders (González de Juana et al., 1980), which outcrop at some places in the Perijá Range and the Andean region near the Colombia-Venezuela border and were likely exposed on the surface in the Paleocene (Van Der Lelij, 2013).

Moreover, the growing demand for energy has sparked global interest in the recovery of coalbed methane (CBM), a clean fossil fuel associated with broad coal deposits (Bustin and Clarkson, 1998). During the coalification processes, considerable amounts of hydrocarbons are generated and, partially, retained in the pore network (Petersen, 2006). Previous studies (Pan and Connell, 2012) have demonstrated that methane retention in the coal matrix can be explained by adsorption. Various factors such as coal petrography, coal rank, permeability, hydrodynamic setting, structure and burial history of the basin control CBM producibility (Scott, 2002; Chalmers et al., 2007; Solano-Acosta, 2007). Methane sorption capacity depends positively on total organic carbon (TOC) content, pore surface area, coal rank or fixed carbon, and inversely on maturity, mineral matter or moisture (Levy et al., 1997; Laxminarayana and Crosdale, 1999; Prinz and Littke, 2005). However,

positive trends exist between gas content (normalized to TOC) and illite content for dried coaly shale samples from SW Canada (Chalmers et al., 2008).

Numerous studies have been conducted on CBM potential of coal basins to improve our understanding of this unconventional energy resource (e.g., Mussa et al., 2021). With respect to the study area, Canónico (2002) and Tyler et al. (2006) estimated CBM resources to be 28-112 and 197-300 billion cubic meters, respectively, for this area on the basis of gas in-situ contents from United States coal (Eddy et al., 1982); since although profuse information is available on geology of coal seams in the Guasare Coalfield, data on gas content and gas distribution trends is very limited. Finally, most Guasare coal gas generation was attributed to thermogenic processes based on carbon isotope values (Berbesi et al., 2009; Quintero et al., 2011).

The main goals of this work are: (i) to characterize the mineralogical and elemental compositions of the mineral matter present in selected Marcelina coal seams (groups 2 to 11) intersected in cored boreholes; ii) to determine the distribution patterns of rare earth elements (REE) in the study coals for the first time; (iii) to investigate the provenance of trace and rare earth elements in coal samples from the Guasare Coalfield; (iv) to evaluate CBM potential of unmined and mineable coal seams at the Paso Diablo and Mina Norte open-pits, and (v) to investigate the role of the illite content with regard to reservoir gas capacity of Guasare coals. This information leads to assess in detail the distribution of the inorganic components in Marcelina coals at a mine-area and a basin-wide scale, and will prompt new exploration for CBM to evaluate its economic use in the study area.

2. Geological background

Geological features of the Sierra de Perijá have been described in literature (e.g., Kellogg, 1981; Audemard, 1991; Taboada et al., 2000; Duerto et al., 2006; Mann et al., 2006; Escalona and Mann,

2011). Uplift of the Sierra de Perijá started during the Oligocene and culminated in the Pliocene-Pleistocene (Kellogg, 1984). The Perijá Range is part of the Andean ridge, which is situated at the northwestern margin of Venezuela, specifically as a ramification towards the north of the Colombian Eastern Cordillera (Miller, 1962). Approximately at 9°N, a modification in trend from N20°W occurs, which is predominant in the northern Eastern Cordillera, to N25°E for the Perijá Range. The Sierra de Perijá remains at the northern edge of the Guajira Plains (latitude 11°10'N), constituting its crest the reference for the Colombia-Venezuela border (Fig. 1b). The main fractures related to the Sierra de Perijá's eastern flank include the Cuiba and Tigre left-lateral strike-slip faults (Bayona et al., 2011), which are oriented in the NE-SW direction and may have been formed along normal faults in the rifted Jurassic South America-African plate boundary (Lugo and Mann, 1995); as well as the El Palmar and Totumo faults with an orientation N-S, defining an abrupt uplift of the Sierra de Perijá, consecutive to that of the adjoining Lake Maracaibo Basin (Alvarado, 2007).

The Guasare Coal Basin and the Manuelote Syncline are structurally bound. This syncline can be defined as a NE-SW stretching tectonic horst, which is a known fold in the area under study and contains an axial plane that shares traits with the direction of the Tigre Fault (Pindell et al., 1998). The average value for total accumulated thickness of coal in the Marcelina Formation is 45-50 m, with scarce partings (González de Juana et al., 1980). This latter feature, along with low sulfur content and ash yield averaging 0.9 and 1.9 wt.% on a dry basis, respectively, are interpreted to be associated with the tectonic conditions ruling through the Paleocene in NW Venezuela; particularly by reason of low rates of subsidence (Hackley and Martínez, 2007). The stratigraphic succession in the Guasare Coalfield is composed of a series of sedimentary rocks of Phanerozoic age (see Fig. 3) overlying metamorphic basement (quartzites, amphibolites, and gneissoid schists being intruded by granite plutons) of the Precambrian Perijá Formation (Pérez et al., 2008). The lithology of the Marcelina Formation comprises sandy shales, black mudstones, grey sandstones, and coal horizons

(Sutton, 1946). At the bottom of the formation, the sandstones are thick, massive, light grey, and locally calcareous. The sandstones become finer upwards and appear to be interbedded with grey shales. Both sandstones and shales have lengthened nodules of blue-grey sandy limestone up to 3 m thick in the lower part of the formation (Escobar et al., 2011). The Marcelina Formation reflects a swamp paleo-depositional environment with similar peat accumulation and subsidence rates (McCabe, 1991), being formed by a deltaic sequence over the shelf edge of the Guasare Formation (González de Juana et al., 1980). In the area around the Paso Diablo mine, the Marcelina Formation conformably underlies the Misoa sands that represent a deltaic shoreface (Parnaud et al., 1995).

Figure 3

In the Paso Diablo mine, coal seams dip considerably (8-12º) to the east; nevertheless, the dip is greater (15º-25º) towards the south and the seams appear to be nearly vertical (Hackley and Martínez, 2007). The structural geology in the Guasare Coalfield is governed by the El Tigre fault and by multiple minor faults oriented in a N45ºW direction and spaced between 60 and 160 m (Alvarado, 2007). Towards the north, the coal seams gradually thin down to become lenses, while towards the south, the thickness of the seams increases. Coal seams are most common in the lower-central part of the Marcelina Formation (Fig. 2).

3. Samples and analytical procedures

Forty-six (46) coal core samples of 16 seams were collected from 16 drilled exploratory boreholes of the Marcelina Formation in the Paso Diablo mine and Mina Norte open-pit (Table 1 and Fig. 1c). About 3 kg of each whole seam sample were obtained from 2-4 individual samples. Then, the coal samples were homogenized using a Jones jaw crusher to obtain 100 g of each. We also provide previous unpublished proximate-ultimate data and gross calorific values (GCV) on additional 66 coals of 31 seams intersected in most wells under consideration (Carruyo, 2017; Tables 1 and 2). The location of the study seams in the stratigraphic column is shown in Figure 2.

Table 1

The coal samples were analyzed for moisture, ash yield, and volatile matter (VM) following the standards ISO 687:2010, ISO 1171:2010, and ISO 562:2010, respectively. The fixed carbon (FC) was calculated by subtracting the sum of these three parameters from the total (100 %). Ultimate analyses were also carried out using a LECO C-H-N 1000 apparatus in accordance with ISO 29541:2010 for C, H and N, and a LECO Truspec micro O analyser for direct O determination. Total sulfur was obtained by using a LECO SC32 apparatus according to ISO 19579:2006. TOC is calculated as the difference between the total carbon content and the inorganic carbon content. A LECO C-144 instrument was used to determine the total carbon content; while total inorganic carbon content was measured by using a CM5017 CO_2 coulometer. GCV values were determined through a Parr 6400 calorimeter following the norm ISO 1928:2009. Methane content of bulk crushed coal samples (50 mesh) was determined by a high-pressure volumetric sorption apparatus. Samples (100 mg) were air dried prior to methane sorption analysis. Each analysis was performed under isothermal conditions at 30°C and 6 MPa in order to compare samples. A value of 0.85 can be assumed to approximate the ratio of volumes of gas adsorbed on wet and dry coal (Kim, 1977). Reproducibility of the sorption analysis was within 3%.

The elemental compositions of raw (un-ashed) samples were obtained after the acid digestion of them following a two-step method devised to retain potentially volatile elements in solution (Querol et al., 1995). Al, Fe, P, Mg, Mn, Ca, Na, K, Ti, Zn, B, Sr, Ba, Cr, V, Ni and Pb were analyzed by inductively coupled plasma atomic emission spectrometry (ICP-AES); while Li, Be, U, Co, Cu, Ga, Ge, As, Rb, Zr, Nb, Mo, Sb, Cs, W, Th, Se, Y, Sc and naturally-occurring lanthanides were analyzed by inductively coupled plasma mass spectrometry (ICP-MS). The international reference material SARM 19 was used to calculate the accuracy of the methods. The element results were treated using SPSS 22.0 package for Windows.

Mineralogical analysis of a subset (16) of core samples of an equal number of seams was performed by semi-quantitative X-ray diffraction (XRD) using a Bruker-AXS D8 Advance diffractometer equipped with a copper anode, CuKα radiation, tube conditions of 40 kV and 30 mA, Δ2θ=4-60º, step size = 0.03º, and time step = 0.1 s. The diffractograms were obtained using the powder technique. The organic carbon was removed from each coal sample by low-temperature oxygen-plasma ashing (LTA) through an IPC-4 chamber following the USGS method (Kolker et al., 2003). Semiquantitative mineralogical compositions (normalized to 100% ash) of coal samples were determined according to the procedure reported by Chung (1974). The clay fraction analyses of the LTA residues from selected coal samples were conducted separately. Such fraction (< 2 μm effective diameter) of each LTA residue was isolated by ultrasonic dispersion in water treated with sodium hexametaphosphate, and further settling. Later, oriented-aggregate XRD technique was performed after treatment with ethylene glycol and heating to a maximum temperature of 550 ºC as routine treatments (Poppe et al., 2001), to investigate the composition of the clay fractions.

4. Results and discussion

4.1. Proximate and ultimate analyses

Table 2 displays values for ultimate and proximate analyses of the coal seams studied. The coals show low moisture contents (0.9-3.8 wt. % on a dry basis; averaging 2.0 wt. %) and are defined by low to medium ash yields between 0.7 and 9.9 wt. % on a dry basis (mean value of 3.0 wt. %). Fixed carbon and volatile matter range, respectively, from 49.0 to 61.6 wt. % on a dry basis (56.1 wt. % average) and from 36.6 to 48.1 wt. % on a dry ash-free basis (mean equals to 41.8 wt. %). In agreement with previous results (e.g., Carruyo, 2017), the measured gross calorific values for the coals (33.30-35.53 MJ/kg on a moist mineral-matter-free basis), along with proximate-ultimate data, denote that they have a rank of high volatile A bituminous following the ASTM D-388 classification. Also, the study coals exhibit low (< 1%) to moderate (1-3%; Chou, 2012) contents of

total sulfur (0.33-1.56 wt. % on a dry basis; averaging 0.74 wt. %), which would indicate the accumulation of precursor organic matter in mostly telmatic depositional settings (Banerjee and Goodarzi, 1990) and an acidic pH during the peatification process (Bechtel et al., 2003). No regular variations in the proximate analysis data are observed either vertically or laterally.

Table 2

Carbon, oxygen, hydrogen, and nitrogen contents (dry basis) for the coals are, respectively, in the 79.66-87.47 wt. %, 6.56-8.56 wt. %, 4.93-5.93 wt. %, and 1.44-1.99 wt. % ranges (Table 2). Carbon and nitrogen contents fall into the high volatile bituminous range reported, but hydrogen and oxygen data are slightly higher and lower than the mean values indicated by Given (1984). O/C atomic ratios below 0.1 and H/C values around 0.8 agree with a high volatile bituminous A rank (Kopp et al., 2000). The study coals, particularly those of the lower Marcelina coal seams (groups 2 and 3), show relatively high H/C values compared to the majority of humic coals. These latter also have the highest volatile matter values (Table 2), thereby indicating that they are perhydrous coals, as previously stated by Escobar et al. (2016). Finally, the high relative proportions of carbon versus nitrogen for all the samples under consideration (Table 2) are typical of humic-type coals (Meyers and Ishiwatari, 1993).

4.2. Geochemistry of minor and trace elements

4.2.1. Element contents

Tables 3, 4, and 5 show the contents of a series of minor (0.01-1.0 wt%), trace (< 100 μg/g; Finkelman, 1993), and rare earth elements on a whole coal basis, as well as average values for world hard coals (Ketris and Yudovich, 2009) and Swaine's worldwide ranges (Swaine, 1990).

Table 3

Table 4

Table 5

The geochemical features of Marcelina coal seams do not vary regularly with depth. Similarly, nor were there significant differences in the element geochemistry of the Paso Diablo coals and those from Mina Norte. However, this latter finding is tentative because it is not supported statistically by enough data. Elemental concentrations in all the coal samples are near or below the lowest values in the Swaine's worldwide concentration ranges in coal (see Tables 3, 4, and 5). These low elemental contents may be explained by little input of detrital materials to domed-ombrogenous deposits protected from sediment influx during peat accumulation in the Guasare Coal Basin (Hackley and Martínez, 2007). Given the similar average ash yields for the Mina Norte (MN) and Paso Diablo (PD) coals (3.6 and 2.9 wt. %, respectively), when comparing elemental concentrations in both subsets of coals (see Tables 3, 4 and 5), results tentatively indicate that MN coals have in general slightly higher average trace element contents than PD coals; while these latter have higher or similar mean concentrations of Fe, Ca, Mg, K, and Na, but not of Al, than those. These features seem to agree with the slightly high contents of kaolinite found in Mina Norte coals with respect to those from Paso Diablo, as previously reported in literature (Hackley et al., 2005).

The coal samples show concentrations of B from 14.1 to 42.7 µg/g, suggesting that the study coals were formed in paleomires developed in freshwater habitats (Dai et al., 2020a), which is consistent with the low total sulfur content and the inferred ombrogenous mire depositional environment of the parent organic matter. However, the concentration of B in coal may be also influenced by factors such as hydrothermal fluids, volcanic activity, and acid waters (Karayiğit et al., 2017). For that reason, the B content can be used as paleosalinity indicator but it must be interpreted with caution. Further, relatively low Ni/Co ratios (mean of ~4) and high Ca/Sr values over 4 (Appendix) suggest an oxic-dysoxic depositional environment with no marine influence in the original peat mires where Marcelina coals were formed (Krejci-Graf, 1984; Rimmer, 2004). The total REE content (also named as REY when Y is included; Dai et al., 2016b) of the 46 coal samples ranges from 1.113 to

16.364 µg/g (Appendix), with a mean value (4.578 µg/g) which is notably lower than the average REY in worldwide bituminous coal (68.6 µg/g; Yudovich and Ketris, 2006).

When comparing mean element concentrations in samples with average values for world hard coals (Ketris and Yudovich, 2009) by the use of concentration coefficients (CC = ratio of element concentration in sampled coals to average for world hard coals; Dai et al., 2016a), B, Ge, Se, and in some cases, Sb appear to be close to the averages for word hard coals ($0.5 < CC < 1$; Dai et al., 2015). The remaining elements analyzed and Cd (average for world hard coals equals 0.2 µg/g and values < 0.01 µg/g for samples; Hackley et al., 2005) are depleted ($CC < 0.5$) in the study coals. It has been also found that only F and Cl concentrations (89 and 380 µg/g) in Marcelina coals are higher than their respective average values (82 and 340 µg/g) for world hard coals (Morán, 1987).

4.2.2. Modes of occurrence of elements

Modes of occurrence of the elements in Marcelina coals were investigated using the Pearson correlation (*r*) between element contents and ash yield, although this statistical analysis should be used with caution (Dai et al., 2020b). Previous research works (e.g., Suárez-Ruiz et al., 2006) have established that elements whose concentration strongly follows the ash trend show a likely inorganic association, while organically-bound elements follow a completely opposite trend to the ash content. Only selenium seems to be mainly associated with the organic matter in sampled coals. The contents of a group of 22 minor, trace and rare earth elements (Table 6), show a weak correlation suggesting a mixed inorganic-organic association in the coal seams under consideration (Dai et al., 2021). The rest of the analyzed elements (Table 6) increases in samples parallel with ash content, which indicates a dominant affiliation with the mineral matter. No or weak correlation of several elements with ash yield may be explained by adsorption on coal surface, various modes of occurrence or anomalous low concentrations (Martínez et al., 2001). Further, positive correlations

of heavy (HREE, from Gd to Lu and Y) and light (LREE, from La to Eu) rare earth elements with Al, Ca, Fe, and P may reveal a terrigenous detrital origin for the REY species (Mishra et al., 2019). Lastly, the weak correlations ($-0.13 < r < +0.26$) between total sulfur and other elements analyzed, and no relationship between total sulfur and ash yield, reflect the mainly organic affiliation of sulfur in Marcelina coals (Hackley et al., 2005; Hackley and Martínez, 2007).

Table 6

Multivariate clustering based on elemental contents was carried out in order to identify the similarity of elements in the study coals and to group those into clusters. In coal geochemistry, this statistical tool has been usually applied in different fields such as the development of neural models to estimate moisture and ash content in coals and coaly shales (Ghosh et al., 2016) or the mode of occurrence of the trace elements in coals (Xu et al., 2021). However, it is necessary to ensure the compositional homogeneity in the dataset (Eskenezy et al., 2010). Cluster analysis was performed following the Ward's method (Everitt, 1993), and similarity percent was obtained after calculating square Euclidean distances (cut-off of 900; Fig. 4). Three groups of elements were determined. The first is wide and includes at least 12 elements within this association. Detailed analysis of these elements suggests three subgroups having a geochemical significance: Na–B and Mn–Ba–Sr, respectively, may be associated with groundwater movement and carbonate minerals (Beaton et al., 1991); while the third is made up of P, V, Zr, Li, Cu, Ni, and Cr, and these seem to be related to primary paleoproductivity and particular paleoredox conditions (Rimmer, 2004). The second group (Fe, Al, Cs, Ca, and Mg, among others) reveals a predominant clay mineral affiliation (Cullers, 1994) and, to a lesser extent, both carbonate and other possible associations. The last group includes some redox-sensitive trace elements (Mo, Rb, Nb, Co, U, Th, As, Be, and Sb; Cullers, 2002), along with another subgroup of elements (Zn, Pb, Ga, Ge, La, S, Sc, and REY) bound in sulfides, sand-forming minerals, and heavy detrital species (Ward, 2016).

Figure 4

4.2.3. Sediment source of elements

In an attempt to identify the source of trace elements in the coals under study, and considering the positive Pearson correlations between Al (Fralick and Kronberg, 1997) and trace elements such as Cr, Co, Th, Sc, La and REEs, which confirms the relative immobility of these lithophile elements (Yan et al., 2006), we can use here these latter elements to investigate the detrital input during peat accumulation in the Guasare Coalfield. In detail, the concentrations of La and Th (enriched in felsic sources) as well as Co and Sc (suggestive of mafic) may allow distinguishing between mafic and felsic provenance (e.g., Cullers, 2002). As shown in Table 7, when comparing La/Sc, Th/Sc, La/Co, and Th/Cr values of Marcelina coals with the ratios of sediments sourced from mafic and felsic rocks (Cullers et al., 1988; Cullers, 2000; Cullers and Podkovyrov, 2000), most samples lay within or closer to the felsic ranges, suggesting a probable granitic or metamorphic felsic nature of the source rocks. The La-Sc-Th ternary diagram can also give information about the provenance characteristics (Cullers, 2002). In this diagram, the average compositions of andesite and basalt (Condie, 1993), as well as some nearby granitoids (El Carmen Granodiorite and El Palmar Granite boulders; Van Der Lelij, 2013), are used for comparison purposes. The majority of samples plot near granitoid compositions (Fig. 5), which indicates that mineral fractions in Marcelina coals were derived presumably by the influence of felsic contribution.

Table 7

Figure 5

The REE distribution pattern in the sedimentary rocks is a very useful tool to unravel the provenance (Taylor and McLennan, 1985). In this regard, to identify a possible igneous source rock, the REE data of Marcelina coals are normalized relative to the chondrite values (Boynton, 1984) and compared with granitic rocks from areas located close to the mines under study. The subscript "*n*" indicates C1- or chondrite-normalized abundances. Typical REE patterns of the Paso Diablo and Mina Norte coal samples are shown in Figure 6. They are significantly similar to each

other and those of the El Palmar Granite and El Carmen Granodiorite boulders in the foothills of the Sierra of Perijá (Van Der Lelij, 2013). The chondrite-normalized patterns of samples from both mines are characterized by a quite flat HREE shape, LREE being nearly three times higher than HREE on average and $Eu_n/Eu^* < 1$ (see Fig. 6 and Appendix A), which agree with felsic sources (e.g., granites, gneisses, and pegmatites) with clear negative Eu anomaly (Armstrong-Altrin et al., 2004), rather than Eu mobility favored by reducing and low temperature conditions during peat accumulation (Eskenazy, 1987). By contrast, granodiorite often shows a positive Eu anomaly (Cullers, 1994). Slightly negative Ce anomalies also support a felsic provenance, although other alternatives to account for a negative Ce anomaly (Ce immobility, in-situ precipitation, and Ce^{+3} to Ce^{+4} oxidation) cannot be fully ruled out (Dai et al., 2016b). Finally, coal samples show Gd_n/Yb_n and Eu_n/Eu^* ratios below 2 and not exceeding 0.85, respectively (Appendix A), which is consistent with K-feldspar-rich granitic source rocks of Cambrian age or younger (McLennan, 1989; Taylor and McLennan, 1985).

Figure 6

4.3. Mineralogy

The mineralogy of the study coal seams is quite uniform (Table 8). Quartz and kaolinite are the predominant mineral species in the low temperature ash of the samples. Although these primary minerals are usually detrital in nature (Karayiğit et al., 2018), their occurrence in the coal samples could also result from authigenic precipitation in the raised peat mires protected from clastic inflow at the time of peatification (Ward, 2016). This would be consistent with a progradational deltaic environment for the Marcelina coals (Hackley and Martínez, 2007). A series of secondary minerals identified in the coal samples include illite, K-feldspar, sphalerite, pyrite, plagioclase, diaspore, hematite, and apatite, among others; which are also present in small proportions (see Table 8).

Table 8

Traces of bassanite were also detected in the LTA residues. Although Ca sulfates may represent either authigenic sediments or crystallization of ions from aqueous solution in the coal pore structure with evaporation, they were probably formed during the LTA process (Koukouzas et al., 2010). Butlerite and whewellite are rare minerals in coals and they are, respectively, a product of oxidation of pyrite (Kruszewski, 2013) and the result of an authigenic accumulation of Ca oxalate in coal seams (Echigo and Kimata, 2010). Carbonate minerals consist of small quantities of ankerite and siderite, which are the dominant iron-bearing species in coals when pyrite is absent or found in very low amounts (Ward et al., 2001), and they both would have been authigenically precipitated within mires in early diagenetic stages into the Paleocene (Ward et al. 1996), which is agreement with the freshwater conditions in which the study coals were formed (Hackley and Martínez, 2007). Oriented-aggregate XRD analysis indicated that kaolinite is the dominant component of the clay fraction of the study coals, and that illite and other clay minerals are usually present in minor and trace amounts, respectively. The predominance of kaolinite over the other minerals in the clay fraction, along with presence of whewellite and bassanite in the LTA materials, agree with a low detrital input to the paleomire and a significant portion of Ca associated to organic macerals (Koukouzas et al., 2010). Differences in illite contents in our samples can reveal subtle changes in provenance and depositional setting (Escobar et al., 2016).

4.4. Coalbed methane in the Marcelina seams

4.4.1. Numerical modeling of gas generated by Guasare coals

Generation of methane during coalification is modeled by calculating the amounts of volatiles in view of the atomic H/C and O/C ratios at the beginning of the high-volatile bituminous rank (0.85 and 0.13; Kopp et al., 2000) and averages of both ratios for Guasare coals (0.78 and 0.066). More exactly, complex organic “molecules” break down, releasing volatiles, and are gradually converted to hard coal and finally graphite, with decreasing atomic H/C and O/C ratios down to near zero

(Suggate, 2002). Only methane, carbon dioxide and water molecules were considered in order to simplify the modeling process. Other assumptions of the model are: methane is not significantly generated during early stages of coalification (Kopp et al., 2000) and the fact that the ratio of carbon dioxide to methane as gases released from organic matter is assumed to be 2 at maturity levels (~0.75%) of high-volatile bituminous A Guasare coals (Kopp et al., 2000; Escobar et al., 2016).

Once the numerical analysis described by Kopp and Bennett (2001) was carried out (Appendix B), we also assumed a mass loss of around 33% during the transition from lignite to high-volatile bituminous A coal (Tang et al., 1996). The model has predicted a methane generative potential of ~11 cm^3 per gram of raw coal and CBM reserves in the Guasare Coalfield near 17.6 billion m^3.

4.4.2. Methane sorption capacity of Guasare coals

Table 2 shows the values for gas volume per unit weight of each sampled coal seam (G_c). High pressure desorption data from dried coal samples indicated methane sorption capacity data ranging from 5.87 to 13.0 cm^3/g, approaching the economic threshold of 9.30 cm^3/g (Tang et al., 1996). These results were slightly lower than the dry, ash-free coalbed gas contents (G_{daf}) estimated theoretically by an indirect method from seam depth and proximate data (1.60-16.4 cm^3/g; Juliao, 2010), which reveals that Guasare coals could accommodate more gas than it would be present in them. Experimental data are also coherent with methane storage capacities (3.42-13.0 cm^3/g) of raw Guasare coals reported by Tyler et al. (2006), thereby suggesting that Marcelina seams can be considered to contain notable amounts of coal-bed methane.

The gas content values (G_c) for the Guasare Coalfield represents only the total volume of gas that is adsorbed by van der Waals forces to coal's interior surface area, but not to gas retention in other forms such as free gas present in the open pore spaces of coal and within natural cleats and

fractures, dissolved in formation water, and trapped gas within the matrix porosity (Clarkson and Bustin, 1996). Our results tend to underestimate the methane sorption capacity of Guasare coals due to gas loss after sampling and during crushing of samples. Hence, according to Strapóc et al. (2007), the measured gas content is equivalent to the residual gas fraction and to a part of the desorbed gas.

4.4.3. Clay content and CBM accumulation

Among the few studies have been carried out on the role of clays in methane sorption capacity of coal, Lu et al. (1995) indicated that illite is able to sorb methane at pressures from 1 to 7 MPa. Knowing that moisture in coal reduces the ability of the clay fraction to retain methane because moisture occupies sorption sites within the clays (Chalmers et al., 2008), total clay and illite contents are plotted versus the gas content on 16 dried samples (Fig. 7) in order to evaluate possible secondary influences of both variables on methane sorption capacity. Normalized data are presented on a per unit TOC volume basis assuming that the density of kerogen remains constant.

Figure 7

Negligible trend exists between gas content normalized to TOC and total clay content (Fig. 7a), in contrast to the positive relationship between methane sorption capacity normalized to TOC and illite content considering a sufficiently broad range (0.5-5%) of the latter variable (Fig. 7b), reflecting the notion that kaolinite and quartz have low sorption capacity compared to illite and the positive relationship of the latter clay with the surface area (Chalmers et al., 2008).

5. Conclusions

The high volatile bituminous A coals of the Guasare Coalfield contain low proportions of mineral matter and show no regular vertical and lateral variation in mineralogy and inorganic geochemistry. Kaolinite and quartz are the dominant mineral phases in selected Marcelina coal seams. In general, mean values of trace element concentrations in Marcelina coals generally indicate strong depletion

compared to the averages for world hard coals. Although this latter geochemical characteristic can make difficult a reliable statistical analysis to elucidate the modes of occurrence of elements, they all (except Se) show inorganic affinity or intermediate association and mixed mode of occurrence.

Regarding the provenance of trace and rare earth elements in Marcelina coals, Th/Sc, Th/Co, Th/Cr, La/Sc, LREE enrichment, and clear negative Eu anomalies reveal the predominant felsic character of the source rocks. Similarly, La-Th-Sc values and low Eu_n/Eu^* ratios are in agreement with Phanerozoic granitoids and their metamorphic equivalents as source rocks. Lastly, although a sediment contribution from methamorphic rocks of the Perijá Formation and other possibilities (as la Luna carbonate rocks and relatively nearby La Quinta mafic volcanoclastic materials; see Haze, 1984) cannot be completely dismissed, the comparison of REE patterns and Eu anomalies to the source rocks suggests that the mineral matter in Marcelina coals was, in part, a result of detrital input derived from granitoids such as the El Palmar Granite and El Carmen Granodiorite boulders or other similar granitic rocks. Data from raw Guasare coals indicates that methane contents range from 5 to 11 cm^3/g, values similar to that obtained from the numerical model (near 11 cm^3/g). Finally, the illite content showed a positive relationship with gas storage capacity when this latter is normalized to TOC on dried coal samples.

CRediT author statement

Gonzalo Márquez: Conceptualization, Writing - Original Draft, Investigation, Supervision; **Manuel Martínez**: Writing - Review & Editing, Formal analysis, Validation; **Gabriela Carruyo**: Visualization, Investigation; **Carlos Boente**: Writing - Review & Editing, Formal analysis; **Erika Lorenzo**: Investigation, Data curation; **Rafael Tocco**: Writing - Review & Editing, Resources.

Declaration of competing interest

The authors declare that they have no known competing financial interests or personal relationships that could have appeared to influence the work reported in this paper. There are no conflicts of interest to declare.

Acknowledgments

The authors are grateful to the company Carbozulia-PDVSA for facilitating access to the samples. We also thank Professor Marcos Escobar[†](LUZ) for scientific assistance. Finally, Dr. Shifeng Dai and the anonymous reviewer are thanked for their comments on the manuscript document.

References

Alvarado, D., 2007. Geological-structural interpretation of the northeast area of the Paso Diablo mine, Mara Municipality, Zulia State, on the basis of information from description of cores. BSc Thesis. Central University of Venezuela, Caracas, Venezuela, 145 p.

Armstrong-Altrin, J.S., Lee, Y.I., Verma, S.P., Ramasamy, S., 2004. Geochemistry of Sandstones from the Upper Miocene Kudankulam Formation, Southern India: Implications for provenance, weathering, and tectonic setting. J. Sediment. Res. 74, 285–297. https://doi.org/10.1306/082803740285

Audemard, F., 1991. Tectonics of Western Venezuela. PhD Thesis. Rice University, Houston, pp. 1-245.

Banerjee, I., Goodarzi, F., 1990. Paleoenvironment and sulfur-boron content of the Mannville (Lower Cretaceous) coals of southern Alberta, Canada. Sediment. Geol. 67, 297–310. https://doi.org/10.1016/0037-0738(90)90040-Z

Bayona, G., Montes, C., Cardona, A., Jaramillo, C., Ojeda, G., Valencia, V., Ayala-Calvo, C., 2011. Intraplate subsidence and basin filling adjacent to an oceanic arc-continent collision: a case from the southern Caribbean-South America plate margin. Basin Res. 23, 403–422. https://doi.org/10.1111/j.1365-2117.2010.00495.x

Beaton, A.P., Goodarzi, F., Potter, J., 1991. The petrography, mineralogy and geochemistry of a Paleocene lignite from southern Saskatchewan, Canada. Int. J. Coal Geol. 17, 117–148. https://doi.org/10.1016/0166-5162(91)90007-6

Bechtel, A., Gruber, W., Sachsenhofer, R.., Gratzer, R., Lücke, A., Püttmann, W., 2003. Depositional environment of the Late Miocene Hausruck lignite (Alpine Foreland Basin): insights from petrography, organic geochemistry, and stable carbon isotopes. Int. J. Coal Geol. 53, 153–180. https://doi.org/10.1016/S0166-5162(02)00194-5

Berbesi, L.A., Márquez, G., Martínez, M., Requena, A., 2009. Evaluating the gas content of coals and isolated maceral concentrates from the Paleocene Guasare Coalfield, Venezuela. Appl. Geochem. 24, 1817–1824. https://doi.org/10.1016/j.apgeochem.2009.06.003

Boynton, W.V., 1984. Geochemistry of the rare earth elements: meteorite studies, in: Henderson, P. (Ed.), Rare earth element geochemistry. Elsevier, Amsterdam, pp. 63-114. https://doi.org/10.1016/B978-0-444-42148-7.50008-3

Bustin, R., Clarkson, C., 1998. Geological controls on coalbed methane reservoir capacity and gas content. Int. J. Coal Geol. 38, 3–26. https://doi.org/10.1016/S0166-5162(98)00030-5

Canónico, U., 2002. Evaluation of the gas storage capacity in coals from western Venezuela. BSc Thesis. Central University of Venezuela, Caracas, pp. 1-88.

Canónico, U., Tocco, R., Ruggiero, A., Suárez, H., 2004. Organic geochemistry and petrology of coals and carbonaceous shales from western Venezuela. Int. J. Coal Geol. 57, 151–165. https://doi.org/10.1016/j.coal.2003.10.002

Carruyo, G., 2017. Geochemistry and use of coals from the Paleocene Marcelina Formation at Paso Diablo mine, Zulia, Venezuela. PhD Thesis. University of Zulia, Maracaibo, pp. 1-229.

Chalmers, G., Bustin, R., 2007. On the effects of petrographic composition on coalbed methane sorption. Int. J. Coal Geol. 69, 288-304. https://doi.org/10.1016/j.coal.2006.06.002

Chalmers, G., Bustin, R., 2008. Lower Cretaceous gas shales in northeastern British Columbia, Part I: geological controls on methane sorption capacity. B. Can. Petrol. Geol. 56, 1-21. https://doi.org/10.2113/gscpgbull.56.1.1

Chou, C.-L., 2012. Sulfur in coals: A review of geochemistry and origins. Int. J. Coal Geol. 100, 1-13. https://doi.org/10.1016/j.coal.2012.05.009

Chung, F.H., 1974. Quantitative interpretation of X-ray diffraction patterns of mixtures. I. Matrix-flushing method for quantitative multicomponent analysis. J. Appl. Chrystallogr. 7, 519-525. https://doi.org/10.1107/S0021889874010375

Clarkson, C.R., Bustin, R.M., 1996. Variation in micropore capacity and size distribution with composition in bituminous coal of the western Canadian sedimentary Basin. Fuel 75, 1483-1498. https://doi.org/10.1016/0016-2361(96)00142-1

Condie, K.C., 1993. Chemical composition and evolution of the upper continental crust: Contrasting results from surface samples and shales. Chem. Geol. 104, 1-37. https://doi.org/10.1016/0009-2541(93)90140-E

Cullers, R.L., 2002. Implications of elemental concentrations for provenance, redox conditions, and metamorphic studies of shales and limestones near Pueblo, CO, USA. Chem. Geol. 191, 305-327. https://doi.org/10.1016/S0009-2541(02)00133-X

Cullers, R.L., 2000. The geochemistry of shales, siltstones and sandstones of Pennsylvanian–Permian age, Colorado, USA: implications for provenance and metamorphic studies. Lithos 51, 181–203. https://doi.org/10.1016/S0024-4937(99)00063-8

Cullers, R.L., Podkovyrov, V.N., 2000. Geochemistry of the Mesoproterozoic Lakhanda shales in southeastern Yakutia, Russia: implications for mineralogical and provenance control, and recycling. Precambrian Res. 104, 77-93. https://doi.org/10.1016/S0301-9268(00)00090-5

Cullers, R.L., 1994. The controls on the major and trace element variation of shales, siltstones, and sandstones of Pennsylvanian-Permian age from uplifted continental blocks in Colorado to platform sediment in Kansas, USA. Geochim. Cosmochim. Ac. 58, 4955-4972. https://doi.org/10.1016/0016-7037(94)90224-0

Cullers, R.L., Basu, A., Suttner, L.J., 1988. Geochemical signature of provenance in sand-size material in soils and stream sediments near the Tobacco Root batholith, Montana, U.S.A. Chem. Geol. 70, 335-348. https://doi.org/10.1016/0009-2541(88)90123-4

Dai, S., Bechtel, A., Eble, C.F., Flores, R.M., French, D., Graham, I.T., Hood, M. M., Hower, J.C., Korasidis, V.A., Moore, T.A., Puttmann, W., Wei, Q., Zhao, L., O'Keefe, J.M.K., 2020a. Recognition of peat depositional environments in coal: A review. Int. J. Coal Geol. 219, 103383. https://doi.org/10.1016/j.coal.2019.103383

Dai, S., Finkelman, R.B., French, D., Hower, J.C., Graham, I.T., Zhao, F., 2021. Modes of occurrence of elements in coal: a critical evaluation. Earth-Science Reviews 222, 103815. https://doi.org/10.1016/j.earscirev.2021.103815

Dai, S., Graham, I.T., Ward, C.R., 2016a. A review of anomalous rare earth elements and yttrium in coal. Int. J. Coal Geol. 159, 82–95. https://doi.org/10.1016/j.coal.2016.04.005

Dai, S., Hower, J.C., Finkelman, R.B., Graham, I.T., French, D., Ward, C.R., Eskenazy, G., Wei, Q., Zhao, L., 2020b. Organic associations of non-mineral elements in coal: a review. Int. J. Coal Geol. 218, 103347. https://doi.org/10.1016/j.coal.2019.103347

Dai, S., Liu, J., Ward, C.R., Hower, J.C., French, D., Jia, S., Hood, M.M., Garrison, T.M., 2016b. Mineralogical and geochemical compositions of Late Permian coals and host rocks from the Guxu Coalfield, Sichuan Province, China, with emphasis on enrichment of rare metals. Int. J. Coal Geol. 166, 71–95. https://doi.org/10.1016/j.coal.2015.12.004

Dai, S., Ren, D., Chou, C.-L., Finkelman, R.B., Seredin, V. V., Zhou, Y., 2012. Geochemistry of trace elements in Chinese coals: A review of abundances, genetic types, impacts on human health, and industrial utilization. Int. J. Coal Geol. 94, 3–21. https://doi.org/10.1016/j.coal.2011.02.003

Dai, S., Seredin, V.V., Ward, C.R., Hower, J.C., Xing, Y., Zhang, W., Song, W., Wang, P., 2015. Enrichment of U–Se–Mo–Re–V in coals preserved within marine carbonate successions: geochemical and mineralogical data from the Late Permian Guiding Coalfield, Guizhou, China. Miner Deposita 50, 159–186. https://doi.org/10.1007/s00126-014-0528-1

Duerto, L., Escalona, A., Mann, P., 2006. Deep structure of the Mérida Andes and Sierra de Perijá mountain fronts, Maracaibo Basin, Venezuela. AAPG Bull. 90, 505–528. https://doi.org/10. 1306/10080505033

Echigo, T., Kimata, M., 2010. Crystal chemistry and genesis of organic minerals: A review of oxalate and polycyclic aromatic hydrocarbon minerals. Can. Mineral. 48, 1329-1358. https://doi.org/10.3749/canmin.48.5.1329

Eddy, G.E., Rightmire, C.T., Byrer, C., 1982. Relationship of methane content of coal, rank and depth. Proceedings of the Society of Petroleum Engineers/Department of Energy Unconventional Gas Recovery Symp., Pittsburgh, Pennsylvania, vol. 10800. Society of Petroleum Engineers/Department of Energy, pp. 117-122. https://doi.org/10.2118/10800-MS

Escalona, A., Mann, P., 2011. Tectonics, basin subsidence mechanisms, and paleogeography of the Caribbean-South American plate boundary zone. Mar. Petrol. Geol. 28, 8–39. https://doi.org/10. 1016/ j.marpetgeo.2010.01.016

Escobar, M., Márquez, G., Inciarte, S., Rojas, J., Esteves, I., Malandrino, G., 2011. The organic geochemistry of oil seeps from the Sierra de Perijá eastern foothills, Lake Maracaibo Basin, Venezuela. Org. Geochem. 42, 727-738. https://doi.org/10.1016/j.orggeochem.2011.06.005

Escobar, M., Márquez, G., Suárez-Ruiz, I., Juliao, T.M., Carruyo, G., Martínez, M., 2016. Source-rock potential of the lowest coal seams of the Marcelina Formation at the Paso Diablo mine in the Venezuelan Guasare Basin: Evidence for the correlation of Amana oils with these Paleocene coals. Int. J. Coal Geol. 163, 149-165. https://doi.org/10.1016/j.coal.2016.07.003

Eskenazy, G.M., 1987. Rare earth elements and yttrium in lithotypes of Bulgarian coals. Org. Geochem. 11, 83-89. https://doi.org/10.1016/0146-6380(87)90030-1

Eskenazy, G., Finkelman, R. B., Chattarjee, S., 2010. Some considerations concerning the use of correlation coefficients and cluster analysis in interpreting coal geochemistry data. Int. J. Coal Geol. 83, 491–493. https://doi.org/10.1016/j.coal.2010.05.006

Everitt, B.S., 1993. Cluster Analysis. In: E. Arnold ed. Multivariate statistics. Oxford University Press, London, pp. 42–50.

Finkelman, R.B., 1993. Trace and Minor Elements in Coal. In: M.H. Engel and S.A. Macko eds. Organic Geochemistry: Principles and Applications. Springer, Berlin, pp. 593–607.

Fralick, P.W., Kronberg, B.I., 1997. Geochemical discrimination of clastic sedimentary rock sources. Sediment. Geol. 113, 111–124. https://doi.org/10.1016/S0037-0738(97)00049-3

Ghosh, S., Chatterjee, R., Shanker, P. 2016. Estimation of ash, moisture content and detection of coal lithofacies from well logs using regression and artificial neural network modelling. Fuel 177, 279–287. https://doi.org/10.1016/j.fuel.2016.03.001

Given, P.H., 1984. An essay on the organic geochemistry of coal. In: Gorbaty, M.L., Larsen, J.W., Wender, I. (Eds.), Coal Science, Vol. III. Academic Press, New York, pp. 63-252.

González de Juana, C., Iturralde de Arozarena, J.M., Picard, X., 1980. Geology of Venezuela and the petroliferous Venezuelan basins, Vol. I. Ediciones Foninves, Caracas, 407 p.

Hackley, P.C., Martinez, M., 2007. Organic petrology of Paleocene Marcelina Formation coals, Paso Diablo mine, western Venezuela: Tectonic controls on coal type. Int. J. Coal Geol. 71, 505–526. https://doi.org/10.1016/j.coal.2006.05.002

Hackley, P.C., Warwick, P.D., González, E., 2005. Petrology, mineralogy and geochemistry of mined coals, western Venezuela. Int. J. Coal Geol. 63, 68–97. https://doi.org/10.1016/j.coal.2005.02.006

Haze, W.B., 1984. Jurassic La Quinta Formation in the Sierra de Perijá, northwestern Venezuela: Geology and tectonic environment of red beds and volcanic rocks, in: Bonini, W.E., Hargraves, R.B., Shagam, R. (Eds.), The Caribbean-South American plate boundary and regional tectonics, Geological Society of America 162, pp. 263-282. https://doi.org/10.1130/MEM162

ISO 19579, 2006. Solid mineral fuels – Determination of sulfur by IR spectrometry. International Organization for Standardization, Geneva.

ISO 1928, 2009. Solid mineral fuels – Determination of gross calorific value by the bomb calorimetric method and calculation of net calorific value. International Organization for Standardization, Geneva.

ISO 562, 2010. Hard coal and coke – Determination of volatile matter. International Organization for Standardization, Geneva.

ISO 687, 2010. Solid mineral fuels – Coke – Determination of moisture in the general analysis test sample. International Organization for Standardization, Geneva.

ISO 1171, 2010. Solid mineral fuels –Determination of ash. International Organization for Standardization, Geneva.

ISO 29541, 2010. Solid mineral fuels – Determination of total carbon, hydrogen and nitrogen content – Instrumental method. International Organization for Standardization, Geneva.

Juliao, T.M., 2010. Geochemistry and Exploration of Coalbed Methane in a South-West Section of Paso Diablo Mine, Guasare Basin, Zulia. MSc Thesis. University of Zulia, Maracaibo, pp. 1-118.

Karayiğit, A.İ., Mastalerz, M., Oskay, R.G., Gayer, R.A., 2018. Coal petrography, mineralogy, elemental compositions and palaeoenvironmental interpretation of Late Carboniferous coal seams in

three wells from the Kozlu coalfield (Zonguldak Basin, NW Turkey). Int. J. Coal Geol. 187, 54-70. https://doi.org/10.1016/j.coal.2017.12.007

Karayiğit, A.I., Bircan, C., Mastalerz, M., Oskay, R.G., Querol, X., Lieberman, N.R., Türkmen, I., 2017. Coal characteristics, elemental composition and modes of occurrence of some elements in the İsaalan coal (Balıkesir, NW Turkey). Int. J. Coal Geol. 172, 43-59. https://doi.org/10.1016/j.coal. 2017.01.016

Kellogg, J., 1981. The Cenozoic basement tectonics of Sierra de Perijá, Venezuela and Colombia: PhD Thesis. Princeton University, Princeton, USA, 241 p.

Kellogg, J., 1984. Cenozoic tectonic history of the Sierra de Perijá, Venezuela, Colombia, and adjacent basins, in: Bonini, W.E., Hargraves, R.B., Shagam, R. (Eds.), The Caribbean–South American plate boundary and regional tectonics: Geological Society of America 162, 239–261.

Ketris, M.P., Yudovich, Ya.E., 2009. Estimations of Clarkes for Carbonaceous biolithes: World average for trace element contents in black shales and coals. Int. J. Coal Geol. 78, 135-148. https://doi.org/10.1016/j.coal.2009.01.002

Kim, A.G., 1977. Estimating methane content of bituminous coal-beds from adsorption data. Report of investigations, United States Bureau of Mines RI 8245.

Kolker, A., Palmer, C.A., Ruppert, L.F., 2003. USGS Short Course C, Modes of Occurrence of Trace Elements in Coals (151 slides).

Kopp, O.C., Bennett III, M.E., 2001. A comparison of the loss of CO and CO_2 during coalification. Int. J. Coal Geol. 47, 63–66.

Kopp, O.C., Bennett III, M.E., Clark, C.E., 2000. Volatiles lost during coalification. Int. J. Coal Geol. 44, 69-84. https://doi.org/10.1016/S0166-5162(99)00069-5

Koukouzas, N., Kalaitzidis, S.P., Ward, C.R., 2010. Organic petrographical, mineralogical and geochemical features of the Achlada and Mavropigi lignite deposits, NW Macedonia, Greece. Int. J. Coal Geol. 83, 387-395. https://doi.org/10.1016/j.coal.2010.05.004

Krejci-Graf, K., 1984. Uber die Elemente in Kohlen. Erdoel Kohle, Erdgas, Petrochem. 37, 451-457.

Kretz, R., 1983. Symbols for rock-forming minerals. Am. Mineral. 68, 277-279.

Kruszewski, Ł., 2013. Supergene sulphate minerals from the burning coal mining dumps in the Upper Silesian Coal Basin, South Poland. Int. J. Coal Geol. 105, 91-109. https://doi.org/10.1016/j.coal.2012.12.007

Laxminarayana, C. and Crosdale, P.J. 1999. Role of coal type and rank on methane sorption characteristics of Bowen Basin, Australia coals. Int. J. Coal Geol. 40, 309–325. https://doi.org/10.1016/S0166-5162(99)00005-1

Levy, J.H., Day, S.J., Killingly, J.S. 1997. Methane capacities of Bowen Basin coals related to coal properties. Fuel 76, 813–819. https://doi.org/10.1016/S0016-2361(97)00078-1

Li, X., Dai, S., Zhang, W., Li, T., Zheng, X., Chen, W., 2014. Determination of As and Se in coal and coal combustion products using closed vessel microwave digestion and collision/reaction cell technology (CCT) of inductively coupled plasma mass spectrometry (ICP-MS). Int. J. Coal Geol. 124, 1-4. https://doi.org/10.1016/j.coal.2014.01.002

Lu, X.C., Li, F.C., Watson, A.T., 1995. Adsorption measurements in Devonian shales. Fuel 74, 599–603. https://doi.org/10.1016/0016-2361(95)98364-K

Lugo, J., Mann, P., 1995. Jurassic-Eocene tectonic evolution of Maracaibo Basin, Venezuela, in: Tankard, A.J., Suárez, S., Welsink, H.J. (Eds.), Petroleum basins of South America. AAPG Memoir 62, pp. 699-725.

Mann, P., Escalona, A., Castillo, M.V., 2006. Regional geologic and tectonic setting of the Maracaibo supergiant basin, western Venezuela. AAPG Bull. 90, 445–477. https://doi.org/10.1306/10110505031

Martínez, M., Escobar, M., Esteves, I., Lopez, C., Galarraga, F., González, R., 2001. Trace elements of Paleocene Táchira coals, southwestern Venezuela: a geochemical study. J. S. Am. Earth Sci. 14, 387– 399. https://doi.org/10.1016/S0895-9811(01)00035-9

Martínez, M., Escobar, M., Galárraga, F. 1989. Preliminary geochemical characterization of some Venezuelan coals. In: Memoirs of the VII Venezuelan Geological Congress, Part IV. The Venezuelan Society of Geologists, Barquisimeto, November 15-18, pp. 1877–1896

McCabe, P.J., 1991. Tectonic controls on coal accumulation. B. Soc. Geol. Fr. 162, 277–282.

McLennan, S.M., 1989. Rare earth elements in sedimentary rocks: influence of provenance and sedimentary processes, in: Lipin, B. and McKay, G., (Eds.), Geochemistry and Mineralogy of Rare Earth Elements, Mineralogical Society of America, Reviews in Minerology 21, pp. 169-200.

Meyers, P.A., Ishiwatari, R., 1993. Lacustrine organic geochemistry—an overview of indicators of organic matter sources and diagenesis in lake sediments. Org. Geochem. 20, 867–900. https://doi.org/10.1016/0146-6380(93)90100-P

Miller, J.B., 1962. Tectonic trends in Sierra de Perijá and adjacent parts of Venezuela and Colombia. AAPG Bull. 46, 1565–1595.

Mishra, V., Chakravarty, S., Finkelman, R.B., Varma, A.K., 2019. Geochemistry of Rare Earth Elements in Lower Gondwana Coals of the Talchir Coal Basin, India. J. Geochem. Explor. 204, 43-56. https://doi.org/10.1016/j.gexplo.2019.04.006

Moore, F., Esmaeili, A., 2012. Mineralogy and geochemistry of the coals from the Karmozd and Kiasar coal mines, Mazandaran province, Iran. Int. J. Coal Geol. 96/97, 9–21. https://doi.org/10.1016/j.coal.2012.02.012

Morán, R., 1987. Evaluation of metals in Venezuelan coals as a source of air pollution. MSc Thesis. University of Zulia, Maracaibo, Venezuela, 92 p.

Mussa, A., Kalkreuth, W., Pimentel Mizusaki, A.M., Müller Bicca, M., 2021. Geochemical characterization of selected organic-rich shales from the Devonian Pimenteiras Formation, Parnaíba Basin, Brazil – Implications for methane adsorption capacity. J. S. Am. Earth Sci. 112, 103507. https://doi.org/10.1016/j.jsames.2021.103507

Pan, Z., Connell, L.D., 2012. Modelling permeability for coal reservoirs: a review of analytical models and testing data. Int. J. Coal Geol. 92, 1–44. https://doi.org/10.1016/j.coal.2011.12.009

Pardo, A., 2004. Paleocene-Eocene Palynology and Palynofacies from Northeastern Colombia and Western Venezuela. PhD Thesis. Université de Liège, Liege, Belgium, 322 p.

Parnaud, F., Gou, Y., Pascual, J.C., Capello, M.A., Truskowski, I., Passalacqua, H., 1995. Stratigraphic synthesis of western Venezuela, in: Tankard, A.J., Suárez, S., Welsink, H.J. (Eds.), Petroleum basins of South America. AAPG Memoir 62, 667–679.

Pérez. K.J., Soriano, R.E., Valenzuela, A.E., 2008. Updating of the geology at a 1:100000 scale of a sector of the Sierra de Perijá through the use of satellite images landsat 7 etm (coordinates 72º00' to 73º00'W and 10º40' to 11º00'N). BSc Thesis, Central University of Venezuela, Caracas, 106 p.

Petersen H.I., 2006. The petroleum generation potential and effective oil window of humic coals related to coal composition and age. Int. J. Coal Geol. 67, 221–248. https://doi.org/10.1016/j.coal.2006.01.005

Petersen, H.I., Lindström, S., Nytoft, H.P., Rosenberg, P., 2009. Composition, peat-forming vegetation and kerogen paraffinicity of Cenozoic coals: Relationship to variations in the petroleum

generation potential (Hydrogen Index). Int. J. Coal Geol. 78, 119–134. https://doi.org/10.1016/j.coal.2008.11.003

Pindell, J.L., Higgs, R., Dewey, J.F., 1998. Cenozoic palinspastic reconstruction, paleogeographic evolution, and hydrocarbon setting of the northern margin of South America, in: Pindell, J.L., Drake, C.L. (Eds.), Paleogeographic Evolution and Non-Glacial Eustasy, northern South America. Society for Sedimentary Geology Special Publication 58, 45–86.

Poppe, L.J., Paskevich, V.F., Hathaway, J.C., Blackwood, D.S., 2001. A Laboratory Manual for X-Ray Powder Diffraction. U.S. Geological Survey Open-File Report 01-041, Denver, 1-88. https://doi.org/10.3133/ofr0141

Prinz, D., Littke, R. 2005. Development of the micro- and ultramicroporous structure of coals with rank as deduced from the accessibility to water. Fuel 84, 1645–1652. https://doi.org/10.1016/j.fuel.2005.01.010

Qin, S., Lu, Q., Li, Y., Wang, J., Zhao, Q., Gao, K., 2018. Relationships between trace elements and organic matter in coals. J. Geochem. Explor. 188, 101-110. https://doi.org/10.1016/j.gexplo.2018.01.015

Querol, X., Fernández-Turiel, J., López-Soler, A., 1995. Trace elements in coal and their behaviour during combustion in a large power station. Fuel 74, 331–343. https://doi.org/10.1016/0016-2361(95)93464-O

Quintero, K., Martínez, M., Hackley, P., Márquez, G., Garbán, G., Esteves, I., Escobar, M., 2011. Organic geochemical investigation and coal-bed methane characteristics of the Guasare coals (Paso Diablo mine, western Venezuela). Energ. Source., Part A: Recovery, Utilization, and Environmental Effects 33, 959–971. https://doi.org/10.1080/15567030903330728

Rimmer, S.M., 2004. Geochemical paleoredox indicators in Devonian–Mississippian black shales, Central Appalachian Basin (USA). Chem. Geol. 206, 373-391. https://doi.org/10.1016/j.chemgeo. 2003.12.029

Scott, A.R., 2002. Hydrogeologic factors affecting gas content distribution in coal beds. Int. J. Coal Geol. 50: 363-387. https://doi.org/10.1016/S0166-5162(02)00135-0

Solano-Acosta, W., 2007. Controls on coalbed methane potential and gas sorption characteristics of high-volatile bituminous coals in Indiana. PhD Thesis. Indiana University, Bloomington, 366 p.

Strapóc, D., Masterlerz, M., Eble, C., Schimmelmann, A., 2007. Characterization of the origin of coalbed gases in southeastern Illinois Basin by compound-specific carbon and hydrogen stable isotope ratios. Org. Geochem. 38: 267-287. https://doi.org/10.1016/j.orggeochem.2006.09.005

Suárez-Ruiz, I., Flores, D., Marques, M.M., Martinez-Tarazona, M.R., Pis, J., Rubiera, F., 2006. Geochemistry, mineralogy and technological properties of coals from Rio Maior (Portugal) and Peñarroya (Spain) basins. Int. J. Coal Geol. 67, 171-190. https://doi.org/10.1016/j.coal.2005.11.004

Suggate, R., 2002. Application of Rank (Sr), a maturity index based on chemical analyses of coals. Mar. Petrol. Geol. 19, 929–950. https://doi.org/10.1016/S0264-8172(02)00117-4

Sutton, F.A., 1946. Geology of Maracaibo Basin, Venezuela. AAPG Bull. 30, 1621–1741.

Swaine, D. J., 1990. Trace Elements in Coal. Butterworths, London, 294 p. https://doi.org/10.1016/C2013-0-00949-8

Taboada, A., Rivera, L.A., Fuenzalida, A., Cisternas, A., Philip, H., Bijwaard, H., Olaya, J., Rivera, C., 2000. Geodynamics of the northern Andes: Subductions and intracontinental deformation (Colombia). Tectonics 19, 787–813. https://doi.org/10.1029/2000TC900004

Tang, Y., Jenden, P., Nigrini, A., Teerman, S., 1996. Modeling early methane generation in coal. Energ. Fuel. 10, 659–671. https://doi.org/10.1021/ef950153l

Taylor, S.R., McLennan, S.M., 1985. The Continental Crust: Its Composition and Evolution. Blackwell Publishing, Oxford, 312 p.

Tyler, R., Tyler, N., Tocco, R., Savian, V., 2006. The potential for Coalbed Gas Resource Development, Western Maracaibo Basin, Venezuela. AAPG-Annual Convention, April 9-12 (paper # 100904). Houston.

Van Der Lelij, R., 2013. Reconstructing north-western Gondwana with implications for the evolution of the Iapetus and Rheic Oceans: A geochronological, thermochronological, and geochemical study. PhD Thesis, Université de Genève, 221 p.

Ward, C.R., 2016. Analysis, origin and significance of mineral matter in coal: An updated review. Int. J. Coal Geol. 165, 1-27. https://doi.org/10.1016/j.coal.2016.07.014

Ward, C.R., Bocking, M., Ruan, C.-D., 2001. Mineralogical analysis of coals as an aid to seam correlation in the Gloucester Basin, New South Wales, Australia. Int. J. Coal Geol. 47, 31-49. https://doi.org/10.1016/S0166-5162(01)00025-8

Ward, C.R., Corcoran, J.F., Saxby, J.D., Read, H.W., 1996. Occurrence of phosphorus minerals in Australian coal seams. Int. J. Coal Geol. 31, 185-210. https://doi.org/10.1016/0166-5162(95)00055-0

Xu, N., Finkelman, R. B., Dai, S., Xu, C., Peng, M., 2021. Average linkage hierarchical clustering algorithm for determining the relationships between elements in coal. ACS Omega 6, 6206–6217. https://doi.org//10.1021/acsomega.0c05758

Yan, Y., Xia, B., Lin, G., Cui, X., Hu, X., Yan, P., Zhang, F., 2007. Geochemistry of the sedimentary rocks from the Nanxiong Basin, South China and implications for provenance, paleoenvironment and paleoclimate at the K/T boundary. Sediment. Geol. 197, 127-140. https://doi.org/10.1016/j.sedgeo.2006.09.004

Yang, N., Tang, S., Zhang, S., Xi, Z., Li, J., Yuan, Y., Guo, Y., 2018. In seam variation of element-oxides and trace elements in coal from the eastern Ordos Basin, China. Int. J. Coal Geol. 197, 31-41. https://doi.org/10.1016/j.coal.2018.08.002

Yudovich, Y.E., Ketris, M.P., 2006. Valuable trace elements in coal. Ekaterinburg. Komi Scientific Center/Institute of Geology/Ural Division, RAS, pp. 1-538.

Figure 1: a) and b), respectively, maps showing the location of the Guasare Coalfield in NW Venezuela and the Paso Diablo and open-pit mines in this basin (modified from Escobar et al., 2016); c) situation of exploratory boreholes.

Figure 2: Stratigraphic units in the Sierra of Perijá (modified from Escobar et al., 2016).

Figure 3: Lithologic column of the Paso Diablo and Mina Norte open-cut mines showing coal seam names and stratigraphic position of coal samples (modified from Quintero et al., 2011).

Figure 4: Dendogram showing correlation of elements in the Marcelina coal seams.

Figure 5: La-Sc-Th triangular diagram for the coals under study. Data from local granitoids (El Palmar Granite and El Carmen Granodiorite; Van Der Lelij, 2013) are included.

Figure 6: Chondrite-normalized REE plots for the Guasare coals, El Palmar and El Carmen granitoids.

Figure 7: Plots of gas content normalized to per-unit TOC on a dried basis with the total clay (a) and illite (b) contents.

Elemental composition and mineralogy of NW Venezuelan Guasare coals: Provenance study and role of illite in methane sorption capacity

G. MÁRQUEZ[a,*], M. MARTÍNEZ[b], G. CARRUYO[c], C. BOENTE[a], E. LORENZO[d] and R. TOCCO[e]

[a] Center for Research in Sustainable Chemistry (CIQSO), University of Huelva, 21006 Huelva, Spain
[b] Institute of Earth Sciences, Faculty of Sciences, Central University of Venezuela, Caracas 3895-1010A, Venezuela
[c] School of Chemical Engineering, Faculty of Engineering, University of Zulia, Maracaibo 4002-A, Venezuela
[d] School of Engineering Sciences, State University Santa Elena Peninsula, 240204 La Libertad, Ecuador
[d] Independent Petroleum Geochemistry Consultant, Madrid, 28410, Spain

Abstract: A series of coal seams (groups 4 to 11) of Paleocene age in the Marcelina Formation have been open pit exploited in two mines (Paso Diablo and Mina Norte) in the Guasare Coalfield (NW Venezuela). An investigation has been conducted on the elemental composition, mineralogy, and coalbed methane (CBM) in Guasare coals. For this study, 46 core coal samples of 16 seams (groups 2 to 7) were collected from 16 exploratory boreholes that were drilled in both mines. It was also considered unpublished proximate-ultimate and gross calorific data of other 66 coals of 31 seams intersected in most of these wells. The coals under study showed low ash yields (3.4 wt. % on average) and were classified as high volatile bituminous A. Mean values of trace element and lanthanide (REE) contents in Marcelina coals generally indicate depletion compared to average values for world hard coals. The statistical evaluations indicate that elements (except Se) show inorganic affinity or intermediate association and mixed mode of occurrence. La/Sc, Th/Sc, La/Co, and Th/Cr ratios support a felsic or metamorphic felsic source for the mineral matter present in Marcelina coals. Most coal samples exhibited similar normalized REE patterns, showing light REE enriched, as well as negative Ce and Eu anomalies. The comparison of REE patterns to those of some nearby granitoids suggests that Marcelina coals received a supply of sediments from theses granitic source rocks. The mineralogical compositions of representative coal samples are notably similar, kaolinite and quartz were noted as the major mineral species in all coal seams. The measured gas volumes available for CBM production from Marcelina seams vary approximately between 5 and 11 cm^3/g. Variation in the illite content has an appreciable positive effect on gas adsorption capacity of Guasare coals. Lastly, a numerical model of the gas generative potential of the coals in the Marcelina Formation was also developed.

Key-words: bituminous coal, Guasare Coalfield, elemental composition, mineralogy, CBM, illite content.

1. Introduction

Venezuela hosts potential resources of approximately ten billion metric tons of coal, 80 percent of them located in the Paleocene aged Guasare Coalfield (e.g., Carruyo, 2017). This basin stretches over a relatively small (55×5 km) geographical zone in the NW sector of Zulia State (Fig. 1a), 85 km northwest of the city of Maracaibo (Escobar et al., 1997). The Guasare Coalfield contains the majority (~1.6 billion tons) of the Venezuelan bituminous coal reserves and holds about 30 coal

seams in the Paleocene Marcelina Formation, with good lateral continuity and thicknesses ranging from 2 to 13 m (Quintero et al., 2011; Escobar et al., 2016). The Marcelina coal seams have been exploited in two mines (Paso Diablo and Mina Norte), operated by open-cast methods, since 1987 (Carruyo, 2017). The Paso Diablo mine and the nearby Mina Norte open-pit are located in the eastern flank of the Sierra de Perijá, between the Oca Fault northwards and the Totumo-Inciarte uplift southwards (Fig. 1b). According to Hackley and Martínez (2007), coal seams in both mines are classified into 11 groups (numbered from bottom to top; see Fig. 2) which, in turn, have been divided into seams so that the stratigraphically highest bed is assigned a Latin capital letter and each of the next lower seams are given letters farther down along the alphabet.

Figure 1

Figure 2

Previous geological studies have been conducted on the mineable and unmined Marcelina coal seams (e.g., Martínez et al., 1989; Juliao, 2010). The Guasare Coalfield has been studied in terms of coal-bed methane potential (Canónico, 2002; Tyler et al., 2006), petrography (Hackley and Martínez, 2007; Escobar et al., 2016), palynology (Pardo, 2004; Petersen et al., 2009), and organic geochemistry (Canónico et al., 2004; Quintero et al., 2011; Escobar et al., 2016). However, very few studies focused on the mineralogical and inorganic geochemical features of the coals in the basin (Morán, 1987; Hackley et al., 2005; Carruyo, 2017).

The minerals and concentrations of minor and trace elements are important for coal conversion and for evaluation of the paleo-depositional environment (Moore and Esmaeili, 2012; Dai et al., 2020a) by way of examples. Elements in coal appear to be in organic, inorganic and intimate organic associations (Dai et al, 2020b); while elemental concentrations are influenced by factors such as depositional environments of coal genesis, hydrothermal fluids, volcanic ash input, weathering or coalification processes (e.g., Dai et al., 2012). The element contents can also vary notably between

and even within coal seams (Yang et al., 2018). In this regard, mineralogy is useful in determining the modes of occurrence for trace elements. It is used in the correlation of coal seams, the identification of source areas, and the evaluation of environmental and health impacts during coal utilization (Ward, 2016). Statistical relationships between elements and ash yield are also frequently used to study their modes of occurrence (e.g., Qin et al., 2018; Dai et al., 2021).

Regarding the main source rocks at the time of peatification in the Guasare Coalfield, it was inferred that deltaic deposits of the Marcelina Formation were sourced from positive areas including the Guayana Shield (Parnaud et al., 1995). Also, Carruyo (2017) postulated that the source of minor, trace, and rare earth elements (REE) in Marcelina coals may have been partly sourced from granitoids such as the Late Triassic El Palmar Granite and El Carmen Granodiorite boulders (González de Juana et al., 1980), which outcrop at some places in the Perijá Range and the Andean region near the Colombia-Venezuela border and were likely exposed on the surface in the Paleocene (Van Der Lelij, 2013).

Moreover, the growing demand for energy has sparked global interest in the recovery of coalbed methane (CBM), a clean fossil fuel associated with broad coal deposits (Bustin and Clarkson, 1998). During the coalification processes, considerable amounts of hydrocarbons are generated and, partially, retained in the pore network (Petersen, 2006). Previous studies (Pan and Connell, 2012) have demonstrated that methane retention in the coal matrix can be explained by adsorption. Various factors such as coal petrography, coal rank, permeability, hydrodynamic setting, structure and burial history of the basin control CBM producibility (Scott, 2002; Chalmers et al., 2007; Solano-Acosta, 2007). Methane sorption capacity depends positively on total organic carbon (TOC) content, pore surface area, coal rank or fixed carbon, and inversely on maturity, mineral matter or moisture (Levy et al., 1997; Laxminarayana and Crosdale, 1999; Prinz and Littke, 2005). However,

positive trends exist between gas content (normalized to TOC) and illite content for dried coaly shale samples from SW Canada (Chalmers et al., 2008).

Numerous studies have been conducted on CBM potential of coal basins to improve our understanding of this unconventional energy resource (e.g., Mussa et al., 2021). With respect to the study area, Canónico (2002) and Tyler et al. (2006) estimated CBM resources to be 28-112 and 197-300 billion cubic meters, respectively, for this area on the basis of gas in-situ contents from United States coal (Eddy et al., 1982); since although profuse information is available on geology of coal seams in the Guasare Coalfield, data on gas content and gas distribution trends is very limited. Finally, most Guasare coal gas generation was attributed to thermogenic processes based on carbon isotope values (Berbesi et al., 2009; Quintero et al., 2011).

The main goals of this work are: (i) to characterize the mineralogical and elemental compositions of the mineral matter present in selected Marcelina coal seams (groups 2 to 11) intersected in cored boreholes; ii) to determine the distribution patterns of rare earth elements (REE) in the study coals for the first time; (iii) to investigate the provenance of trace and rare earth elements in coal samples from the Guasare Coalfield; (iv) to evaluate CBM potential of unmined and mineable coal seams at the Paso Diablo and Mina Norte open-pits, and (v) to investigate the role of the illite content with regard to reservoir gas capacity of Guasare coals. This information leads to assess in detail the distribution of the inorganic components in Marcelina coals at a mine-area and a basin-wide scale, and will prompt new exploration for CBM to evaluate its economic use in the study area.

2. Geological background

Geological features of the Sierra de Perijá have been described in literature (e.g., Kellogg, 1981; Audemard, 1991; Taboada et al., 2000; Duerto et al., 2006; Mann et al., 2006; Escalona and Mann,

2011). Uplift of the Sierra de Perijá started during the Oligocene and culminated in the Pliocene-Pleistocene (Kellogg, 1984). The Perijá Range is part of the Andean ridge, which is situated at the northwestern margin of Venezuela, specifically as a ramification towards the north of the Colombian Eastern Cordillera (Miller, 1962). Approximately at 9°N, a modification in trend from N20°W occurs, which is predominant in the northern Eastern Cordillera, to N25°E for the Perijá Range. The Sierra de Perijá remains at the northern edge of the Guajira Plains (latitude 11°10'N), constituting its crest the reference for the Colombia-Venezuela border (Fig. 1b). The main fractures related to the Sierra de Perijá's eastern flank include the Cuiba and Tigre left-lateral strike-slip faults (Bayona et al., 2011), which are oriented in the NE-SW direction and may have been formed along normal faults in the rifted Jurassic South America-African plate boundary (Lugo and Mann, 1995); as well as the El Palmar and Totumo faults with an orientation N-S, defining an abrupt uplift of the Sierra de Perijá, consecutive to that of the adjoining Lake Maracaibo Basin (Alvarado, 2007).

The Guasare Coal Basin and the Manuelote Syncline are structurally bound. This syncline can be defined as a NE-SW stretching tectonic horst, which is a known fold in the area under study and contains an axial plane that shares traits with the direction of the Tigre Fault (Pindell et al., 1998). The average value for total accumulated thickness of coal in the Marcelina Formation is 45-50 m, with scarce partings (González de Juana et al., 1980). This latter feature, along with low sulfur content and ash yield averaging 0.9 and 1.9 wt.% on a dry basis, respectively, are interpreted to be associated with the tectonic conditions ruling through the Paleocene in NW Venezuela; particularly by reason of low rates of subsidence (Hackley and Martínez, 2007). The stratigraphic succession in the Guasare Coalfield is composed of a series of sedimentary rocks of Phanerozoic age (see Fig. 3) overlying metamorphic basement (quartzites, amphibolites, and gneissoid schists being intruded by granite plutons) of the Precambrian Perijá Formation (Pérez et al., 2008). The lithology of the Marcelina Formation comprises sandy shales, black mudstones, grey sandstones, and coal horizons

(Sutton, 1946). At the bottom of the formation, the sandstones are thick, massive, light grey, and locally calcareous. The sandstones become finer upwards and appear to be interbedded with grey shales. Both sandstones and shales have lengthened nodules of blue-grey sandy limestone up to 3 m thick in the lower part of the formation (Escobar et al., 2011). The Marcelina Formation reflects a swamp paleo-depositional environment with similar peat accumulation and subsidence rates (McCabe, 1991), being formed by a deltaic sequence over the shelf edge of the Guasare Formation (González de Juana et al., 1980). In the area around the Paso Diablo mine, the Marcelina Formation conformably underlies the Misoa sands that represent a deltaic shoreface (Parnaud et al., 1995).

Figure 3

In the Paso Diablo mine, coal seams dip considerably (8-12º) to the east; nevertheless, the dip is greater (15º-25º) towards the south and the seams appear to be nearly vertical (Hackley and Martínez, 2007). The structural geology in the Guasare Coalfield is governed by the El Tigre fault and by multiple minor faults oriented in a N45ºW direction and spaced between 60 and 160 m (Alvarado, 2007). Towards the north, the coal seams gradually thin down to become lenses, while towards the south, the thickness of the seams increases. Coal seams are most common in the lower-central part of the Marcelina Formation (Fig. 2).

3. Samples and analytical procedures

Forty-six (46) coal core samples of 16 seams were collected from 16 drilled exploratory boreholes of the Marcelina Formation in the Paso Diablo mine and Mina Norte open-pit (Table 1 and Fig. 1c). About 3 kg of each whole seam sample were obtained from 2-4 individual samples. Then, the coal samples were homogenized using a Jones jaw crusher to obtain 100 g of each. We also provide previous unpublished proximate-ultimate data and gross calorific values (GCV) on additional 66 coals of 31 seams intersected in most wells under consideration (Carruyo, 2017; Tables 1 and 2). The location of the study seams in the stratigraphic column is shown in Figure 2.

Table 1

The coal samples were analyzed for moisture, ash yield, and volatile matter (VM) following the standards ISO 687:2010, ISO 1171:2010, and ISO 562:2010, respectively. The fixed carbon (FC) was calculated by subtracting the sum of these three parameters from the total (100 %). Ultimate analyses were also carried out using a LECO C-H-N 1000 apparatus in accordance with ISO 29541:2010 for C, H and N, and a LECO Truspec micro O analyser for direct O determination. Total sulfur was obtained by using a LECO SC32 apparatus according to ISO 19579:2006. TOC is calculated as the difference between the total carbon content and the inorganic carbon content. A LECO C-144 instrument was used to determine the total carbon content; while total inorganic carbon content was measured by using a CM5017 CO_2 coulometer. GCV values were determined through a Parr 6400 calorimeter following the norm ISO 1928:2009. Methane content of bulk crushed coal samples (50 mesh) was determined by a high-pressure volumetric sorption apparatus. Samples (100 mg) were air dried prior to methane sorption analysis. Each analysis was performed under isothermal conditions at 30°C and 6 MPa in order to compare samples. A value of 0.85 can be assumed to approximate the ratio of volumes of gas adsorbed on wet and dry coal (Kim, 1977). Reproducibility of the sorption analysis was within 3%.

The elemental compositions of raw (un-ashed) samples were obtained after the acid digestion of them following a two-step method devised to retain potentially volatile elements in solution (Querol et al., 1995). Al, Fe, P, Mg, Mn, Ca, Na, K, Ti, Zn, B, Sr, Ba, Cr, V, Ni and Pb were analyzed by inductively coupled plasma atomic emission spectrometry (ICP-AES); while Li, Be, U, Co, Cu, Ga, Ge, As, Rb, Zr, Nb, Mo, Sb, Cs, W, Th, Se, Y, Sc and naturally-occurring lanthanides were analyzed by inductively coupled plasma mass spectrometry (ICP-MS). The international reference material SARM 19 was used to calculate the accuracy of the methods. The element results were treated using SPSS 22.0 package for Windows.

Mineralogical analysis of a subset (16) of core samples of an equal number of seams was performed by semi-quantitative X-ray diffraction (XRD) using a Bruker-AXS D8 Advance diffractometer equipped with a copper anode, CuKα radiation, tube conditions of 40 kV and 30 mA, Δ2θ=4-60º, step size = 0.03º, and time step = 0.1 s. The diffractograms were obtained using the powder technique. The organic carbon was removed from each coal sample by low-temperature oxygen-plasma ashing (LTA) through an IPC-4 chamber following the USGS method (Kolker et al., 2003). Semiquantitative mineralogical compositions (normalized to 100% ash) of coal samples were determined according to the procedure reported by Chung (1974). The clay fraction analyses of the LTA residues from selected coal samples were conducted separately. Such fraction (< 2 μm effective diameter) of each LTA residue was isolated by ultrasonic dispersion in water treated with sodium hexametaphosphate, and further settling. Later, oriented-aggregate XRD technique was performed after treatment with ethylene glycol and heating to a maximum temperature of 550 ºC as routine treatments (Poppe et al., 2001), to investigate the composition of the clay fractions.

4. Results and discussion

4.1. Proximate and ultimate analyses

Table 2 displays values for ultimate and proximate analyses of the coal seams studied. The coals show low moisture contents (0.9-3.8 wt. % on a dry basis; averaging 2.0 wt. %) and are defined by low to medium ash yields between 0.7 and 9.9 wt. % on a dry basis (mean value of 3.0 wt. %). Fixed carbon and volatile matter range, respectively, from 49.0 to 61.6 wt. % on a dry basis (56.1 wt. % average) and from 36.6 to 48.1 wt. % on a dry ash-free basis (mean equals to 41.8 wt. %). In agreement with previous results (e.g., Carruyo, 2017), the measured gross calorific values for the coals (33.30-35.53 MJ/kg on a moist mineral-matter-free basis), along with proximate-ultimate data, denote that they have a rank of high volatile A bituminous following the ASTM D-388 classification. Also, the study coals exhibit low (< 1%) to moderate (1-3%; Chou, 2012) contents of

total sulfur (0.33-1.56 wt. % on a dry basis; averaging 0.74 wt. %), which would indicate the accumulation of precursor organic matter in mostly telmatic depositional settings (Banerjee and Goodarzi, 1990) and an acidic pH during the peatification process (Bechtel et al., 2003). No regular variations in the proximate analysis data are observed either vertically or laterally.

Table 2

Carbon, oxygen, hydrogen, and nitrogen contents (dry basis) for the coals are, respectively, in the 79.66-87.47 wt. %, 6.56-8.56 wt. %, 4.93-5.93 wt. %, and 1.44-1.99 wt. % ranges (Table 2). Carbon and nitrogen contents fall into the high volatile bituminous range reported, but hydrogen and oxygen data are slightly higher and lower than the mean values indicated by Given (1984). O/C atomic ratios below 0.1 and H/C values around 0.8 agree with a high volatile bituminous A rank (Kopp et al., 2000). The study coals, particularly those of the lower Marcelina coal seams (groups 2 and 3), show relatively high H/C values compared to the majority of humic coals. These latter also have the highest volatile matter values (Table 2), thereby indicating that they are perhydrous coals, as previously stated by Escobar et al. (2016). Finally, the high relative proportions of carbon versus nitrogen for all the samples under consideration (Table 2) are typical of humic-type coals (Meyers and Ishiwatari, 1993).

4.2. Geochemistry of minor and trace elements

4.2.1. Element contents

Tables 3, 4, and 5 show the contents of a series of minor (0.01-1.0 wt%), trace (< 100 μg/g; Finkelman, 1993), and rare earth elements on a whole coal basis, as well as average values for world hard coals (Ketris and Yudovich, 2009) and Swaine's worldwide ranges (Swaine, 1990).

Table 3

Table 4

Table 5

The geochemical features of Marcelina coal seams do not vary regularly with depth. Similarly, nor were there significant differences in the element geochemistry of the Paso Diablo coals and those from Mina Norte. However, this latter finding is tentative because it is not supported statistically by enough data. Elemental concentrations in all the coal samples are near or below the lowest values in the Swaine's worldwide concentration ranges in coal (see Tables 3, 4, and 5). These low elemental contents may be explained by little input of detrital materials to domed-ombrogenous deposits protected from sediment influx during peat accumulation in the Guasare Coal Basin (Hackley and Martínez, 2007). Given the similar average ash yields for the Mina Norte (MN) and Paso Diablo (PD) coals (3.6 and 2.9 wt. %, respectively), when comparing elemental concentrations in both subsets of coals (see Tables 3, 4 and 5), results tentatively indicate that MN coals have in general slightly higher average trace element contents than PD coals; while these latter have higher or similar mean concentrations of Fe, Ca, Mg, K, and Na, but not of Al, than those. These features seem to agree with the slightly high contents of kaolinite found in Mina Norte coals with respect to those from Paso Diablo, as previously reported in literature (Hackley et al., 2005).

The coal samples show concentrations of B from 14.1 to 42.7 µg/g, suggesting that the study coals were formed in paleomires developed in freshwater habitats (Dai et al., 2020a), which is consistent with the low total sulfur content and the inferred ombrogenous mire depositional environment of the parent organic matter. However, the concentration of B in coal may be also influenced by factors such as hydrothermal fluids, volcanic activity, and acid waters (Karayiğit et al., 2017). For that reason, the B content can be used as paleosalinity indicator but it must be interpreted with caution. Further, relatively low Ni/Co ratios (mean of ~4) and high Ca/Sr values over 4 (Appendix) suggest an oxic-dysoxic depositional environment with no marine influence in the original peat mires where Marcelina coals were formed (Krejci-Graf, 1984; Rimmer, 2004). The total REE content (also named as REY when Y is included; Dai et al., 2016b) of the 46 coal samples ranges from 1.113 to

16.364 µg/g (Appendix), with a mean value (4.578 µg/g) which is notably lower than the average REY in worldwide bituminous coal (68.6 µg/g; Yudovich and Ketris, 2006).

When comparing mean element concentrations in samples with average values for world hard coals (Ketris and Yudovich, 2009) by the use of concentration coefficients (CC = ratio of element concentration in sampled coals to average for world hard coals; Dai et al., 2016a), B, Ge, Se, and in some cases, Sb appear to be close to the averages for word hard coals (0.5 < CC < 1; Dai et al., 2015). The remaining elements analyzed and Cd (average for world hard coals equals 0.2 µg/g and values < 0.01 µg/g for samples; Hackley et al., 2005) are depleted (CC < 0.5) in the study coals. It has been also found that only F and Cl concentrations (89 and 380 µg/g) in Marcelina coals are higher than their respective average values (82 and 340 µg/g) for world hard coals (Morán, 1987).

4.2.2. Modes of occurrence of elements

Modes of occurrence of the elements in Marcelina coals were investigated using the Pearson correlation (*r*) between element contents and ash yield, although this statistical analysis should be used with caution (Dai et al., 2020b). Previous research works (e.g., Suárez-Ruiz et al., 2006) have established that elements whose concentration strongly follows the ash trend show a likely inorganic association, while organically-bound elements follow a completely opposite trend to the ash content. Only selenium seems to be mainly associated with the organic matter in sampled coals. The contents of a group of 22 minor, trace and rare earth elements (Table 6), show a weak correlation suggesting a mixed inorganic-organic association in the coal seams under consideration (Dai et al., 2021). The rest of the analyzed elements (Table 6) increases in samples parallel with ash content, which indicates a dominant affiliation with the mineral matter. No or weak correlation of several elements with ash yield may be explained by adsorption on coal surface, various modes of occurrence or anomalous low concentrations (Martínez et al., 2001). Further, positive correlations

of heavy (HREE, from Gd to Lu and Y) and light (LREE, from La to Eu) rare earth elements with Al, Ca, Fe, and P may reveal a terrigenous detrital origin for the REY species (Mishra et al., 2019). Lastly, the weak correlations ($-0.13 < r < +0.26$) between total sulfur and other elements analyzed, and no relationship between total sulfur and ash yield, reflect the mainly organic affiliation of sulfur in Marcelina coals (Hackley et al., 2005; Hackley and Martínez, 2007).

Table 6

Multivariate clustering based on elemental contents was carried out in order to identify the similarity of elements in the study coals and to group those into clusters. In coal geochemistry, this statistical tool has been usually applied in different fields such as the development of neural models to estimate moisture and ash content in coals and coaly shales (Ghosh et al., 2016) or the mode of occurrence of the trace elements in coals (Xu et al., 2021). However, it is necessary to ensure the compositional homogeneity in the dataset (Eskenezy et al., 2010). Cluster analysis was performed following the Ward's method (Everitt, 1993), and similarity percent was obtained after calculating square Euclidean distances (cut-off of 900; Fig. 4). Three groups of elements were determined. The first is wide and includes at least 12 elements within this association. Detailed analysis of these elements suggests three subgroups having a geochemical significance: Na–B and Mn–Ba–Sr, respectively, may be associated with groundwater movement and carbonate minerals (Beaton et al., 1991); while the third is made up of P, V, Zr, Li, Cu, Ni, and Cr, and these seem to be related to primary paleoproductivity and particular paleoredox conditions (Rimmer, 2004). The second group (Fe, Al, Cs, Ca, and Mg, among others) reveals a predominant clay mineral affiliation (Cullers, 1994) and, to a lesser extent, both carbonate and other possible associations. The last group includes some redox-sensitive trace elements (Mo, Rb, Nb, Co, U, Th, As, Be, and Sb; Cullers, 2002), along with another subgroup of elements (Zn, Pb, Ga, Ge, La, S, Sc, and REY) bound in sulfides, sand-forming minerals, and heavy detrital species (Ward, 2016).

Figure 4

4.2.3. Sediment source of elements

In an attempt to identify the source of trace elements in the coals under study, and considering the positive Pearson correlations between Al (Fralick and Kronberg, 1997) and trace elements such as Cr, Co, Th, Sc, La and REEs, which confirms the relative immobility of these lithophile elements (Yan et al., 2006), we can use here these latter elements to investigate the detrital input during peat accumulation in the Guasare Coalfield. In detail, the concentrations of La and Th (enriched in felsic sources) as well as Co and Sc (suggestive of mafic) may allow distinguishing between mafic and felsic provenance (e.g., Cullers, 2002). As shown in Table 7, when comparing La/Sc, Th/Sc, La/Co, and Th/Cr values of Marcelina coals with the ratios of sediments sourced from mafic and felsic rocks (Cullers et al., 1988; Cullers, 2000; Cullers and Podkovyrov, 2000), most samples lay within or closer to the felsic ranges, suggesting a probable granitic or metamorphic felsic nature of the source rocks. The La-Sc-Th ternary diagram can also give information about the provenance characteristics (Cullers, 2002). In this diagram, the average compositions of andesite and basalt (Condie, 1993), as well as some nearby granitoids (El Carmen Granodiorite and El Palmar Granite boulders; Van Der Lelij, 2013), are used for comparison purposes. The majority of samples plot near granitoid compositions (Fig. 5), which indicates that mineral fractions in Marcelina coals were derived presumably by the influence of felsic contribution.

Table 7

Figure 5

The REE distribution pattern in the sedimentary rocks is a very useful tool to unravel the provenance (Taylor and McLennan, 1985). In this regard, to identify a possible igneous source rock, the REE data of Marcelina coals are normalized relative to the chondrite values (Boynton, 1984) and compared with granitic rocks from areas located close to the mines under study. The subscript "*n*" indicates C1- or chondrite-normalized abundances. Typical REE patterns of the Paso Diablo and Mina Norte coal samples are shown in Figure 6. They are significantly similar to each

other and those of the El Palmar Granite and El Carmen Granodiorite boulders in the foothills of the Sierra of Perijá (Van Der Lelij, 2013). The chondrite-normalized patterns of samples from both mines are characterized by a quite flat HREE shape, LREE being nearly three times higher than HREE on average and $Eu_n/Eu^* < 1$ (see Fig. 6 and Appendix A), which agree with felsic sources (e.g., granites, gneisses, and pegmatites) with clear negative Eu anomaly (Armstrong-Altrin et al., 2004), rather than Eu mobility favored by reducing and low temperature conditions during peat accumulation (Eskenazy, 1987). By contrast, granodiorite often shows a positive Eu anomaly (Cullers, 1994). Slightly negative Ce anomalies also support a felsic provenance, although other alternatives to account for a negative Ce anomaly (Ce immobility, in-situ precipitation, and Ce^{+3} to Ce^{+4} oxidation) cannot be fully ruled out (Dai et al., 2016b). Finally, coal samples show Gd_n/Yb_n and Eu_n/Eu^* ratios below 2 and not exceeding 0.85, respectively (Appendix A), which is consistent with K-feldspar-rich granitic source rocks of Cambrian age or younger (McLennan, 1989; Taylor and McLennan, 1985).

Figure 6

4.3. Mineralogy

The mineralogy of the study coal seams is quite uniform (Table 8). Quartz and kaolinite are the predominant mineral species in the low temperature ash of the samples. Although these primary minerals are usually detrital in nature (Karayiğit et al., 2018), their occurrence in the coal samples could also result from authigenic precipitation in the raised peat mires protected from clastic inflow at the time of peatification (Ward, 2016). This would be consistent with a progradational deltaic environment for the Marcelina coals (Hackley and Martínez, 2007). A series of secondary minerals identified in the coal samples include illite, K-feldspar, sphalerite, pyrite, plagioclase, diaspore, hematite, and apatite, among others; which are also present in small proportions (see Table 8).

Table 8

Traces of bassanite were also detected in the LTA residues. Although Ca sulfates may represent either authigenic sediments or crystallization of ions from aqueous solution in the coal pore structure with evaporation, they were probably formed during the LTA process (Koukouzas et al., 2010). Butlerite and whewellite are rare minerals in coals and they are, respectively, a product of oxidation of pyrite (Kruszewski, 2013) and the result of an authigenic accumulation of Ca oxalate in coal seams (Echigo and Kimata, 2010). Carbonate minerals consist of small quantities of ankerite and siderite, which are the dominant iron-bearing species in coals when pyrite is absent or found in very low amounts (Ward et al., 2001), and they both would have been authigenically precipitated within mires in early diagenetic stages into the Paleocene (Ward et al. 1996), which is agreement with the freshwater conditions in which the study coals were formed (Hackley and Martínez, 2007). Oriented-aggregate XRD analysis indicated that kaolinite is the dominant component of the clay fraction of the study coals, and that illite and other clay minerals are usually present in minor and trace amounts, respectively. The predominance of kaolinite over the other minerals in the clay fraction, along with presence of whewellite and bassanite in the LTA materials, agree with a low detrital input to the paleomire and a significant portion of Ca associated to organic macerals (Koukouzas et al., 2010). Differences in illite contents in our samples can reveal subtle changes in provenance and depositional setting (Escobar et al., 2016).

4.4. Coalbed methane in the Marcelina seams

4.4.1. Numerical modeling of gas generated by Guasare coals

Generation of methane during coalification is modeled by calculating the amounts of volatiles in view of the atomic H/C and O/C ratios at the beginning of the high-volatile bituminous rank (0.85 and 0.13; Kopp et al., 2000) and averages of both ratios for Guasare coals (0.78 and 0.066). More exactly, complex organic “molecules” break down, releasing volatiles, and are gradually converted to hard coal and finally graphite, with decreasing atomic H/C and O/C ratios down to near zero

(Suggate, 2002). Only methane, carbon dioxide and water molecules were considered in order to simplify the modeling process. Other assumptions of the model are: methane is not significantly generated during early stages of coalification (Kopp et al., 2000) and the fact that the ratio of carbon dioxide to methane as gases released from organic matter is assumed to be 2 at maturity levels (~0.75%) of high-volatile bituminous A Guasare coals (Kopp et al., 2000; Escobar et al., 2016).

Once the numerical analysis described by Kopp and Bennett (2001) was carried out (Appendix B), we also assumed a mass loss of around 33% during the transition from lignite to high-volatile bituminous A coal (Tang et al., 1996). The model has predicted a methane generative potential of ~11 cm^3 per gram of raw coal and CBM reserves in the Guasare Coalfield near 17.6 billion m^3.

4.4.2. Methane sorption capacity of Guasare coals

Table 2 shows the values for gas volume per unit weight of each sampled coal seam (G_c). High pressure desorption data from dried coal samples indicated methane sorption capacity data ranging from 5.87 to 13.0 cm^3/g, approaching the economic threshold of 9.30 cm^3/g (Tang et al., 1996). These results were slightly lower than the dry, ash-free coalbed gas contents (G_{daf}) estimated theoretically by an indirect method from seam depth and proximate data (1.60-16.4 cm^3/g; Juliao, 2010), which reveals that Guasare coals could accommodate more gas than it would be present in them. Experimental data are also coherent with methane storage capacities (3.42-13.0 cm^3/g) of raw Guasare coals reported by Tyler et al. (2006), thereby suggesting that Marcelina seams can be considered to contain notable amounts of coal-bed methane.

The gas content values (G_c) for the Guasare Coalfield represents only the total volume of gas that is adsorbed by van der Waals forces to coal's interior surface area, but not to gas retention in other forms such as free gas present in the open pore spaces of coal and within natural cleats and

fractures, dissolved in formation water, and trapped gas within the matrix porosity (Clarkson and Bustin, 1996). Our results tend to underestimate the methane sorption capacity of Guasare coals due to gas loss after sampling and during crushing of samples. Hence, according to Strapóc et al. (2007), the measured gas content is equivalent to the residual gas fraction and to a part of the desorbed gas.

4.4.3. Clay content and CBM accumulation

Among the few studies have been carried out on the role of clays in methane sorption capacity of coal, Lu et al. (1995) indicated that illite is able to sorb methane at pressures from 1 to 7 MPa. Knowing that moisture in coal reduces the ability of the clay fraction to retain methane because moisture occupies sorption sites within the clays (Chalmers et al., 2008), total clay and illite contents are plotted versus the gas content on 16 dried samples (Fig. 7) in order to evaluate possible secondary influences of both variables on methane sorption capacity. Normalized data are presented on a per unit TOC volume basis assuming that the density of kerogen remains constant.

Figure 7

Negligible trend exists between gas content normalized to TOC and total clay content (Fig. 7a), in contrast to the positive relationship between methane sorption capacity normalized to TOC and illite content considering a sufficiently broad range (0.5-5%) of the latter variable (Fig. 7b), reflecting the notion that kaolinite and quartz have low sorption capacity compared to illite and the positive relationship of the latter clay with the surface area (Chalmers et al., 2008).

5. Conclusions

The high volatile bituminous A coals of the Guasare Coalfield contain low proportions of mineral matter and show no regular vertical and lateral variation in mineralogy and inorganic geochemistry. Kaolinite and quartz are the dominant mineral phases in selected Marcelina coal seams. In general, mean values of trace element concentrations in Marcelina coals generally indicate strong depletion

compared to the averages for world hard coals. Although this latter geochemical characteristic can make difficult a reliable statistical analysis to elucidate the modes of occurrence of elements, they all (except Se) show inorganic affinity or intermediate association and mixed mode of occurrence.

Regarding the provenance of trace and rare earth elements in Marcelina coals, Th/Sc, Th/Co, Th/Cr, La/Sc, LREE enrichment, and clear negative Eu anomalies reveal the predominant felsic character of the source rocks. Similarly, La-Th-Sc values and low Eu_n/Eu^* ratios are in agreement with Phanerozoic granitoids and their metamorphic equivalents as source rocks. Lastly, although a sediment contribution from methamorphic rocks of the Perijá Formation and other possibilities (as la Luna carbonate rocks and relatively nearby La Quinta mafic volcanoclastic materials; see Haze, 1984) cannot be completely dismissed, the comparison of REE patterns and Eu anomalies to the source rocks suggests that the mineral matter in Marcelina coals was, in part, a result of detrital input derived from granitoids such as the El Palmar Granite and El Carmen Granodiorite boulders or other similar granitic rocks. Data from raw Guasare coals indicates that methane contents range from 5 to 11 cm^3/g, values similar to that obtained from the numerical model (near 11 cm^3/g). Finally, the illite content showed a positive relationship with gas storage capacity when this latter is normalized to TOC on dried coal samples.

CRediT author statement

Gonzalo Márquez: Conceptualization, Writing - Original Draft, Investigation, Supervision; **Manuel Martínez**: Writing - Review & Editing, Formal analysis, Validation; **Gabriela Carruyo**: Visualization, Investigation; **Carlos Boente**: Writing - Review & Editing, Formal analysis; **Erika Lorenzo**: Investigation, Data curation; **Rafael Tocco**: Writing - Review & Editing, Resources.

Declaration of competing interest

The authors declare that they have no known competing financial interests or personal relationships that could have appeared to influence the work reported in this paper. There are no conflicts of interest to declare.

Acknowledgments

The authors are grateful to the company Carbozulia-PDVSA for facilitating access to the samples. We also thank Professor Marcos Escobar[†](LUZ) for scientific assistance. Finally, Dr. Shifeng Dai and the anonymous reviewer are thanked for their comments on the manuscript document.

References

Alvarado, D., 2007. Geological-structural interpretation of the northeast area of the Paso Diablo mine, Mara Municipality, Zulia State, on the basis of information from description of cores. BSc Thesis. Central University of Venezuela, Caracas, Venezuela, 145 p.

Armstrong-Altrin, J.S., Lee, Y.I., Verma, S.P., Ramasamy, S., 2004. Geochemistry of Sandstones from the Upper Miocene Kudankulam Formation, Southern India: Implications for provenance, weathering, and tectonic setting. J. Sediment. Res. 74, 285–297. https://doi.org/10.1306/082803740285

Audemard, F., 1991. Tectonics of Western Venezuela. PhD Thesis. Rice University, Houston, pp. 1-245.

Banerjee, I., Goodarzi, F., 1990. Paleoenvironment and sulfur-boron content of the Mannville (Lower Cretaceous) coals of southern Alberta, Canada. Sediment. Geol. 67, 297–310. https://doi.org/10.1016/0037-0738(90)90040-Z

Bayona, G., Montes, C., Cardona, A., Jaramillo, C., Ojeda, G., Valencia, V., Ayala-Calvo, C., 2011. Intraplate subsidence and basin filling adjacent to an oceanic arc-continent collision: a case from the southern Caribbean-South America plate margin. Basin Res. 23, 403–422. https://doi.org/10.1111/j.1365-2117.2010.00495.x

Beaton, A.P., Goodarzi, F., Potter, J., 1991. The petrography, mineralogy and geochemistry of a Paleocene lignite from southern Saskatchewan, Canada. Int. J. Coal Geol. 17, 117–148. https://doi.org/10.1016/0166-5162(91)90007-6

Bechtel, A., Gruber, W., Sachsenhofer, R.., Gratzer, R., Lücke, A., Püttmann, W., 2003. Depositional environment of the Late Miocene Hausruck lignite (Alpine Foreland Basin): insights from petrography, organic geochemistry, and stable carbon isotopes. Int. J. Coal Geol. 53, 153–180. https://doi.org/10.1016/S0166-5162(02)00194-5

Berbesi, L.A., Márquez, G., Martínez, M., Requena, A., 2009. Evaluating the gas content of coals and isolated maceral concentrates from the Paleocene Guasare Coalfield, Venezuela. Appl. Geochem. 24, 1817–1824. https://doi.org/10.1016/j.apgeochem.2009.06.003

Boynton, W.V., 1984. Geochemistry of the rare earth elements: meteorite studies, in: Henderson, P. (Ed.), Rare earth element geochemistry. Elsevier, Amsterdam, pp. 63-114. https://doi.org/10.1016/B978-0-444-42148-7.50008-3

Bustin, R., Clarkson, C., 1998. Geological controls on coalbed methane reservoir capacity and gas content. Int. J. Coal Geol. 38, 3–26. https://doi.org/10.1016/S0166-5162(98)00030-5

Canónico, U., 2002. Evaluation of the gas storage capacity in coals from western Venezuela. BSc Thesis. Central University of Venezuela, Caracas, pp. 1-88.

Canónico, U., Tocco, R., Ruggiero, A., Suárez, H., 2004. Organic geochemistry and petrology of coals and carbonaceous shales from western Venezuela. Int. J. Coal Geol. 57, 151–165. https://doi.org/10.1016/j.coal.2003.10.002

Carruyo, G., 2017. Geochemistry and use of coals from the Paleocene Marcelina Formation at Paso Diablo mine, Zulia, Venezuela. PhD Thesis. University of Zulia, Maracaibo, pp. 1-229.

Chalmers, G., Bustin, R., 2007. On the effects of petrographic composition on coalbed methane sorption. Int. J. Coal Geol. 69, 288-304. https://doi.org/10.1016/j.coal.2006.06.002

Chalmers, G., Bustin, R., 2008. Lower Cretaceous gas shales in northeastern British Columbia, Part I: geological controls on methane sorption capacity. B. Can. Petrol. Geol. 56, 1-21. https://doi.org/10.2113/gscpgbull.56.1.1

Chou, C.-L., 2012. Sulfur in coals: A review of geochemistry and origins. Int. J. Coal Geol. 100, 1-13. https://doi.org/10.1016/j.coal.2012.05.009

Chung, F.H., 1974. Quantitative interpretation of X-ray diffraction patterns of mixtures. I. Matrix-flushing method for quantitative multicomponent analysis. J. Appl. Chrystallogr. 7, 519-525. https://doi.org/10.1107/S0021889874010375

Clarkson, C.R., Bustin, R.M., 1996. Variation in micropore capacity and size distribution with composition in bituminous coal of the western Canadian sedimentary Basin. Fuel 75, 1483-1498. https://doi.org/10.1016/0016-2361(96)00142-1

Condie, K.C., 1993. Chemical composition and evolution of the upper continental crust: Contrasting results from surface samples and shales. Chem. Geol. 104, 1-37. https://doi.org/10.1016/0009-2541(93)90140-E

Cullers, R.L., 2002. Implications of elemental concentrations for provenance, redox conditions, and metamorphic studies of shales and limestones near Pueblo, CO, USA. Chem. Geol. 191, 305-327. https://doi.org/10.1016/S0009-2541(02)00133-X

Cullers, R.L., 2000. The geochemistry of shales, siltstones and sandstones of Pennsylvanian–Permian age, Colorado, USA: implications for provenance and metamorphic studies. Lithos 51, 181–203. https://doi.org/10.1016/S0024-4937(99)00063-8

Cullers, R.L., Podkovyrov, V.N., 2000. Geochemistry of the Mesoproterozoic Lakhanda shales in southeastern Yakutia, Russia: implications for mineralogical and provenance control, and recycling. Precambrian Res. 104, 77-93. https://doi.org/10.1016/S0301-9268(00)00090-5

Cullers, R.L., 1994. The controls on the major and trace element variation of shales, siltstones, and sandstones of Pennsylvanian-Permian age from uplifted continental blocks in Colorado to platform sediment in Kansas, USA. Geochim. Cosmochim. Ac. 58, 4955-4972. https://doi.org/10.1016/0016-7037(94)90224-0

Cullers, R.L., Basu, A., Suttner, L.J., 1988. Geochemical signature of provenance in sand-size material in soils and stream sediments near the Tobacco Root batholith, Montana, U.S.A. Chem. Geol. 70, 335-348. https://doi.org/10.1016/0009-2541(88)90123-4

Dai, S., Bechtel, A., Eble, C.F., Flores, R.M., French, D., Graham, I.T., Hood, M. M., Hower, J.C., Korasidis, V.A., Moore, T.A., Puttmann, W., Wei, Q., Zhao, L., O'Keefe, J.M.K., 2020a. Recognition of peat depositional environments in coal: A review. Int. J. Coal Geol. 219, 103383. https://doi.org/10.1016/j.coal.2019.103383

Dai, S., Finkelman, R.B., French, D., Hower, J.C., Graham, I.T., Zhao, F., 2021. Modes of occurrence of elements in coal: a critical evaluation. Earth-Science Reviews 222, 103815. https://doi.org/10.1016/j.earscirev.2021.103815

Dai, S., Graham, I.T., Ward, C.R., 2016a. A review of anomalous rare earth elements and yttrium in coal. Int. J. Coal Geol. 159, 82–95. https://doi.org/10.1016/j.coal.2016.04.005

Dai, S., Hower, J.C., Finkelman, R.B., Graham, I.T., French, D., Ward, C.R., Eskenazy, G., Wei, Q., Zhao, L., 2020b. Organic associations of non-mineral elements in coal: a review. Int. J. Coal Geol. 218, 103347. https://doi.org/10.1016/j.coal.2019.103347

Dai, S., Liu, J., Ward, C.R., Hower, J.C., French, D., Jia, S., Hood, M.M., Garrison, T.M., 2016b. Mineralogical and geochemical compositions of Late Permian coals and host rocks from the Guxu Coalfield, Sichuan Province, China, with emphasis on enrichment of rare metals. Int. J. Coal Geol. 166, 71–95. https://doi.org/10.1016/j.coal.2015.12.004

Dai, S., Ren, D., Chou, C.-L., Finkelman, R.B., Seredin, V. V., Zhou, Y., 2012. Geochemistry of trace elements in Chinese coals: A review of abundances, genetic types, impacts on human health, and industrial utilization. Int. J. Coal Geol. 94, 3–21. https://doi.org/10.1016/j.coal.2011.02.003

Dai, S., Seredin, V.V., Ward, C.R., Hower, J.C., Xing, Y., Zhang, W., Song, W., Wang, P., 2015. Enrichment of U–Se–Mo–Re–V in coals preserved within marine carbonate successions: geochemical and mineralogical data from the Late Permian Guiding Coalfield, Guizhou, China. Miner Deposita 50, 159–186. https://doi.org/10.1007/s00126-014-0528-1

Duerto, L., Escalona, A., Mann, P., 2006. Deep structure of the Mérida Andes and Sierra de Perijá mountain fronts, Maracaibo Basin, Venezuela. AAPG Bull. 90, 505–528. https://doi.org/10. 1306/10080505033

Echigo, T., Kimata, M., 2010. Crystal chemistry and genesis of organic minerals: A review of oxalate and polycyclic aromatic hydrocarbon minerals. Can. Mineral. 48, 1329-1358. https://doi.org/10.3749/canmin.48.5.1329

Eddy, G.E., Rightmire, C.T., Byrer, C., 1982. Relationship of methane content of coal, rank and depth. Proceedings of the Society of Petroleum Engineers/Department of Energy Unconventional Gas Recovery Symp., Pittsburgh, Pennsylvania, vol. 10800. Society of Petroleum Engineers/Department of Energy, pp. 117-122. https://doi.org/10.2118/10800-MS

Escalona, A., Mann, P., 2011. Tectonics, basin subsidence mechanisms, and paleogeography of the Caribbean-South American plate boundary zone. Mar. Petrol. Geol. 28, 8–39. https://doi.org/10. 1016/ j.marpetgeo.2010.01.016

Escobar, M., Márquez, G., Inciarte, S., Rojas, J., Esteves, I., Malandrino, G., 2011. The organic geochemistry of oil seeps from the Sierra de Perijá eastern foothills, Lake Maracaibo Basin, Venezuela. Org. Geochem. 42, 727-738. https://doi.org/10.1016/j.orggeochem.2011.06.005

Escobar, M., Márquez, G., Suárez-Ruiz, I., Juliao, T.M., Carruyo, G., Martínez, M., 2016. Source-rock potential of the lowest coal seams of the Marcelina Formation at the Paso Diablo mine in the Venezuelan Guasare Basin: Evidence for the correlation of Amana oils with these Paleocene coals. Int. J. Coal Geol. 163, 149-165. https://doi.org/10.1016/j.coal.2016.07.003

Eskenazy, G.M., 1987. Rare earth elements and yttrium in lithotypes of Bulgarian coals. Org. Geochem. 11, 83-89. https://doi.org/10.1016/0146-6380(87)90030-1

Eskenazy, G., Finkelman, R. B., Chattarjee, S., 2010. Some considerations concerning the use of correlation coefficients and cluster analysis in interpreting coal geochemistry data. Int. J. Coal Geol. 83, 491–493. https://doi.org/10.1016/j.coal.2010.05.006

Everitt, B.S., 1993. Cluster Analysis. In: E. Arnold ed. Multivariate statistics. Oxford University Press, London, pp. 42–50.

Finkelman, R.B., 1993. Trace and Minor Elements in Coal. In: M.H. Engel and S.A. Macko eds. Organic Geochemistry: Principles and Applications. Springer, Berlin, pp. 593–607.

Fralick, P.W., Kronberg, B.I., 1997. Geochemical discrimination of clastic sedimentary rock sources. Sediment. Geol. 113, 111–124. https://doi.org/10.1016/S0037-0738(97)00049-3

Ghosh, S., Chatterjee, R., Shanker, P. 2016. Estimation of ash, moisture content and detection of coal lithofacies from well logs using regression and artificial neural network modelling. Fuel 177, 279–287. https://doi.org/10.1016/j.fuel.2016.03.001

Given, P.H., 1984. An essay on the organic geochemistry of coal. In: Gorbaty, M.L., Larsen, J.W., Wender, I. (Eds.), Coal Science, Vol. III. Academic Press, New York, pp. 63-252.

González de Juana, C., Iturralde de Arozarena, J.M., Picard, X., 1980. Geology of Venezuela and the petroliferous Venezuelan basins, Vol. I. Ediciones Foninves, Caracas, 407 p.

Hackley, P.C., Martinez, M., 2007. Organic petrology of Paleocene Marcelina Formation coals, Paso Diablo mine, western Venezuela: Tectonic controls on coal type. Int. J. Coal Geol. 71, 505–526. https://doi.org/10.1016/j.coal.2006.05.002

Hackley, P.C., Warwick, P.D., González, E., 2005. Petrology, mineralogy and geochemistry of mined coals, western Venezuela. Int. J. Coal Geol. 63, 68–97. https://doi.org/10.1016/j.coal.2005.02.006

Haze, W.B., 1984. Jurassic La Quinta Formation in the Sierra de Perijá, northwestern Venezuela: Geology and tectonic environment of red beds and volcanic rocks, in: Bonini, W.E., Hargraves, R.B., Shagam, R. (Eds.), The Caribbean-South American plate boundary and regional tectonics, Geological Society of America 162, pp. 263-282. https://doi.org/10.1130/MEM162

ISO 19579, 2006. Solid mineral fuels – Determination of sulfur by IR spectrometry. International Organization for Standardization, Geneva.

ISO 1928, 2009. Solid mineral fuels – Determination of gross calorific value by the bomb calorimetric method and calculation of net calorific value. International Organization for Standardization, Geneva.

ISO 562, 2010. Hard coal and coke – Determination of volatile matter. International Organization for Standardization, Geneva.

ISO 687, 2010. Solid mineral fuels – Coke – Determination of moisture in the general analysis test sample. International Organization for Standardization, Geneva.

ISO 1171, 2010. Solid mineral fuels –Determination of ash. International Organization for Standardization, Geneva.

ISO 29541, 2010. Solid mineral fuels – Determination of total carbon, hydrogen and nitrogen content – Instrumental method. International Organization for Standardization, Geneva.

Juliao, T.M., 2010. Geochemistry and Exploration of Coalbed Methane in a South-West Section of Paso Diablo Mine, Guasare Basin, Zulia. MSc Thesis. University of Zulia, Maracaibo, pp. 1-118.

Karayiğit, A.İ., Mastalerz, M., Oskay, R.G., Gayer, R.A., 2018. Coal petrography, mineralogy, elemental compositions and palaeoenvironmental interpretation of Late Carboniferous coal seams in

three wells from the Kozlu coalfield (Zonguldak Basin, NW Turkey). Int. J. Coal Geol. 187, 54-70. https://doi.org/10.1016/j.coal.2017.12.007

Karayiğit, A.I., Bircan, C., Mastalerz, M., Oskay, R.G., Querol, X., Lieberman, N.R., Türkmen, I., 2017. Coal characteristics, elemental composition and modes of occurrence of some elements in the İsaalan coal (Balıkesir, NW Turkey). Int. J. Coal Geol. 172, 43-59. https://doi.org/10.1016/j.coal. 2017.01.016

Kellogg, J., 1981. The Cenozoic basement tectonics of Sierra de Perijá, Venezuela and Colombia: PhD Thesis. Princeton University, Princeton, USA, 241 p.

Kellogg, J., 1984. Cenozoic tectonic history of the Sierra de Perijá, Venezuela, Colombia, and adjacent basins, in: Bonini, W.E., Hargraves, R.B., Shagam, R. (Eds.), The Caribbean–South American plate boundary and regional tectonics: Geological Society of America 162, 239–261.

Ketris, M.P., Yudovich, Ya.E., 2009. Estimations of Clarkes for Carbonaceous biolithes: World average for trace element contents in black shales and coals. Int. J. Coal Geol. 78, 135-148. https://doi.org/10.1016/j.coal.2009.01.002

Kim, A.G., 1977. Estimating methane content of bituminous coal-beds from adsorption data. Report of investigations, United States Bureau of Mines RI 8245.

Kolker, A., Palmer, C.A., Ruppert, L.F., 2003. USGS Short Course C, Modes of Occurrence of Trace Elements in Coals (151 slides).

Kopp, O.C., Bennett III, M.E., 2001. A comparison of the loss of CO and CO_2 during coalification. Int. J. Coal Geol. 47, 63–66.

Kopp, O.C., Bennett III, M.E., Clark, C.E., 2000. Volatiles lost during coalification. Int. J. Coal Geol. 44, 69-84. https://doi.org/10.1016/S0166-5162(99)00069-5

Koukouzas, N., Kalaitzidis, S.P., Ward, C.R., 2010. Organic petrographical, mineralogical and geochemical features of the Achlada and Mavropigi lignite deposits, NW Macedonia, Greece. Int. J. Coal Geol. 83, 387-395. https://doi.org/10.1016/j.coal.2010.05.004

Krejci-Graf, K., 1984. Uber die Elemente in Kohlen. Erdoel Kohle, Erdgas, Petrochem. 37, 451-457.

Kretz, R., 1983. Symbols for rock-forming minerals. Am. Mineral. 68, 277-279.

Kruszewski, Ł., 2013. Supergene sulphate minerals from the burning coal mining dumps in the Upper Silesian Coal Basin, South Poland. Int. J. Coal Geol. 105, 91-109. https://doi.org/10.1016/j.coal.2012.12.007

Laxminarayana, C. and Crosdale, P.J. 1999. Role of coal type and rank on methane sorption characteristics of Bowen Basin, Australia coals. Int. J. Coal Geol. 40, 309–325. https://doi.org/10.1016/S0166-5162(99)00005-1

Levy, J.H., Day, S.J., Killingly, J.S. 1997. Methane capacities of Bowen Basin coals related to coal properties. Fuel 76, 813–819. https://doi.org/10.1016/S0016-2361(97)00078-1

Li, X., Dai, S., Zhang, W., Li, T., Zheng, X., Chen, W., 2014. Determination of As and Se in coal and coal combustion products using closed vessel microwave digestion and collision/reaction cell technology (CCT) of inductively coupled plasma mass spectrometry (ICP-MS). Int. J. Coal Geol. 124, 1-4. https://doi.org/10.1016/j.coal.2014.01.002

Lu, X.C., Li, F.C., Watson, A.T., 1995. Adsorption measurements in Devonian shales. Fuel 74, 599–603. https://doi.org/10.1016/0016-2361(95)98364-K

Lugo, J., Mann, P., 1995. Jurassic-Eocene tectonic evolution of Maracaibo Basin, Venezuela, in: Tankard, A.J., Suárez, S., Welsink, H.J. (Eds.), Petroleum basins of South America. AAPG Memoir 62, pp. 699-725.

Mann, P., Escalona, A., Castillo, M.V., 2006. Regional geologic and tectonic setting of the Maracaibo supergiant basin, western Venezuela. AAPG Bull. 90, 445–477. https://doi.org/10.1306/10110505031

Martínez, M., Escobar, M., Esteves, I., Lopez, C., Galarraga, F., González, R., 2001. Trace elements of Paleocene Táchira coals, southwestern Venezuela: a geochemical study. J. S. Am. Earth Sci. 14, 387– 399. https://doi.org/10.1016/S0895-9811(01)00035-9

Martínez, M., Escobar, M., Galárraga, F. 1989. Preliminary geochemical characterization of some Venezuelan coals. In: Memoirs of the VII Venezuelan Geological Congress, Part IV. The Venezuelan Society of Geologists, Barquisimeto, November 15-18, pp. 1877–1896

McCabe, P.J., 1991. Tectonic controls on coal accumulation. B. Soc. Geol. Fr. 162, 277–282.

McLennan, S.M., 1989. Rare earth elements in sedimentary rocks: influence of provenance and sedimentary processes, in: Lipin, B. and McKay, G., (Eds.), Geochemistry and Mineralogy of Rare Earth Elements, Mineralogical Society of America, Reviews in Minerology 21, pp. 169-200.

Meyers, P.A., Ishiwatari, R., 1993. Lacustrine organic geochemistry—an overview of indicators of organic matter sources and diagenesis in lake sediments. Org. Geochem. 20, 867–900. https://doi.org/10.1016/0146-6380(93)90100-P

Miller, J.B., 1962. Tectonic trends in Sierra de Perijá and adjacent parts of Venezuela and Colombia. AAPG Bull. 46, 1565–1595.

Mishra, V., Chakravarty, S., Finkelman, R.B., Varma, A.K., 2019. Geochemistry of Rare Earth Elements in Lower Gondwana Coals of the Talchir Coal Basin, India. J. Geochem. Explor. 204, 43-56. https://doi.org/10.1016/j.gexplo.2019.04.006

Moore, F., Esmaeili, A., 2012. Mineralogy and geochemistry of the coals from the Karmozd and Kiasar coal mines, Mazandaran province, Iran. Int. J. Coal Geol. 96/97, 9–21. https://doi.org/10.1016/j.coal.2012.02.012

Morán, R., 1987. Evaluation of metals in Venezuelan coals as a source of air pollution. MSc Thesis. University of Zulia, Maracaibo, Venezuela, 92 p.

Mussa, A., Kalkreuth, W., Pimentel Mizusaki, A.M., Müller Bicca, M., 2021. Geochemical characterization of selected organic-rich shales from the Devonian Pimenteiras Formation, Parnaíba Basin, Brazil – Implications for methane adsorption capacity. J. S. Am. Earth Sci. 112, 103507. https://doi.org/10.1016/j.jsames.2021.103507

Pan, Z., Connell, L.D., 2012. Modelling permeability for coal reservoirs: a review of analytical models and testing data. Int. J. Coal Geol. 92, 1–44. https://doi.org/10.1016/j.coal.2011.12.009

Pardo, A., 2004. Paleocene-Eocene Palynology and Palynofacies from Northeastern Colombia and Western Venezuela. PhD Thesis. Université de Liège, Liege, Belgium, 322 p.

Parnaud, F., Gou, Y., Pascual, J.C., Capello, M.A., Truskowski, I., Passalacqua, H., 1995. Stratigraphic synthesis of western Venezuela, in: Tankard, A.J., Suárez, S., Welsink, H.J. (Eds.), Petroleum basins of South America. AAPG Memoir 62, 667–679.

Pérez. K.J., Soriano, R.E., Valenzuela, A.E., 2008. Updating of the geology at a 1:100000 scale of a sector of the Sierra de Perijá through the use of satellite images landsat 7 etm (coordinates 72º00' to 73º00'W and 10º40' to 11º00'N). BSc Thesis, Central University of Venezuela, Caracas, 106 p.

Petersen H.I., 2006. The petroleum generation potential and effective oil window of humic coals related to coal composition and age. Int. J. Coal Geol. 67, 221–248. https://doi.org/10.1016/j.coal.2006.01.005

Petersen, H.I., Lindström, S., Nytoft, H.P., Rosenberg, P., 2009. Composition, peat-forming vegetation and kerogen paraffinicity of Cenozoic coals: Relationship to variations in the petroleum

generation potential (Hydrogen Index). Int. J. Coal Geol. 78, 119–134. https://doi.org/10.1016/j.coal.2008.11.003

Pindell, J.L., Higgs, R., Dewey, J.F., 1998. Cenozoic palinspastic reconstruction, paleogeographic evolution, and hydrocarbon setting of the northern margin of South America, in: Pindell, J.L., Drake, C.L. (Eds.), Paleogeographic Evolution and Non-Glacial Eustasy, northern South America. Society for Sedimentary Geology Special Publication 58, 45–86.

Poppe, L.J., Paskevich, V.F., Hathaway, J.C., Blackwood, D.S., 2001. A Laboratory Manual for X-Ray Powder Diffraction. U.S. Geological Survey Open-File Report 01-041, Denver, 1-88. https://doi.org/10.3133/ofr0141

Prinz, D., Littke, R. 2005. Development of the micro- and ultramicroporous structure of coals with rank as deduced from the accessibility to water. Fuel 84, 1645–1652. https://doi.org/10.1016/j.fuel.2005.01.010

Qin, S., Lu, Q., Li, Y., Wang, J., Zhao, Q., Gao, K., 2018. Relationships between trace elements and organic matter in coals. J. Geochem. Explor. 188, 101-110. https://doi.org/10.1016/j.gexplo.2018.01.015

Querol, X., Fernández-Turiel, J., López-Soler, A., 1995. Trace elements in coal and their behaviour during combustion in a large power station. Fuel 74, 331–343. https://doi.org/10.1016/0016-2361(95)93464-O

Quintero, K., Martínez, M., Hackley, P., Márquez, G., Garbán, G., Esteves, I., Escobar, M., 2011. Organic geochemical investigation and coal-bed methane characteristics of the Guasare coals (Paso Diablo mine, western Venezuela). Energ. Source., Part A: Recovery, Utilization, and Environmental Effects 33, 959–971. https://doi.org/10.1080/15567030903330728

Rimmer, S.M., 2004. Geochemical paleoredox indicators in Devonian–Mississippian black shales, Central Appalachian Basin (USA). Chem. Geol. 206, 373-391. https://doi.org/10.1016/j.chemgeo. 2003.12.029

Scott, A.R., 2002. Hydrogeologic factors affecting gas content distribution in coal beds. Int. J. Coal Geol. 50: 363-387. https://doi.org/10.1016/S0166-5162(02)00135-0

Solano-Acosta, W., 2007. Controls on coalbed methane potential and gas sorption characteristics of high-volatile bituminous coals in Indiana. PhD Thesis. Indiana University, Bloomington, 366 p.

Strapóc, D., Masterlerz, M., Eble, C., Schimmelmann, A., 2007. Characterization of the origin of coalbed gases in southeastern Illinois Basin by compound-specific carbon and hydrogen stable isotope ratios. Org. Geochem. 38: 267-287. https://doi.org/10.1016/j.orggeochem.2006.09.005

Suárez-Ruiz, I., Flores, D., Marques, M.M., Martinez-Tarazona, M.R., Pis, J., Rubiera, F., 2006. Geochemistry, mineralogy and technological properties of coals from Rio Maior (Portugal) and Peñarroya (Spain) basins. Int. J. Coal Geol. 67, 171-190. https://doi.org/10.1016/j.coal.2005.11.004

Suggate, R., 2002. Application of Rank (Sr), a maturity index based on chemical analyses of coals. Mar. Petrol. Geol. 19, 929–950. https://doi.org/10.1016/S0264-8172(02)00117-4

Sutton, F.A., 1946. Geology of Maracaibo Basin, Venezuela. AAPG Bull. 30, 1621–1741.

Swaine, D. J., 1990. Trace Elements in Coal. Butterworths, London, 294 p. https://doi.org/10.1016/C2013-0-00949-8

Taboada, A., Rivera, L.A., Fuenzalida, A., Cisternas, A., Philip, H., Bijwaard, H., Olaya, J., Rivera, C., 2000. Geodynamics of the northern Andes: Subductions and intracontinental deformation (Colombia). Tectonics 19, 787–813. https://doi.org/10.1029/2000TC900004

Tang, Y., Jenden, P., Nigrini, A., Teerman, S., 1996. Modeling early methane generation in coal. Energ. Fuel. 10, 659–671. https://doi.org/10.1021/ef950153l

Taylor, S.R., McLennan, S.M., 1985. The Continental Crust: Its Composition and Evolution. Blackwell Publishing, Oxford, 312 p.

Tyler, R., Tyler, N., Tocco, R., Savian, V., 2006. The potential for Coalbed Gas Resource Development, Western Maracaibo Basin, Venezuela. AAPG-Annual Convention, April 9-12 (paper # 100904). Houston.

Van Der Lelij, R., 2013. Reconstructing north-western Gondwana with implications for the evolution of the Iapetus and Rheic Oceans: A geochronological, thermochronological, and geochemical study. PhD Thesis, Université de Genève, 221 p.

Ward, C.R., 2016. Analysis, origin and significance of mineral matter in coal: An updated review. Int. J. Coal Geol. 165, 1-27. https://doi.org/10.1016/j.coal.2016.07.014

Ward, C.R., Bocking, M., Ruan, C.-D., 2001. Mineralogical analysis of coals as an aid to seam correlation in the Gloucester Basin, New South Wales, Australia. Int. J. Coal Geol. 47, 31-49. https://doi.org/10.1016/S0166-5162(01)00025-8

Ward, C.R., Corcoran, J.F., Saxby, J.D., Read, H.W., 1996. Occurrence of phosphorus minerals in Australian coal seams. Int. J. Coal Geol. 31, 185-210. https://doi.org/10.1016/0166-5162(95)00055-0

Xu, N., Finkelman, R. B., Dai, S., Xu, C., Peng, M., 2021. Average linkage hierarchical clustering algorithm for determining the relationships between elements in coal. ACS Omega 6, 6206–6217. https://doi.org//10.1021/acsomega.0c05758

Yan, Y., Xia, B., Lin, G., Cui, X., Hu, X., Yan, P., Zhang, F., 2007. Geochemistry of the sedimentary rocks from the Nanxiong Basin, South China and implications for provenance, paleoenvironment and paleoclimate at the K/T boundary. Sediment. Geol. 197, 127-140. https://doi.org/10.1016/j.sedgeo.2006.09.004

Yang, N., Tang, S., Zhang, S., Xi, Z., Li, J., Yuan, Y., Guo, Y., 2018. In seam variation of element-oxides and trace elements in coal from the eastern Ordos Basin, China. Int. J. Coal Geol. 197, 31-41. https://doi.org/10.1016/j.coal.2018.08.002

Yudovich, Y.E., Ketris, M.P., 2006. Valuable trace elements in coal. Ekaterinburg. Komi Scientific Center/Institute of Geology/Ural Division, RAS, pp. 1-538.

Figure 1: a) and b), respectively, maps showing the location of the Guasare Coalfield in NW Venezuela and the Paso Diablo and open-pit mines in this basin (modified from Escobar et al., 2016); c) situation of exploratory boreholes.

Figure 2: Stratigraphic units in the Sierra of Perijá (modified from Escobar et al., 2016).

Figure 3: Lithologic column of the Paso Diablo and Mina Norte open-cut mines showing coal seam names and stratigraphic position of coal samples (modified from Quintero et al., 2011).

Figure 4: Dendogram showing correlation of elements in the Marcelina coal seams.

Figure 5: La-Sc-Th triangular diagram for the coals under study. Data from local granitoids (El Palmar Granite and El Carmen Granodiorite; Van Der Lelij, 2013) are included.

Figure 6: Chondrite-normalized REE plots for the Guasare coals, El Palmar and El Carmen granitoids.

Figure 7: Plots of gas content normalized to per-unit TOC on a dried basis with the total clay (a) and illite (b) contents.

Figure 1

Click here to access/download;Figure;Figura1abc_vertical.tif

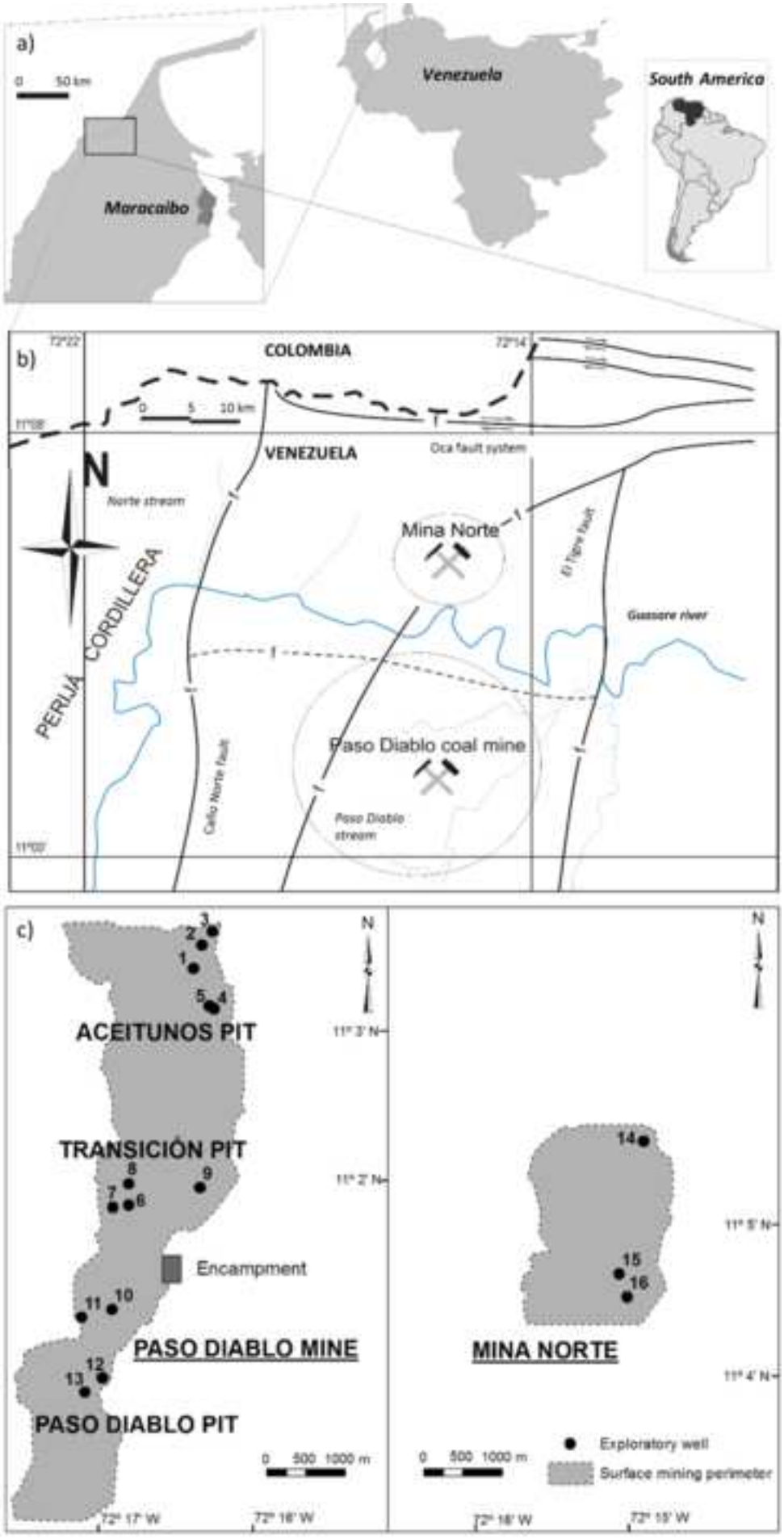

Figure 2

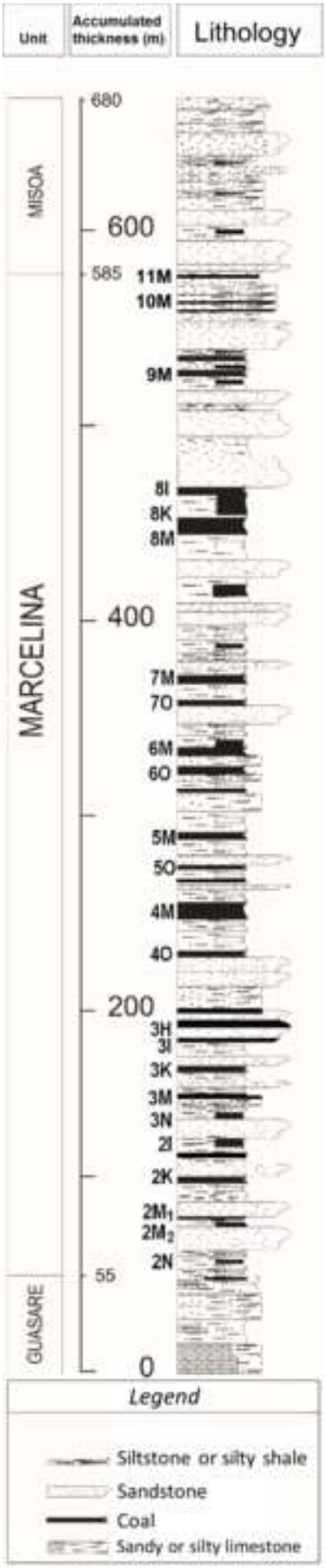

Figure 3

Click here to access/download;Figure;Figura3.tif

Figure 4

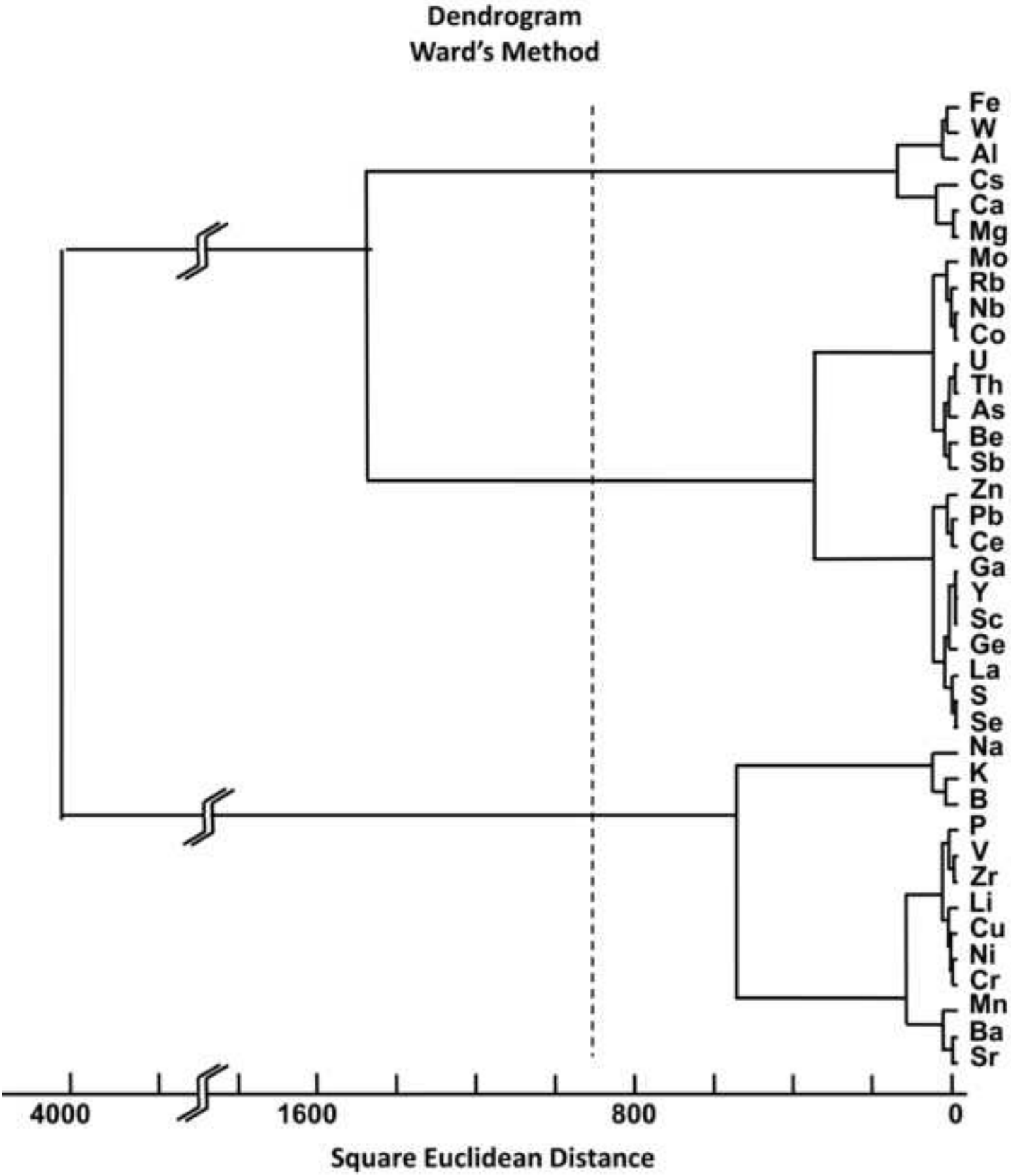

Figure 5

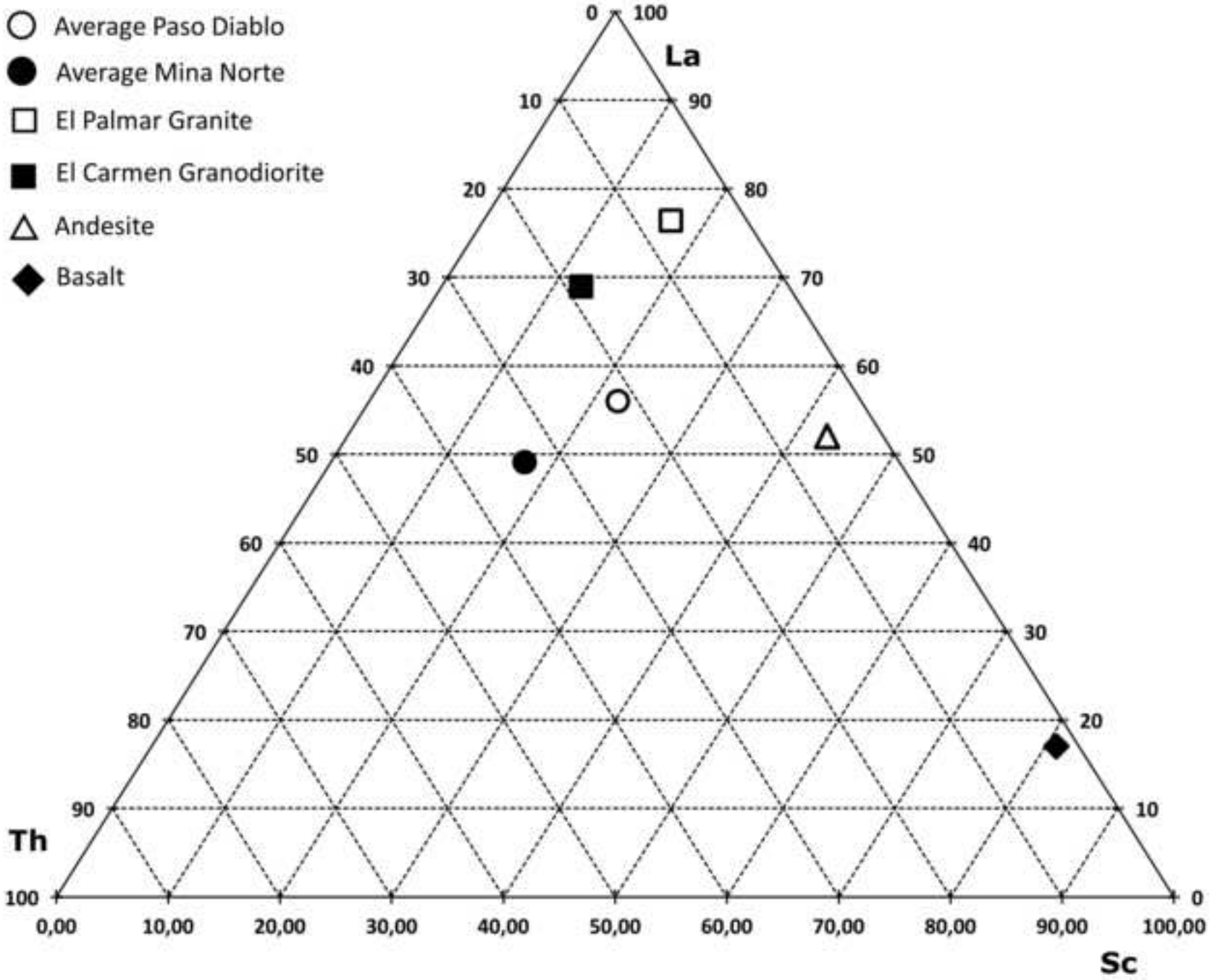

Figure 6

Click here to access/download;Figure;Fig6_REV_DEF.tif

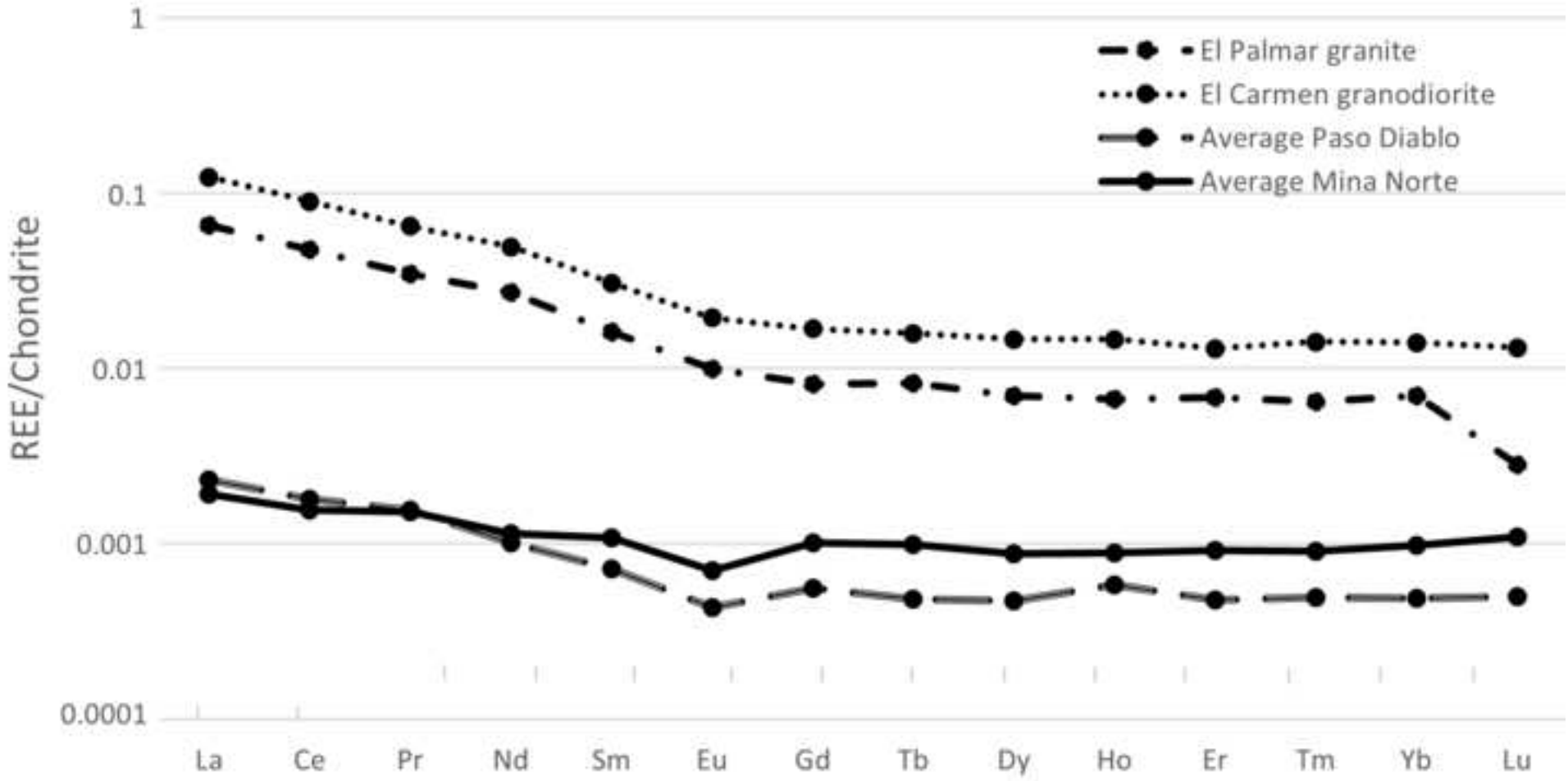

Figure 7

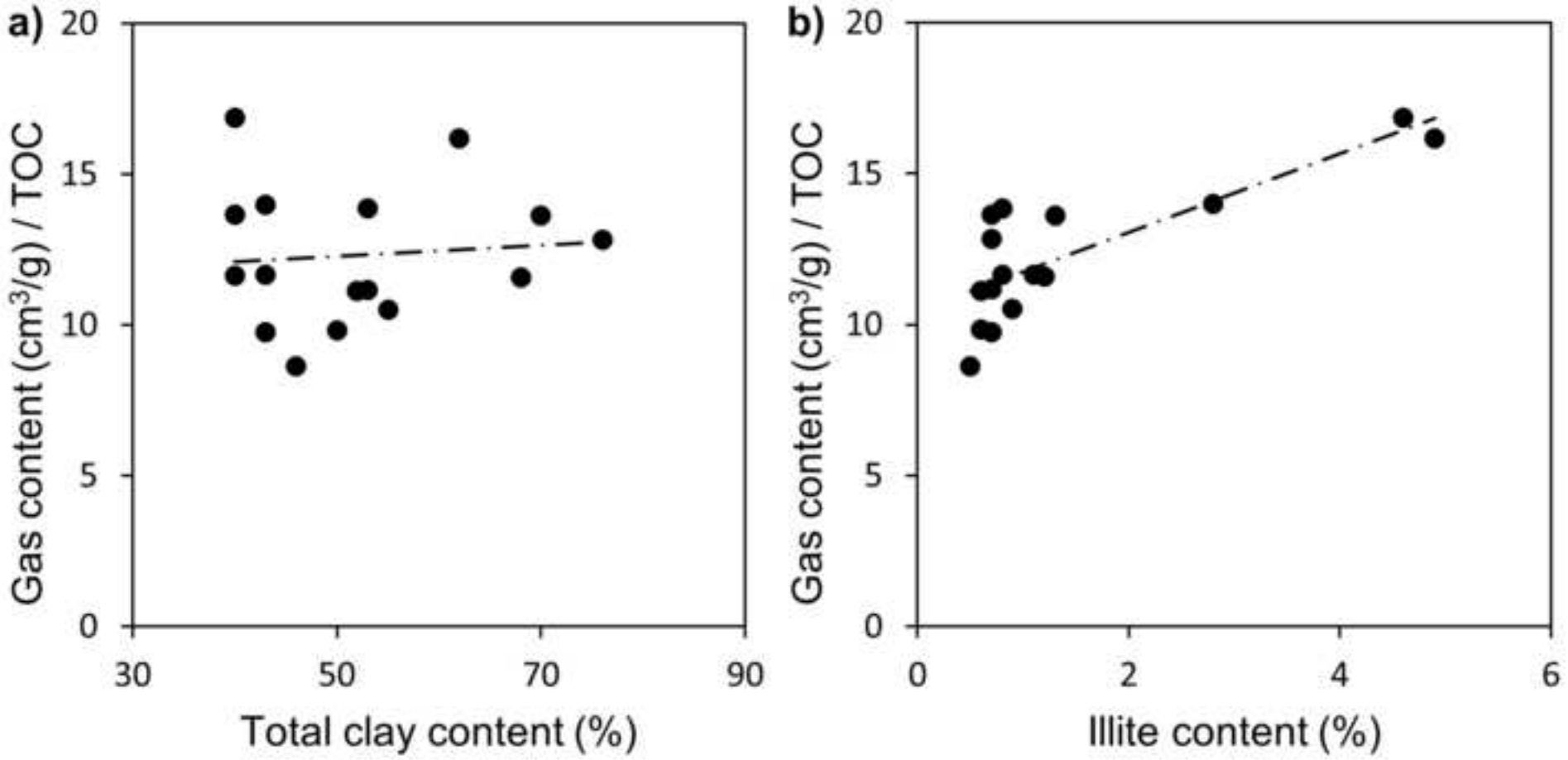

Table 1: Coordinates of exploratory wells and list of coal seams under study. Codes in boldface represent the sampled coal seams.

Pit area	Well	Latitude	Longitude	Studied coal seams
Aceitunos	1	11°03′34″N	72°16′22″W	4MO/**5O**
	2	11°03′46″N	72°15′44″W	2J/**2M**/**3K**/3M/4MO
	3	11°03′47″N	72°15′36″W	2I/2J/2M/**2O**/3G/3H/3K/3M/**4MO**
	4	11°03′14″N	72°15′58″W	**4MO**/5M/**5O**/6K/**6M**/**6O**/**6Q**/7M/**7O**/8KM
	5	11°03′15″N	72°15′59″W	**4MO**/5M/**5O**/**6MO**/**6Q**/7M/**7O**/8I/8KM/9O
Baqueta	6	11°01′45″N	72°16′40″W	**4M**/**4O**/**5M**
	7	11°01′44″N	72°17′03″W	**4M**/5M/6K/**6MO**/6Q/7M/**7O**
	8	11°01′58″N	72°16′43″W	3G/3H/**3K**/4O
	9	11°01′57″N	72°16′21″W	**4M**/**4O**/**5O**/6K/**6MO**/6Q/7M/**7O**/8K/8M
Paso Diablo	10	11°00′41″N	72°16′42″W	3G/**4MO**/5M/**5O**/5Q/6K/**6MO**/6Q
	11	11°00′37″N	72°17′20″W	2I/2K/**2M1**/**2M2**/2N/3H/3I/**3K**/3M/3N
	12	11°00′06″N	72°16′42″W	3G/**4MO**/5M/**5O**/**6MO**/6Q/7M/7O/8I/8K/8M/9G/9J/9K/9M/9O/10M/10N/11M
	13	10°59′49″N	72°17′04″W	**4MO**/5M/**5O**/5Q/6K/**6MO**/7M/**7O**/8I/8K
Mina Norte	14	11°05′35″N	71°14′55″W	**4M**
	15	11°04′39″N	72°15′05″W	**2I**/**3K**
	16	11°04′30″N	72°15′01″W	**2K**/**3I**

Table 2: Depths (m), thicknesses (m), TOC (wt.%), proximate-ultimate parameters and gross calorific values (MJ/Kg on a moist ash-free basis), G_{daf} and G_c (cm^3/g) for Marcelina coal seams studied. The codes for coal seam numbering precede those for exploratory wells in sampling nomenclature.

Coal	Depth	Thickness	Moisture	Ash yield	VM	FC	C	H	N	O	S_t	TOC	GCV	H/C	O/C	G_{daf}	G_c
5O/1	37.8	1.9	1.7	9.9	42.3	50.8	82.54	5.44	1.87	7.42	0.57	73.07	34.48	0.79	0.067	7.14	6.31
4MO/1	78.7	14.5	1.9	1.9	39.2	59.6	84.24	5.42	1.91	7.58	0.44	--	34.99	0.77	0.068	10.4	--
4MO/2	34.7	14.8	2.4	1.7	39.9	59.0	87.47	4.93	1.68	7.87	0.45	--	35.32	0.67	0.066	7.78	--
3K/2	125.4	2.3	2.1	3.9	43.5	54.3	82.61	5.77	1.67	7.43	0.57	78.32	33.69	0.83	0.068	11.5	9.17
3M/2	131.6	1.8	1.6	2.8	43.3	55.4	81.06	5.59	1.84	7.29	0.69	--	34.23	0.82	0.067	11.9	--
2J/2	150.7	0.7	3.3	4.5	44.3	52.2	83.85	5.73	1.90	6.94	0.65	--	35.41	0.82	0.062	11.9	--
2M/2	159.8	2.6	2.9	1.4	43.6	55.6	84.52	5.74	1.72	7.24	0.83	79.43	34.29	0.81	0.064	12.7	11.1
4MO/3	48.0	14.6	2.1	2.1	39.7	59.0	85.02	5.30	1.83	7.65	0.51	79.21	35.07	0.74	0.067	8.72	7.19
3G/3	89.4	0.5	2.3	2.5	43.2	55.4	80.85	5.84	1.73	7.07	0.84	--	34.54	0.86	0.065	10.4	--
3H/3	99.4	1.0	0.9	2.6	45.5	53.0	81.82	5.74	1.85	7.36	1.00	--	34.72	0.84	0.067	10.8	--
3K/3	139.3	2.4	2.5	4.6	45.2	51.3	82.03	5.65	1.86	6.86	0.47	--	34.61	0.82	0.062	11.6	--
3M/3	144.5	2.1	3.3	1.6	45.1	53.9	82.82	5.80	1.88	7.45	0.73	--	35.11	0.84	0.066	12.1	--
2I/3	158.1	0.8	1.8	2.0	44.2	54.6	82.59	5.82	1.87	7.13	0.63	--	33.85	0.84	0.064	12.6	--
2J/3	162.5	0.5	3.8	4.4	42.6	51.9	84.04	5.72	1.71	7.56	0.79	--	35.46	0.81	0.068	12.1	--
2M/3	177.3	3.3	2.9	1.9	45.2	53.7	82.79	5.85	1.98	7.45	0.60	--	35.16	0.84	0.067	12.9	--
2O/3	198.2	1.5	1.9	1.8	44.6	54.4	82.09	5.78	1.66	7.38	0.38	73.20	34.81	0.84	0.067	13.6	12.3
8KM/4	0.9	3.0	1.3	1.6	41.5	57.5	81.32	5.03	1.84	7.31	0.72	--	33.51	0.74	0.067	1.60	--
7M/4	11.1	4.0	2.1	1.5	39.3	59.8	86.04	5.16	1.75	7.74	1.06	--	35.25	0.71	0.068	5.18	--
7O/4	23.2	3.8	1.7	0.9	41.6	57.6	81.86	5.21	1.76	7.36	0.59	80.04	33.93	0.76	0.065	6.76	5.92
6K/4	38.4	0.5	1.0	4.5	37.0	60.1	84.10	5.36	1.91	8.20	1.25	--	33.65	0.76	0.073	8.09	--
6M/4	49.1	3.1	2.1	1.3	40.6	58.6	86.87	5.05	1.87	7.81	1.56	73.22	35.33	0.69	0.067	8.81	7.14
6O/4	52.7	2.9	1.9	1.9	40.3	58.2	86.32	5.29	1.96	7.76	0.56	74.06	35.48	0.73	0.065	8.98	7.28
6Q/4	65.4	0.7	1.8	5.0	42.1	58.5	81.79	5.46	1.85	7.35	1.32	77.85	34.32	0.79	0.063	9.32	7.75
5M/4	78.6	3.9	1.8	1.5	40.4	58.7	84.00	5.52	1.70	8.56	0.80	--	35.09	0.78	0.070	10.4	--
5O/4	107.3	2.8	2.0	2.5	40.0	58.4	83.99	5.58	1.80	8.15	0.84	79.26	35.18	0.79	0.072	11.3	9.36
4MO/4	148.9	13.2	1.6	1.3	38.4	60.7	86.64	5.12	1.76	6.79	0.69	80.59	35.35	0.71	0.060	13.0	10.4
9O/5	37.7	1.9	2.2	2.8	42.8	55.6	81.69	5.40	1.85	8.35	0.57	--	34.22	0.79	0.076	7.76	--
8I/5	47.8	1.9	2.3	3.5	42.4	55.5	84.98	5.62	1.93	7.28	0.64	--	34.25	0.79	0.064	8.37	--
8KM/5	53.6	2.7	1.9	1.4	39.3	59.8	83.99	5.67	1.70	7.19	1.01	--	34.10	0.80	0.066	9.17	--
7M/5	62.2	3.9	2.6	1.3	41.2	56.8	84.87	5.47	1.92	7.27	0.81	--	34.01	0.77	0.064	9.42	--
7O/5	74.9	3.6	1.9	1.1	41.4	57.9	82.46	5.14	1.77	7.42	0.67	80.31	34.03	0.74	0.067	10.2	8.18
6MO/5	102.0	6.2	2.1	2.0	40.5	58.2	83.43	5.06	1.89	8.05	0.89	79.57	34.25	0.72	0.072	11.2	8.93

Sample	Depth	Thickness	Moisture	Ash yield	VM	FC	C	H	N	O	St	TOC	GCV	H/C	O/C	G_{daf}	G_c
6Q/5	117.7	0.9	1.7	4.2	42.9	55.4	82.27	5.48	1.86	7.40	1.04	76.80	34.45	0.79	0.067	11.3	8.94
5M/5	132.6	4.2	1.7	1.7	40.6	58.3	85.93	5.71	1.75	7.28	0.75	--	34.37	0.79	0.063	12.3	--
5O/5	160.0	2.8	2.1	1.3	39.6	59.5	84.72	5.22	1.92	7.62	0.89	78.17	35.01	0.73	0.065	13.1	10.4
4MO/5	201.2	13.5	1.9	1.4	38.4	60.7	84.35	5.42	1.91	7.59	0.33	78.26	35.01	0.77	0.066	14.2	11.3
5M/6	77.1	5.8	1.5	0.9	40.3	59.1	84.16	5.36	1.91	8.37	0.98	77.51	34.93	0.76	0.071	10.4	8.62
4M/6	102.3	2.5	2.2	1.6	41.9	57.1	83.74	5.28	1.90	6.92	0.79	78.01	34.66	0.75	0.061	11.1	8.89
4O/6	138.0	8.8	1.9	1.1	42.5	56.5	81.75	5.46	1.85	7.35	0.63	79.84	34.30	0.79	0.067	12.3	9.80
7M/7	97.4	1.9	2.5	1.5	42.9	56.5	84.20	5.67	1.91	7.57	0.82	--	35.37	0.80	0.067	10.9	--
7O/7	107.4	3.9	1.0	2.8	41.9	56.4	82.38	5.24	1.77	7.17	0.75	80.88	34.16	0.76	0.065	11.3	9.03
6K/7	128.1	1.0	2.3	4.9	43.1	53.1	85.49	5.30	1.94	8.24	1.05	--	33.85	0.74	0.070	11.4	--
6MO/7	137.1	5.5	1.7	3.8	42.1	55.6	84.07	5.50	1.71	7.56	0.78	77.93	35.08	0.78	0.068	12.0	9.53
6Q/7	152.8	1.0	2.1	5.3	43.4	53.3	85.75	5.73	1.64	7.26	0.77	--	34.38	0.79	0.064	12.0	--
5M/7	163.6	3.8	1.8	2.9	43.1	55.3	81.75	5.46	1.85	7.35	0.96	--	34.29	0.80	0.069	12.7	--
4M/7	222.3	9.9	1.8	1.0	42.7	56.7	83.47	5.54	1.89	7.01	0.51	78.67	35.06	0.79	0.063	14.3	11.5
4O/8	27.4	2.8	1.3	3.0	42.0	56.3	84.21	5.53	1.91	7.57	0.82	--	35.17	0.78	0.066	7.01	--
3G/8	51.5	0.6	2.8	4.8	44.2	53.9	82.39	5.66	1.87	7.41	0.74	--	34.77	0.82	0.069	8.33	--
3H/8	61.3	0.8	1.6	4.5	44.9	52.5	82.65	5.81	1.74	7.43	0.97	--	35.09	0.84	0.065	8.94	--
3K/8	96.1	1.1	2.0	3.5	44.0	54.0	79.66	5.73	1.81	7.16	0.94	76.64	34.01	0.86	0.065	10.5	8.93
8K/9	93.0	3.9	2.7	4.4	42.1	52.9	85.22	5.17	1.93	7.66	0.99	--	34.99	0.72	0.065	10.3	--
8M/9	100.1	0.9	2.4	4.5	38.8	57.3	81.43	5.41	1.84	7.31	0.78	--	34.21	0.79	0.068	10.8	--
7M/9	115.4	3.1	2.7	1.5	41.4	57.7	82.18	5.14	1.86	7.39	0.68	--	33.94	0.75	0.066	11.6	--
7O/9	129.4	3.7	2.6	3.7	43.0	54.0	81.41	5.40	1.84	6.92	0.96	76.77	34.13	0.79	0.065	11.6	9.14
6K/9	149.4	0.8	1.7	3.1	42.9	58.1	84.59	5.61	1.92	7.24	1.09	--	34.35	0.79	0.064	12.4	--
6MO/9	159.1	6.8	2.9	1.7	40.5	58.4	82.99	5.22	1.68	7.46	0.99	79.18	34.37	0.75	0.063	12.8	10.3
6Q/9	174.4	0.9	2.2	5.8	42.9	52.1	83.35	5.38	1.79	8.23	1.51	--	34.66	0.77	0.070	12.4	--
5O/9	216.0	2.5	2.1	1.7	41.7	57.3	82.95	5.40	1.88	7.46	0.81	79.84	34.58	0.78	0.069	14.1	11.2
4M/9	254.7	8.8	2.6	1.1	39.7	59.7	85.78	4.97	1.94	7.72	0.56	77.92	34.85	0.69	0.066	15.1	11.9
4O/9	272.3	6.6	3.1	5.6	44.7	54.4	84.11	5.35	1.91	7.56	0.49	81.99	34.85	0.76	0.067	13.0	8.95
6K/10	14.9	1.6	1.2	4.9	36.6	59.5	85.32	5.26	1.63	6.82	0.93	--	33.55	0.73	0.060	5.73	--
6MO/10	25.4	4.6	2.0	1.5	41.0	58.2	84.66	5.48	1.92	7.25	0.62	79.09	33.94	0.77	0.064	6.96	5.87
6Q/10	43.6	0.9	1.3	4.9	42.7	52.3	85.93	5.27	1.95	7.28	1.03	--	33.72	0.73	0.063	7.98	--
5M/10	64.7	5.5	1.7	2.4	41.2	57.3	82.82	4.98	1.88	7.45	0.94	--	33.94	0.72	0.067	9.54	--
5O/10	91.2	2.8	1.9	1.3	40.7	58.6	81.86	5.42	1.76	7.36	0.56	80.24	34.23	0.79	0.068	10.9	8.88
5Q/10	129.7	1.2	1.8	5.4	39.5	55.4	82.27	5.10	1.66	7.40	0.92	--	33.94	0.74	0.067	11.6	--

Sample	Depth	Thickness	Moisture	Ash yield	VM	FC	C	H	N	O	St	TOC	GCV	H/C	O/C	G_{daf}	G_c
4MO/10	223.2	9.6	1.6	4.3	41.6	57.3	81.84	5.48	1.85	7.36	0.66	80.38	34.34	0.79	0.068	14.0	11.0
3G/10	254.3	0.5	2.4	3.2	43.4	54.8	81.54	5.71	1.68	8.33	0.84	--	33.93	0.84	0.071	14.4	--
3H/11	60.1	1.0	1.3	4.6	43.7	53.3	82.95	5.71	1.88	6.86	0.85	--	35.03	0.82	0.062	8.96	--
3I/11	70.8	0.6	1.2	3.7	45.6	51.1	80.46	5.74	1.82	8.21	0.87	--	34.29	0.85	0.070	9.45	--
3K/11	96.3	1.6	2.4	3.3	43.4	54.8	81.58	5.87	1.85	8.34	0.92	76.26	34.18	0.86	0.076	10.6	8.45
3M/11	100.6	0.6	1.2	7.3	43.1	52.7	84.13	5.80	1.72	7.57	0.81	--	33.60	0.82	0.068	10.4	--
3N/11	106.3	0.9	1.2	1.4	43.4	55.8	81.47	5.88	1.85	7.33	0.49	--	34.12	0.86	0.063	11.3	--
2I/11	116.8	1.0	2.7	3.0	48.1	50.3	84.65	5.82	1.92	7.25	0.58	--	34.42	0.82	0.064	11.0	--
2K/11	123.6	0.5	1.1	5.2	44.9	52.2	82.65	5.81	1.87	7.43	0.85	--	35.08	0.84	0.066	11.3	--
2M1/11	128.4	1.1	2.9	1.8	43.4	55.6	83.26	5.66	1.79	7.19	0.93	77.09	35.25	0.81	0.064	11.8	9.39
2M2/11	130.0	1.4	1.5	3.2	43.3	54.8	82.82	5.75	1.78	7.45	0.69	76.90	33.74	0.83	0.065	11.8	9.42
2N/11	147.3	1.0	2.6	2.7	45.9	51.6	82.86	5.85	1.88	8.45	0.96	--	35.21	0.84	0.071	12.0	--
11M/12	11.2	0.5	2.7	3.7	38.6	58.3	80.32	5.18	1.82	7.22	0.68	--	33.40	0.77	0.063	5.04	--
10M/12	38.0	2.8	0.9	5.0	40.0	57.0	81.30	5.03	1.84	7.31	0.54	--	33.49	0.74	0.069	7.84	--
10N/12	45.8	1.9	1.1	4.7	39.4	57.8	85.63	5.68	1.56	6.56	0.56	--	33.63	0.79	0.058	8.41	--
9G/12	105.2	5.3	3.1	2.0	42.0	55.9	80.52	5.22	1.83	6.95	0.59	--	33.51	0.77	0.064	11.0	--
9J/12	126.6	0.9	1.6	2.8	39.9	58.4	80.58	5.36	1.83	7.24	0.75	--	33.79	0.79	0.068	12.0	--
9K/12	128.1	1.5	0.9	1.0	39.8	59.5	81.68	5.45	1.85	7.34	0.33	--	33.66	0.79	0.063	12.3	--
9M/12	140.6	0.5	3.2	5.9	37.0	56.8	86.11	5.27	1.95	7.74	0.62	--	35.39	0.73	0.067	11.9	--
9O/12	144.8	0.7	1.1	4.0	39.6	57.9	85.47	5.53	1.94	8.24	0.46	--	33.94	0.77	0.072	12.4	--
8I/12	184.5	1.2	1.0	4.3	40.7	56.8	84.52	5.64	1.62	7.60	0.67	--	35.53	0.79	0.065	13.3	--
8K/12	191.6	1.6	1.6	7.2	41.7	52.9	82.69	4.99	1.87	7.44	0.64	--	33.89	0.72	0.067	12.8	--
8M/12	194.4	1.1	1.2	5.1	41.4	55.5	81.32	5.11	1.74	7.31	0.83	--	33.64	0.75	0.068	13.3	--
7M/12	210.9	3.0	1.2	1.6	39.1	59.9	83.10	5.07	1.88	7.47	0.49	--	34.12	0.73	0.066	14.4	--
7O/12	225.8	3.4	2.5	0.9	41.7	57.7	84.95	5.70	1.93	7.28	0.48	--	34.34	0.80	0.064	14.4	--
6MO/12	255.2	6.7	1.4	3.2	42.6	56.5	83.09	5.27	1.88	6.97	0.47	81.09	34.40	0.76	0.062	14.7	11.2
6Q/12	271.3	1.4	3.0	4.6	42.3	53.6	82.56	5.38	1.87	7.43	1.55	--	34.41	0.78	0.066	14.4	--
5M/12	289.3	5.9	1.4	2.7	40.8	57.6	83.07	5.51	1.88	7.47	0.90	--	34.82	0.79	0.065	15.5	--
5O/12	308.8	2.5	1.6	0.7	38.0	61.6	85.04	5.65	1.56	7.11	0.64	79.99	34.51	0.79	0.063	16.4	13.0
4MO/12	345.6	11.0	1.7	1.3	42.3	56.9	83.75	5.56	1.90	7.53	0.47	80.51	35.03	0.79	0.068	16.4	12.8
3G/12	377.4	0.5	0.9	3.6	44.9	49.0	82.94	5.85	1.85	7.06	0.87	--	35.23	0.84	0.063	16.1	--
8I/13	61.8	1.1	1.2	0.7	38.1	61.4	85.04	5.62	1.93	7.20	0.79	--	33.96	0.79	0.062	9.86	--
8K/13	70.0	1.4	3.1	5.1	37.3	58.2	81.61	5.43	1.84	8.33	0.54	--	33.82	0.79	0.072	9.57	--
7M/13	90.8	2.8	2.6	1.2	42.7	56.5	85.48	5.65	1.94	8.32	0.52	--	33.91	0.79	0.071	10.7	--

Sample	Depth	Thickness	Moisture	Ash yield	VM	FC	C	H	N	O	St	TOC	GCV	H/C	O/C	G_{daf}	G_c
7O/13	105.3	3.1	2.2	1.1	42.8	56.5	83.72	4.97	1.99	7.54	0.59	79.16	34.18	0.71	0.062	11.2	8.92
6K/13	131.6	1.6	0.9	4.5	41.9	52.0	82.50	5.13	1.86	7.48	0.91	--	34.07	0.74	0.068	11.7	--
6MO/13	135.0	4.8	2.2	1.7	43.2	55.8	83.83	5.08	1.73	7.14	0.61	78.76	34.38	0.72	0.063	12.1	9.34
5M/13	168.1	5.2	1.9	2.5	42.3	56.3	82.50	5.50	1.67	7.41	0.48	--	34.66	0.79	0.066	12.9	--
5O/13	184.0	2.2	2.0	3.0	41.2	57.0	83.54	5.20	1.89	7.51	0.50	79.55	34.45	0.74	0.067	13.3	10.3
5Q/13	209.8	0.7	1.2	2.5	41.0	57.5	82.60	5.39	1.87	7.43	0.70	--	34.44	0.78	0.066	14.1	--
4MO/13	228.7	9.2	1.4	1.4	41.4	57.8	83.26	5.50	1.69	7.08	0.40	--	34.85	0.79	0.064	14.6	--
4M/14	147.4	1.6	2.8	1.8	38.1	59.9	82.39	5.52	1.50	8.27	0.42	79.11	34.11	0.79	0.075	12.7	10.2
2I/15	171.2	1.0	1.4	5.4	43.5	53.3	83.48	5.74	1.69	7.51	0.69	80.89	33.30	0.82	0.067	12.5	11.0
3K/15	105.4	0.8	1.9	3.2	47.0	51.0	85.00	5.84	1.59	6.87	0.70	78.76	34.70	0.82	0.061	10.7	8.69
2K/16	181.6	1.9	3.4	5.0	44.9	49.0	81.71	5.73	1.85	7.35	0.49	75.00	34.63	0.84	0.067	10.1	8.69
3I/16	97.7	1.4	2.5	2.5	43.7	54.9	85.22	5.93	1.44	6.60	0.81	74.11	33.77	0.86	0.059	13.1	12.0

Notes: Proximate-ultimate data in wt. % on a dry basis, except VM (wt. % on a dry ash-free basis), H/C and O/C (atomic ratios); depth, moisture and ash yield are expressed by “h”, “m” and “a”; $G_{daf} = 0.01 \cdot (100 - m - a) \cdot [(0.8 \cdot FC/VM + 5.6) \cdot (0.096 \cdot h)^{0.315} \cdot (0.096 \cdot h)^{0.01 \cdot VM/FC} - 0.14 \cdot (0.018 \cdot h + 11)]$ (Kim, 1977).

Table 3: Contents, means and concentration coefficients (CC) of minor and trace elements determined by ICP-AES in Marcelina coal samples (µg/g unless indicated %).

Sample	Al,%	Fe,%	P	Mg	Mn	Ca	Na	K	Ti	Zn	B	Sr	Ba	Cr	V	Ni	Pb
5O/1	0.44	0.40	126.0	202.1	17.6	508.8	432.8	297.8	177.9	6.6	36.2	16.9	30.5	6.0	8.4	8.3	2.6
3K/2	0.26	0.13	8.1	42.3	5.0	64.1	133.0	9.4	24.6	**2.5**	26.3	**9.8**	**6.5**	1.1	**1.7**	1.1	**1.9**
2M/2	0.14	0.03	8.0	2.6	**0.9**	22.8	101.5	16.7	23.1	**2.5**	30.6	**5.4**	**10.2**	1.4	5.0	2.1	2.3
4MO/3	0.15	0.07	15.6	22.7	**3.2**	32.9	109.0	11.2	39.9	**1.3**	17.2	**4.5**	**4.1**	1.8	2.2	2.2	2.3
2O/3	0.06	0.07	9.2	128.6	7.4	440.3	102.8	11.0	36.9	**0.6**	18.1	10.6	**4.3**	1.4	2.2	1.0	2.5
7O/4	0.03	0.13	7.7	24.3	**4.7**	68.7	222.2	37.8	14.1	**1.1**	19.3	**4.4**	**6.3**	1.1	**1.0**	1.0	**1.8**
6M/4	0.02	0.19	23.5	88.0	6.7	156.8	129.0	14.8	29.4	**0.7**	25.9	14.4	**14.6**	2.0	2.7	0.6	**0.7**
6O/4	0.18	0.15	32.9	60.4	6.7	168.2	170.7	106.7	37.2	**1.6**	37.5	**9.8**	**2.2**	2.2	3.5	1.4	2.0
6Q/4	0.49	0.24	44.7	12.7	**1.7**	52.7	166.6	322.0	97.8	**0.9**	23.5	13.2	**5.7**	5.0	6.6	6.1	**1.9**
5O/4	0.03	0.11	8.4	2.5	**0.5**	32.6	53.2	293.3	181.5	**1.0**	20.6	**5.0**	**4.8**	1.6	5.5	4.4	**1.2**
4MO/4	0.14	0.07	19.2	16.4	**1.7**	84.9	155.3	36.5	87.0	**1.0**	22.6	14.1	**16.3**	2.1	4.1	1.9	**1.8**
7O/5	0.08	0.29	7.2	136.7	15.3	344.1	190.0	29.5	42.9	**1.1**	34.1	**9.9**	**10.1**	2.3	5.3	2.3	2.0
6MO/5	0.23	0.14	11.2	70.2	16.3	184.8	289.1	154.0	60.9	**3.9**	16.8	**8.8**	**7.0**	2.4	4.0	2.0	2.1
6Q/5	0.47	0.06	104.5	4.7	**3.5**	400.7	157.7	13.8	25.5	**1.3**	13.2	27.6	**3.9**	1.4	**0.9**	1.9	**1.7**
5O/5	0.19	0.08	24.7	12.3	**2.6**	24.7	270.8	12.7	61.2	5.2	41.7	**5.9**	**6.3**	5.3	8.8	5.0	**1.3**
4MO/5	0.10	0.08	15.2	20.2	**1.9**	112.5	190.0	20.8	62.4	**0.5**	16.2	15.3	**17.1**	1.5	**1.2**	1.5	**1.2**
5M/6	0.13	0.17	6.8	306.0	12.0	24.0	161.5	51.2	153.0	**2.6**	26.0	**5.1**	**14.5**	1.7	4.2	3.6	**1.1**
4M/6	0.12	0.30	12.8	286.1	19.7	472.6	126.4	22.0	53.4	**0.9**	16.1	17.6	**5.7**	1.5	2.0	1.1	**1.8**
4O/6	0.14	0.51	19.2	84.4	6.3	272.3	152.8	23.7	103.8	**2.1**	29.6	13.4	**10.4**	2.4	5.6	4.2	2.2
7O/7	0.19	0.30	15.2	302.8	23.5	704.7	179.4	43.8	129.6	**1.7**	24.8	19.6	27.5	1.9	4.6	2.5	2.1
6MO/7	0.23	0.11	13.2	84.9	**4.2**	276.4	227.0	129.4	165.0	**1.7**	33.9	28.7	**11.1**	3.1	7.1	6.0	**1.6**
4M/7	0.03	0.09	5.6	10.8	**3.8**	24.9	184.6	314.4	34.2	**1.6**	29.7	**5.5**	**8.9**	1.9	**1.9**	1.5	**1.6**
3K/8	0.25	0.30	19.3	204.3	18.6	460.2	168.1	95.6	87.9	**3.3**	32.3	18.0	21.6	3.1	8.5	3.6	2.6
7O/9	0.36	0.22	16.8	22.9	5.8	76.7	138.3	129.7	70.2	**1.0**	18.9	**9.1**	25.7	1.2	**1.0**	0.7	**1.1**
6MO/9	0.05	0.47	72.7	84.1	16.3	232.8	265.6	94.0	111.0	**3.4**	18.4	21.5	**7.4**	2.3	3.1	1.2	**1.6**
5O/9	0.04	0.25	16.0	11.8	11.6	42.4	272.4	44.9	40.8	**3.7**	33.1	**9.2**	**5.4**	1.9	3.9	5.5	**0.5**
4M/9	0.11	0.27	8.8	12.7	11.3	92.2	175.5	14.0	28.8	**1.5**	15.2	**5.9**	**4.3**	1.8	**1.2**	0.9	**1.2**
4O/9	0.19	0.11	14.8	4.2	**1.4**	16.6	216.7	34.8	29.4	**1.1**	18.0	**4.5**	**10.9**	1.4	**1.4**	2.6	**0.1**
6MO/10	0.02	0.18	4.9	8.6	**3.5**	68.9	105.4	17.0	68.4	**2.5**	18.1	**9.0**	**6.5**	1.6	2.0	1.6	**1.6**
5O/10	0.16	0.13	34.0	46.3	12.3	68.5	211.3	64.5	30.6	**3.9**	28.8	**4.2**	**11.8**	1.6	2.2	5.5	2.2
4MO/10	0.49	0.27	26.4	56.0	**2.6**	182.2	334.2	286.0	114.9	**4.6**	19.8	18.1	**18.8**	4.1	6.3	2.6	2.5

Sample	Al,%	Fe,%	P	Mg	Mn	Ca	Na	K	Ti	Zn	B	Sr	Ba	Cr	V	Ni	Pb
3K/11	0.26	0.18	32.9	4.8	25.2	12.7	121.5	274.6	77.7	**1.8**	27.0	**2.9**	**11.5**	0.9	6.1	2.4	4.1
2M1/11	0.03	0.23	23.2	38.0	15.5	52.1	159.0	41.2	60.3	**1.6**	39.9	**8.9**	**4.9**	5.3	7.6	3.8	2.1
2M2/11	0.29	0.42	52.7	48.9	18.6	36.8	405.8	26.0	58.2	**4.4**	14.2	**8.9**	**8.9**	1.6	**1.2**	1.2	**0.6**
6MO/12	0.04	0.14	28.8	21.5	**2.2**	52.6	285.4	11.6	51.0	**1.8**	29.3	13.1	**9.7**	3.6	6.6	3.6	**0.2**
5O/12	0.01	0.03	10.0	4.9	**0.7**	16.2	162.4	11.5	26.7	**2.0**	31.8	**3.0**	**5.3**	2.1	2.9	4.3	2.3
4MO/12	0.22	0.22	25.2	28.7	**3.7**	96.9	242.9	34.1	65.4	**0.6**	22.7	**8.5**	**10.2**	2.0	3.5	2.9	2.0
7O/13	0.03	0.27	8.7	182.3	23.0	512.8	118.8	24.1	43.8	**2.3**	24.4	**8.4**	**12.7**	1.9	2.3	2.5	2.4
6MO/13	0.12	0.12	7.2	40.6	**4.6**	76.7	152.5	19.2	48.9	**0.9**	23.9	**7.0**	**4.4**	2.0	6.0	4.8	2.1
5O/13	0.11	0.10	24.9	31.7	6.3	152.3	198.2	74.6	68.1	**2.8**	36.1	**5.6**	**4.1**	3.3	7.0	4.9	**1.4**
4MO/13	0.03	0.06	4.0	8.2	0.5	22.9	147.8	11.5	44.4	**0.5**	35.8	**4.0**	**8.0**	1.7	3.0	6.0	2.2
PD mean	*0.16*	*0.20*	*23.6*	*67.9*	*8.5*	*164.6*	*189.8*	*80.1*	*67.6*	***2.1***	*25.5*	*10.4*	***10.3***	*2.3*	*4.0*	*2.9*	***1.8***
4M/14	0.19	0.22	28.0	36.0	0.7	118.0	196.0	44.2	26.4	**2.3**	14.1	**6.2**	**6.9**	3.7	**1.2**	0.6	**0.6**
2I/15	0.29	0.11	26.7	69.2	21.0	192.1	148.3	197.0	220.2	**0.4**	34.2	31.3	29.7	7.5	10.8	9.0	2.0
3K/15	0.04	0.18	3.6	55.5	**1.3**	218.0	108.9	31.0	30.9	**1.6**	37.1	16.4	**19.4**	1.6	4.0	2.2	**0.2**
2K/16	0.42	0.15	36.4	98.1	16.5	170.3	186.0	40.6	34.2	**0.3**	29.6	39.5	37.0	6.1	7.4	6.9	3.6
3I/16	0.43	0.14	34.0	79.3	9.9	150.2	99.6	251.0	124.8	**1.4**	25.1	19.0	20.8	9.6	13.6	3.0	2.5
MN mean	*0.27*	*0.16*	*25.7*	*67.2*	*9.8*	*169.7*	*147.8*	*112.7*	*87.3*	***1.2***	*28.0*	*24.0*	*22.7*	*5.7*	*7.4*	*4.3*	***1.8***
Total mean	*0.18*	*0.19*	*23.9*	*67.8*	*8.7*	*165.1*	*185.3*	*83.6*	*69.7*	***2.0***	*25.8*	*11.9*	***11.6***	*2.7*	*4.4*	*3.1*	***1.8***
CC	--	--	0.09	--	0.12	--	--	--	0.08	0.07	0.55	0.12	0.08	0.16	0.15	0.18	0.19
World range	--	--	1-3000	--	5-300	--	--	--	--	5-300	5-400	10-500	20-1000	0.5-60	2-100	0.5-50	2-80
Hard coal avg.	--	--	250	--	71	--	--	--	890	28	47	100	150	17	28	17	9.0
LODs	0.7	0.5	0.9	0.1	0.1	0.2	1.2	0.6	0.1	0.1	0.6	0.1	0.1	0.1	0.2	0.2	0.1

Notes: Values in boldface are below Swaine´s world ranges in coal; mean values in cursive; LODs = detection limits (µg/g)

Table 4: Concentrations (µg/g), average values and concentration coefficients (CC) of trace elements in Marcelina coal samples determined by ICP-MS.

Sample	Li	Be	U	Co	Cu	Ga	Ge	As	Rb	Zr	Nb	Mo	Sb	Cs	W	Th	Se
5O/1	4.71	0.453	**0.430**	2.39	4.21	2.95	1.32	0.696	2.39	11.50	1.66	1.58	0.342	**0.106**	**0.263**	0.726	0.542
3K/2	**0.980**	0.251	**0.082**	**0.374**	2.11	**0.661**	1.58	**0.298**	**0.160**	**3.078**	**0.232**	0.110	**0.093**	**0.006**	**0.106**	**0.243**	1.18
2M/2	**0.541**	0.301	**0.095**	0.638	3.03	**0.752**	1.55	**0.089**	**0.339**	**3.596**	**0.354**	0.289	0.901	**0.013**	**0.089**	**0.167**	0.604
4MO/3	5.04	0.100	**0.148**	0.560	3.24	**0.841**	**0.235**	**0.114**	**0.257**	**4.303**	**0.334**	0.202	0.872	**0.016**	**0.053**	**0.284**	0.796
2O/3	3.05	0.109	**0.199**	0.507	0.722	**0.710**	**0.086**	**0.198**	**0.095**	**2.780**	**0.262**	0.498	**0.049**	**0.007**	**0.055**	**0.436**	0.671
7O/4	**0.929**	0.130	**0.083**	**0.257**	0.872	**0.429**	**0.349**	**0.095**	**0.215**	**2.652**	**0.248**	**0.037**	**0.061**	**0.019**	**0.082**	**0.173**	2.00
6M/4	4.55	0.214	**0.124**	0.501	2.57	**0.885**	**0.264**	**0.223**	**0.268**	**3.863**	**0.468**	0.434	**0.083**	**0.020**	**0.069**	**0.217**	0.851
6O/4	5.99	0.529	**0.219**	0.785	4.90	2.91	2.01	0.555	**0.799**	5.414	**0.748**	1.353	0.530	**0.069**	**0.083**	**0.389**	0.981
6Q/4	8.61	0.593	**0.101**	1.30	**0.293**	2.50	1.78	**0.165**	2.01	7.581	3.18	0.863	1.14	**0.091**	0.503	**0.245**	0.830
5O/4	3.70	0.160	**0.159**	0.633	3.22	**0.983**	0.588	**0.117**	**0.213**	**4.775**	**0.404**	0.443	0.229	**0.010**	**0.075**	**0.268**	0.771
4MO/4	2.20	0.157	**0.081**	**0.296**	1.02	**0.346**	0.744	**0.032**	**0.085**	**1.858**	**0.181**	0.106	**0.069**	**0.004**	**0.206**	**0.195**	0.728
7O/5	2.36	0.379	**0.113**	**0.449**	2.36	**0.684**	1.41	**0.274**	**0.675**	8.098	**0.416**	0.304	0.113	**0.058**	**0.086**	**0.201**	0.904
6MO/5	6.20	0.102	**0.167**	0.684	2.86	**0.709**	0.555	0.518	**0.998**	**3.368**	**0.316**	0.645	**0.091**	**0.078**	**0.046**	**0.326**	1.04
6Q/5	1.82	**0.027**	**0.049**	**0.252**	1.89	2.08	**0.451**	**0.063**	**0.158**	**2.016**	**0.162**	0.262	**0.061**	**0.006**	**0.086**	**0.137**	0.786
5O/5	**0.972**	0.780	**0.118**	1.70	2.24	2.16	2.90	0.665	**0.991**	12.00	**0.228**	1.49	0.520	**0.069**	**0.084**	**0.351**	0.923
4MO/5	2.77	**0.089**	**0.067**	**0.322**	2.01	**0.382**	**0.193**	**0.078**	**0.187**	1.834	**0.156**	0.295	**0.047**	**0.008**	**0.029**	**0.126**	0.660
5M/6	1.90	0.247	**0.069**	**0.425**	0.605	**0.537**	1.64	**0.159**	**0.170**	5.494	**0.441**	0.521	0.267	**0.023**	**0.122**	**0.124**	1.03
4M/6	2.59	0.083	**0.088**	**0.372**	0.740	**0.585**	0.843	**0.138**	**0.092**	**2.677**	**0.240**	0.352	0.254	**0.008**	**0.063**	**0.199**	0.763
4O/6	6.92	0.352	**0.176**	1.06	2.28	**0.293**	2.25	0.957	**0.258**	9.326	**0.583**	2.13	0.582	**0.022**	**0.151**	**0.314**	1.452
7O/7	2.01	0.248	**0.168**	0.511	3.60	**0.710**	2.60	**0.137**	**0.954**	**3.293**	**0.348**	0.449	0.114	**0.066**	**0.096**	**0.287**	0.793
6MO/7	12.1	0.470	**0.134**	1.58	3.07	1.62	1.70	**0.277**	**0.281**	8.858	**0.701**	0.817	0.784	**0.021**	**0.120**	**0.228**	0.959
4M/7	1.77	0.334	**0.078**	0.509	4.73	**0.497**	**0.494**	**0.289**	**0.219**	**1.563**	**0.686**	0.372	0.115	**0.017**	**0.078**	**0.134**	1.83
3K/8	1.42	0.629	**0.192**	1.30	3.78	1.14	0.604	**0.373**	**1.32**	6.656	**0.150**	0.896	0.455	**0.081**	**0.196**	**0.325**	0.666
7O/9	3.56	0.158	**0.073**	**0.320**	1.16	**0.331**	0.825	**0.171**	**0.154**	**2.424**	**0.184**	0.425	**0.053**	**0.012**	**0.051**	**0.182**	0.840
6MO/9	3.20	**0.070**	**0.148**	0.686	1.09	**0.693**	**0.210**	**0.334**	**0.647**	**3.129**	**0.442**	0.938	0.122	**0.053**	**0.087**	**0.271**	0.981
5O/9	1.72	0.418	**0.079**	0.719	**0.484**	1.01	0.894	**0.423**	**0.191**	6.892	**0.327**	0.184	0.447	**0.017**	**0.108**	**0.137**	0.782
4M/9	2.44	**0.027**	**0.065**	**0.257**	0.824	**0.434**	**0.126**	**0.060**	**0.054**	**1.933**	**0.152**	**0.081**	**0.079**	**0.006**	**0.039**	**0.123**	1.00
4O/9	1.29	**0.047**	**0.054**	0.526	2.90	**0.388**	0.741	**0.179**	**0.260**	**1.718**	**0.188**	**0.097**	0.154	**0.012**	**0.064**	**0.127**	0.849
6MO/10	3.02	**0.053**	**0.102**	**0.365**	3.08	**0.385**	**0.068**	**0.206**	**0.468**	**2.182**	**0.219**	0.697	1.036	**0.034**	**0.032**	**0.172**	1.01
5O/10	1.62	0.324	**0.115**	0.656	0.742	**0.684**	2.10	**0.076**	**0.192**	5.254	**0.440**	0.142	0.884	**0.017**	**0.090**	**0.194**	0.949
4MO/10	3.23	0.146	**0.234**	0.805	3.29	2.21	0.629	**0.360**	2.65	5.585	**0.722**	0.496	0.168	**0.103**	**0.153**	**0.401**	1.10

Sample	Li	Be	U	Co	Cu	Ga	Ge	As	Rb	Zr	Nb	Mo	Sb	Cs	W	Th	Se
3K/11	15.5	0.316	**0.144**	0.915	**0.709**	1.00	2.01	**0.084**	**1.16**	6.760	3.48	0.261	0.834	**0.085**	**0.333**	**0.246**	0.913
2M1/11	1.99	0.653	**0.203**	1.80	**0.661**	1.69	1.43	**0.356**	**0.952**	7.590	**0.689**	**0.085**	0.569	**0.062**	**0.095**	**0.371**	0.735
2M2/11	2.06	**0.028**	**0.076**	**0.385**	**0.752**	**0.429**	**0.078**	**0.178**	**0.041**	**2.005**	**0.162**	**0.086**	**0.069**	**0.004**	**0.018**	**0.185**	0.696
6MO/12	4.27	0.335	**0.173**	0.997	**0.841**	1.52	0.705	**0.261**	**0.296**	5.270	**0.333**	0.656	0.244	**0.025**	**0.066**	**0.292**	0.938
5O/12	1.95	0.414	**0.098**	0.803	**0.710**	1.04	2.95	**0.068**	**0.405**	6.422	1.89	0.441	0.178	**0.017**	**0.122**	**0.292**	1.44
4MO/12	4.78	0.238	**0.108**	0.679	**0.429**	**0.958**	0.876	0.753	**0.289**	**4.476**	**0.374**	0.300	0.320	**0.013**	**0.051**	**0.282**	1.06
7O/13	5.01	0.234	**0.132**	0.667	**0.885**	**0.524**	1.14	**0.167**	**0.443**	**2.971**	**0.233**	0.154	1.09	**0.029**	**0.078**	**0.292**	0.693
6MO/13	4.57	0.192	**0.186**	0.736	2.91	**0.554**	0.576	**0.267**	**0.213**	**2.574**	**0.266**	0.628	0.253	**0.012**	**0.054**	**0.484**	1.03
5O/13	2.51	0.665	**0.160**	1.18	**0.831**	1.40	1.00	**0.210**	**1.52**	11.01	**0.272**	0.285	0.409	**0.013**	**0.123**	**0.281**	0.700
4MO/13	7.57	0.458	**0.151**	1.69	**0.983**	1.43	1.85	**0.108**	**0.108**	5.266	**0.641**	0.363	0.802	**0.007**	**0.134**	**0.289**	1.00
PD mean	*3.74*	*0.281*	***0.144***	*0.783*	*1.94*	*1.03*	*1.08*	***0.262***	***0.564***	***4.879***	***0.572***	*0.51*	*0.38*	***0.033***	***0.109***	***0.264***	*0.94*
4M/14	1.49	**0.042**	**0.121**	**0.401**	**0.346**	**0.494**	**0.371**	**0.309**	**0.504**	**2.161**	**0.313**	**0.075**	**0.093**	**0.052**	**0.039**	**0.311**	1.10
2I/15	5.23	0.692	**0.356**	3.02	**0.684**	1.97	3.53	**0.248**	**1.06**	13.64	1.68	0.158	0.510	**0.101**	**0.192**	0.604	0.694
3K/15	1.97	0.475	**0.284**	0.574	2.95	1.30	2.92	0.562	**0.528**	7.828	**0.381**	0.303	0.815	**0.033**	**0.121**	**0.479**	0.834
2K/16	1.56	0.237	**0.406**	0.765	1.81	**0.831**	1.52	**0.255**	**0.243**	11.35	4.18	0.279	0.413	**0.115**	**0.190**	0.725	0.774
3I/16	19.7	0.194	**0.381**	2.52	2.16	3.32	3.82	**0.432**	**1.84**	15.77	**0.620**	1.06	0.353	**0.109**	**0.155**	0.647	0.801
MN mean	*5.99*	*0.328*	***0.216***	*0.889*	*1.59*	*1.58*	*2.43*	***0.361***	***0.84***	*10.15*	*1.43*	*0.37*	*0.436*	***0.082***	***0.139***	*0.553*	*0.84*
Total mean	*3.98*	*0.286*	***0.152***	*0.866*	*1.91*	*1.08*	*1.23*	***0.273***	***0.59***	*5.45*	***0.67***	*0.49*	*0.39*	***0.038***	***0.112***	***0.292***	*0.93*
CC	0.28	0.14	0.08	0.14	0.12	0.18	0.51	0.03	0.03	0.15	0.16	0.23	0.39	0.03	0.11	0.07	0.58
World range	1-80	0.1-15	0.5-10	0.5-30	0.5-50	1-20	0.5-50	0.5-80	2-50	5-200	1-20	0.1-10	0.1-10	0.3-5	0.5-5	0.5-10	0.2-10
Hard coal av.	14	2.0	1.9	6.0	16	6.0	2.4	9.0	18	36	4.0	2.1	1.00	1.1	0.99	3.2	1.6
LODs	0.2	0.2	0.2	0.2	0.2	0.2	0.3	0.3	0.2	0.2	0.3	0.2	0.3	0.1	0.1	0.2	0.3

Note: As and Se were determined by using collision/reaction cell technology (CCT) of ICP-MS according to Li et al. (2014). Detection limits (LODs) expressed in ng/g.

Table 5: Contents in µg/g, means and concentration coefficients (CC) for rare-earth elements (REEs) analyzed in Marcelina coal samples by ICP-MS.

Sample	La	Ce	Pr	Nd	Sm	Eu	Gd	Tb	Dy	Ho	Er	Tm	Yb	Lu	Y	Sc
5O/1	2.15	5.92	**0.979**	**2.04**	0.567	0.116	0.428	**0.099**	0.549	0.108	**0.294**	**0.043**	**0.474**	**0.041**	2.56	**0.679**
3K/2	**0.367**	**0.677**	**0.081**	**0.321**	**0.077**	**0.038**	0.302	**0.050**	**0.227**	0.133	**0.133**	**0.020**	**0.126**	**0.018**	**0.209**	**0.405**
2M/2	**0.323**	**0.638**	**0.074**	**0.307**	**0.073**	**0.021**	0.103	**0.018**	**0.122**	**0.028**	**0.084**	**0.012**	**0.085**	**0.012**	**0.744**	**0.356**
4MO/3	**0.752**	**1.35**	**0.148**	**0.547**	**0.098**	**0.022**	0.099	**0.013**	**0.079**	**0.015**	**0.043**	**0.006**	**0.041**	**0.005**	**0.384**	**0.135**
2O/3	**0.569**	**1.03**	**0.111**	**0.425**	**0.083**	**0.019**	0.087	**0.012**	**0.070**	**0.039**	**0.039**	**0.005**	**0.036**	**0.005**	**0.368**	**0.120**
6M/4	**0.415**	**0.779**	**0.086**	**0.337**	**0.069**	**0.017**	0.091	**0.015**	**0.102**	**0.023**	**0.070**	**0.010**	**0.068**	**0.010**	**0.583**	**0.243**
6O/4	**0.616**	**1.06**	**0.118**	**0.440**	**0.092**	**0.027**	0.118	**0.023**	**0.139**	**0.034**	**0.096**	**0.017**	**0.098**	**0.016**	**0.718**	**0.346**
6Q/4	**0.875**	**1.86**	**0.248**	**1.04**	**0.242**	**0.069**	0.263	**0.041**	**0.226**	**0.050**	**0.135**	**0.022**	**0.128**	**0.021**	**1.14**	**0.631**
5O/4	1.38	2.01	**0.317**	**0.723**	**0.328**	**0.055**	0.204	**0.045**	**0.366**	0.181	0.514	**0.063**	0.419	0.084	2.34	**0.964**
4MO/4	**0.838**	**1.51**	**0.171**	**0.651**	**0.128**	**0.031**	0.131	**0.019**	**0.105**	**0.021**	**0.056**	**0.008**	**0.054**	**0.007**	**0.482**	**0.212**
7O/4	**0.305**	**0.562**	**0.062**	**0.239**	**0.047**	**0.012**	0.058	**0.009**	**0.057**	**0.012**	**0.037**	**0.005**	**0.036**	**0.005**	**0.355**	**0.130**
7O/5	**0.667**	**1.21**	**0.138**	**0.530**	**0.106**	**0.026**	0.130	**0.022**	**0.152**	**0.036**	**0.108**	**0.016**	**0.113**	**0.016**	**0.895**	**0.355**
6MO/5	1.03	2.02	**0.227**	**0.877**	**0.168**	**0.038**	0.159	**0.023**	**0.128**	**0.025**	**0.070**	**0.010**	**0.065**	**0.009**	**0.556**	**0.182**
6Q/5	**0.290**	**0.537**	**0.058**	**0.219**	**0.051**	**0.020**	0.105	**0.021**	**0.080**	**0.023**	**0.054**	**0.014**	**0.056**	**0.014**	**0.417**	**0.254**
5O/5	**0.668**	**1.24**	**0.160**	**0.717**	**0.207**	**0.069**	0.357	**0.070**	0.517	0.127	**0.406**	**0.066**	0.284	0.072	2.17	**0.712**
4MO/5	**0.435**	**0.772**	**0.085**	**0.318**	**0.057**	**0.014**	0.056	**0.008**	**0.042**	**0.008**	**0.024**	**0.003**	**0.023**	**0.003**	**0.204**	**0.078**
5M/6	**0.520**	**0.956**	**0.111**	**0.408**	**0.084**	**0.011**	0.035	**0.005**	**0.028**	**0.006**	**0.015**	**0.002**	**0.015**	**0.002**	**0.147**	**0.046**
4M/6	**0.396**	**0.713**	**0.078**	**0.295**	**0.056**	**0.014**	0.058	**0.008**	**0.048**	**0.029**	**0.029**	**0.004**	**0.029**	**0.004**	**0.269**	**0.155**
4O/6	2.66	4.21	**0.472**	**1.78**	**0.310**	**0.026**	0.080	**0.012**	**0.085**	**0.019**	**0.058**	**0.009**	**0.061**	**0.009**	**0.530**	**0.235**
7O/7	**0.660**	**1.21**	**0.138**	**0.532**	**0.109**	**0.032**	0.125	**0.021**	**0.121**	**0.026**	**0.077**	**0.011**	**0.075**	**0.011**	**0.687**	**0.284**
6MO/7	**0.620**	**0.993**	**0.124**	**0.505**	**0.131**	**0.042**	0.158	**0.032**	**0.167**	**0.041**	**0.107**	**0.021**	**0.105**	**0.020**	**0.832**	**0.546**
4M/7	**0.439**	**0.796**	**0.092**	**0.361**	**0.073**	**0.018**	0.089	**0.013**	**0.082**	**0.018**	**0.053**	**0.007**	**0.048**	**0.007**	**0.560**	**0.138**
3K/8	1.143	2.17	**0.261**	**1.05**	**0.225**	**0.061**	0.289	**0.047**	**0.319**	**0.073**	**0.219**	**0.033**	**0.212**	**0.032**	**1.92**	**0.778**
7O/9	**0.449**	**0.854**	**0.096**	**0.369**	**0.068**	**0.017**	0.079	**0.011**	**0.074**	**0.017**	**0.051**	**0.007**	**0.053**	**0.007**	**0.491**	**0.174**
6MO/9	1.13	2.05	**0.228**	**0.824**	**0.146**	**0.035**	0.141	**0.022**	**0.106**	**0.025**	**0.063**	**0.012**	**0.061**	**0.012**	**0.477**	**0.178**
5O/9	**0.753**	**1.28**	**0.134**	**0.482**	**0.093**	**0.024**	0.112	**0.019**	**0.121**	**0.029**	**0.087**	**0.015**	**0.096**	**0.015**	**0.712**	**0.464**
4M/9	**0.211**	**0.392**	**0.046**	**0.174**	**0.037**	**0.010**	0.037	**0.006**	**0.029**	**0.007**	**0.016**	**0.004**	**0.016**	**0.003**	**0.125**	**0.056**
4O/9	**0.244**	**0.472**	**0.055**	**0.220**	**0.046**	**0.012**	0.044	**0.007**	**0.032**	**0.008**	**0.020**	**0.004**	**0.020**	**0.004**	**0.164**	**0.079**
6MO/10	**0.454**	**0.859**	**0.097**	**0.365**	**0.069**	**0.015**	0.069	**0.009**	**0.053**	**0.010**	**0.029**	**0.004**	**0.029**	**0.004**	**0.239**	**0.072**
5O/10	**0.339**	**0.647**	**0.075**	**0.299**	**0.067**	**0.018**	0.084	**0.015**	**0.097**	**0.023**	**0.071**	**0.011**	**0.078**	**0.011**	**0.594**	**0.345**
4MO/10	1.62	2.89	**0.336**	**1.28**	**0.237**	**0.053**	0.226	**0.031**	**0.181**	**0.037**	**0.107**	**0.016**	**0.106**	**0.015**	**1.17**	**0.251**

Sample	La	Ce	Pr	Nd	Sm	Eu	Gd	Tb	Dy	Ho	Er	Tm	Yb	Lu	Y	Sc
3K/11	1.00	3.56	1.02	**1.50**	0.539	0.103	0.464	**0.084**	0.596	0.147	**0.216**	**0.081**	**0.251**	**0.033**	**0.871**	**0.297**
2M1/11	1.42	2.83	**0.323**	**1.30**	**0.303**	**0.048**	0.132	**0.022**	**0.149**	**0.035**	**0.107**	**0.017**	**0.115**	**0.017**	**0.877**	**0.477**
2M2/11	**0.535**	**0.966**	**0.108**	**0.405**	**0.075**	**0.018**	0.054	**0.009**	**0.048**	**0.009**	**0.024**	**0.003**	**0.022**	**0.003**	**0.887**	**0.069**
6MO/12	**0.622**	**1.17**	**0.141**	**0.570**	**0.129**	**0.040**	0.161	**0.029**	**0.157**	**0.036**	**0.097**	**0.016**	**0.090**	**0.015**	**0.857**	**0.376**
5O/12	**0.363**	**0.647**	**0.075**	**0.307**	**0.065**	**0.017**	0.083	**0.014**	**0.101**	**0.024**	**0.074**	**0.011**	**0.080**	**0.012**	**0.622**	**0.395**
4MO/12	**0.612**	**1.13**	**0.127**	**0.489**	**0.098**	**0.024**	0.111	**0.017**	**0.104**	**0.022**	**0.064**	**0.009**	**0.062**	**0.009**	**0.553**	**0.258**
7O/13	**0.512**	**0.972**	**0.109**	**0.430**	**0.087**	**0.023**	0.114	**0.019**	**0.130**	**0.032**	**0.099**	**0.015**	**0.102**	**0.015**	**0.842**	**0.280**
6MO/13	**0.541**	**1.01**	**0.116**	**0.463**	**0.099**	**0.025**	0.120	**0.018**	**0.110**	**0.025**	**0.071**	**0.010**	**0.066**	**0.010**	**0.649**	**0.249**
5O/13	**0.816**	**1.54**	**0.182**	**0.072**	**0.152**	**0.039**	0.180	**0.029**	**0.195**	0.144	**0.144**	**0.023**	**0.158**	**0.024**	**1.18**	**0.716**
4MO/13	1.13	2.03	**0.227**	**0.852**	**0.150**	**0.029**	0.164	**0.024**	**0.153**	**0.034**	**0.101**	**0.015**	**0.101**	**0.014**	**0.854**	**0.487**
PD mean	***0.75***	***1.45***	***0.19***	***0.61***	***0.141***	***0.032***	*0.144*	***0.023***	***0.152***	***0.042***	***0.101***	***0.016***	***0.102***	***0.016***	***0.76***	***0.326***
4M/14	**0.473**	**0.953**	**0.208**	**0.169**	**0.101**	**0.014**	0.114	**0.019**	**0.107**	**0.027**	**0.031**	**0.010**	**0.075**	**0.018**	**0.299**	**0.080**
2I/15	1.24	**1.82**	**0.501**	**1.18**	0.506	0.112	0.539	0.108	0.580	**0.095**	0.507	**0.038**	0.372	0.052	**1.87**	**0.237**
3K/15	**0.602**	**0.990**	**0.117**	**0.483**	**0.118**	**0.052**	0.399	**0.062**	**0.332**	**0.074**	**0.213**	**0.031**	**0.206**	**0.030**	**0.818**	**0.499**
2K/16	**0.344**	**0.556**	**0.064**	**0.249**	**0.053**	**0.014**	0.065	**0.011**	**0.075**	**0.018**	**0.037**	**0.029**	**0.063**	**0.009**	**0.431**	**0.206**
3I/16	1.40	2.00	**0.042**	**1.35**	**0.292**	**0.068**	0.222	**0.041**	**0.324**	0.107	**0.176**	**0.039**	0.308	0.068	**1.90**	**0.408**
MN mean	***0.81***	***1.26***	***0.187***	***0.686***	***0.211***	***0.052***	*0.263*	***0.047***	***0.283***	***0.064***	***0.192***	***0.029***	***0.204***	***0.035***	***1.06***	***0.286***
Total mean	***0.76***	***1.43***	***0.19***	***0.61***	***0.149***	***0.035***	*0.157*	***0.026***	***0.167***	***0.045***	***0.111***	***0.017***	***0.113***	***0.018***	***0.79***	***0.322***
CC	0.07	0.06	0.06	0.05	0.07	0.08	0.06	0.09	0.08	0.08	0.11	0.06	0.11	0.09	0.10	0.09
World range	1-40	2-70	1-10	3-30	0.5-6	0.1-2	0-4	0.1-1	0.5-4	0.1-2	0.5-3	0.1-1	0.3-3	0.05-1	2-50	1-10
Hard coal av.	11	23	3.4	12	2.2	0.43	2.7	0.31	2.1	0.57	1.00	0.30	1.0	0.20	8.2	3.7
Chondrite	310	808	122	600	195	73.5	259	47.4	322	71.8	210	32.4	209	32	--	--
LODs	0.2	0.2	0.2	0.3	0.3	0.1	0.3	0.1	0.1	0.1	0.1	0.1	0.1	0.1	0.2	0.2

Notes: Chondrite values used to normalize concentrations of REE; LODs expressed in ng/g.

Table 6: Elemental affinities deduced from the Pearson correlations.

Significant correlation with ash yield ($r > + 0.50$) Al, P, K, Ti, Sr, Ba, Cr, V, U, Co, Ga, Rb, Zr, Nb, Cs, W, Th, Pr, Sm, Eu, Gd, Tb, Dy, Ho, Er, Yb, and Lu
Weak or no correlation with ash yield ($0 < r < + 0.50$) Fe, Ca, Mg, Na, Mn, B, Zn, Ni, Pb, Li, Be, Cu, Ge, As, Mo, Sb, La, Ce, Nd, Tm, Y, and Sc
Inverse correlation with ash yield ($r = - 0.35$) Se

Table 7: Ranges of metal ratios of Marcelina coals compared to the ratios in sediments sourced from mafic rocks and felsic rocks, as well as values for El Carmen and El Palmar granitoids.

Ratio	Coal samples	Mafic sources	Felsic sources	El Carmen	El Palmar
La/Sc	0.91 – 11.31	0.43 – 0.86	2.50 – 16.3	5.51	4.55
Th/Sc	0.25 – 3.89	0.05 – 0.22	0.84 – 20.5	1.48	0.40
La/Co	0.41 – 2.51	0.14 – 0.38	1.8 – 13.8	8.72	7.81
Th/Cr	0.049 – 0.312	0.018 – 0.046	0.13 – 2.70	2.56	0.60

Note: Data from granitoids after Van Der Lelij (2013).

Table 8: Mineral content in some coals from sampled seams as deduced from semiquantitative X-ray analysis plus total clay and illite contents. Data in wt.% of LTA residue (+++ = dominant phase > 20 wt.%; ++ = abundant phase 3-20 wt.%; + = minor phase 1-3 wt.%; O = accessory phase < 1 wt.%).

Sample	Kln	Ill	Rct	Py	Sp	Qtz	Ap	Kfs	Pl	Ank	Sd	Dsp	Bas	Hem	Whe	But	Clay	Illite
5O/1	+++	O	O	O	O	+++	+	O	+	O	O	O	O	O	O	O	46.0	0.5
2M/2	+++	+	--	O	O	+++	--	--	O	--	--	--	--	--	--	--	43.0	2.8
2O/3	+++	++	O	O	--	+++	--	--	O	O	--	--	O	--	O	--	40.0	4.6
6M/4	+++	O	--	O	--	+++	O	--	O	O	O	--	--	O	--	--	43.0	0.7
6O/4	+++	O	O	O	--	+++	O	O	O	O	O	--	--	O	--	--	50.0	0.6
6Q/5	+++	O	O	O	--	+++	+	--	O	--	--	O	--	--	--	--	40.0	0.8
5M/6	+++	O	O	O	O	+++	--	O	O	O	O	--	O	--	O	--	52.0	0.6
7O/7	+++	O	O	O	--	+++	O	O	O	+	O	--	O	O	O	O	53.0	0.7
3K/8	+++	+	O	O	O	+++	O	O	O	+	O	--	O	O	O	O	43.0	1.1
4O/9	+++	O	O	O	--	+++	O	O	O	--	--	--	--	--	--	--	55.0	0.9
4MO/10	+++	O	O	O	O	+++	O	+	O	O	O	--	--	O	--	O	40.0	0.7
6MO/12	+++	O	--	O	--	+++	O	--	O	--	O	--	--	--	--	--	53.0	0.8
4M/14	+++	O	O	O	O	+++	O	O	O	--	O	--	--	--	--	O	76.0	0.7
2I/15	+++	+	O	O	--	+++	O	+	+	O	--	--	--	--	--	--	70.0	1.3
2K/16	+++	+	O	O	--	+++	O	O	--	O	O	O	--	--	--	--	68.0	1.2
3I/16	+++	++	O	O	--	+++	O	+	--	O	--	O	--	--	--	--	62.0	4.9

Notes: Mineral abbreviations after Kretz (1983): Kln = kaolinite; Ill = illite; Rct = smectite; Ap = apatite; Sd = siderite; Kfs = k-feldspar; Py = pyrite; Pl = plagioclase; Sp = spharelite; Qtz = quartz; Bas = bassanite; Dsp = diaspore; Whe = whewellite; Hem = hematite; Ank = ankerite; But = butlerite.

Appendix A. Total, light REE and heavy REE contents (µg/g), Ce and Eu anomalies as well as element ratios in Guasare coals.

Sample	Ca/Sr	Ni/Co	Th/Sc	Th/Cr	La/Co	La/Sc	REY	LREE	HREE	Ce_n/Ce^*	Eu_n/Eu^*	$(Gd/Yb)_n$
5O/1	24.55	3.47	1.07	0.121	0.90	3.16	16.36	11.77	4.592	0.99	0.62	0.72
3K/2	6.54	2.93	0.57	0.221	0.92	0.91	2.779	1.561	1.218	0.93	0.84	1.93
2M/2	4.22	3.28	0.47	0.119	0.50	0.91	2.644	1.436	1.208	0.98	0.76	0.98
4MO/3	7.31	3.92	2.10	0.158	1.34	5.56	3.599	2.915	0.685	0.94	0.70	1.94
2O/3	41.53	1.97	3.63	0.311	1.12	4.75	2.893	2.232	0.661	0.95	0.70	1.95
7O/4	15.61	3.88	0.71	0.157	1.62	1.71	2.675	1.703	0.972	0.97	0.68	1.08
6M/4	10.88	1.19	0.63	0.108	1.23	1.78	3.608	2.349	1.259	0.92	0.77	0.97
6O/4	17.16	1.78	0.62	0.177	1.11	1.39	6.359	4.334	2.024	0.97	0.84	1.66
6Q/4	3.99	4.67	0.25	0.049	1.06	1.44	9.030	4.817	4.213	0.73	0.52	0.39
5O/4	6.52	6.94	1.26	0.167	1.32	3.95	4.215	3.332	0.883	0.94	0.74	1.96
4MO/4	6.02	6.42	1.50	0.093	1.03	2.35	1.801	1.227	0.574	0.96	0.73	1.30
7O/5	34.75	5.11	0.57	0.087	1.48	1.88	4.160	2.672	1.488	0.93	0.68	0.93
6MO/5	21.00	2.92	1.79	0.136	1.50	5.66	5.396	4.351	1.045	0.99	0.70	1.97
6Q/5	14.51	7.53	0.54	0.098	1.14	1.13	1.959	1.175	0.784	0.97	0.85	1.49
5O/5	4.18	2.94	0.49	0.066	0.41	0.94	7.135	4.072	3.063	0.91	0.78	1.02
4MO/5	7.35	4.65	1.62	0.084	1.35	5.58	2.052	1.681	0.371	0.94	0.76	1.96
5M/6	4.70	8.46	2.69	0.073	1.22	11.30	2.344	2.089	0.255	0.94	0.46	1.89
4M/6	26.85	2.95	1.28	0.132	1.06	2.55	2.030	1.552	0.478	0.95	0.77	1.61
4O/6	20.32	3.59	1.34	0.131	2.51	11.31	10.32	9.454	0.863	0.87	0.31	1.06
7O/7	25.95	4.89	1.01	0.151	1.29	2.32	3.836	2.682	1.154	0.94	0.84	1.34
6MO/7	16.35	3.79	0.42	0.074	0.41	1.13	3.898	2.415	1.483	0.84	0.85	1.21
4M/7	4.52	2.94	0.97	0.071	0.86	3.18	2.656	1.779	0.877	0.93	0.72	1.49
3K/8	25.56	2.76	0.41	0.105	0.88	1.47	8.052	4.911	3.141	0.95	0.75	1.10
7O/9	8.42	2.18	1.05	0.152	1.41	2.58	2.643	1.853	0.790	0.98	0.74	1.20
6MO/9	10.82	1.74	1.52	0.118	1.65	6.34	5.336	4.416	0.919	0.95	0.73	1.86
5O/9	4.60	7.64	0.30	0.072	1.04	1.63	3.976	2.769	1.206	0.93	0.73	0.94
4M/9	15.62	3.49	2.19	0.068	0.82	3.77	1.113	0.870	0.243	0.95	0.81	1.87
4O/9	3.68	4.93	1.61	0.091	0.46	3.09	1.351	1.049	0.303	0.97	0.79	1.77
6MO/10	7.65	4.37	2.39	0.107	1.25	6.31	2.305	1.859	0.446	0.97	0.68	1.91
5O/10	16.30	8.38	0.56	0.121	0.51	0.99	2.429	1.445	0.984	0.96	0.73	0.87
4MO/10	10.06	3.22	1.59	0.098	2.02	6.47	8.306	6.415	1.891	0.92	0.70	1.72
3K/11	4.37	2.62	0.83	0.273	1.09	3.37	10.47	7.728	2.743	0.76	0.55	1.49

Sample	Ca/Sr	Ni/Co	Th/Sc	Th/Cr	La/Co	La/Sc	REY	LREE	HREE	Ce_n/Ce^*	Eu_n/Eu^*	$(Gd/Yb)_n$
2M1/11	5.85	2.11	0.78	0.070	0.79	2.97	7.690	6.219	1.471	0.99	0.55	0.93
2M2/11	4.13	3.11	2.68	0.116	1.39	7.76	3.166	2.107	1.059	0.94	0.76	1.98
6MO/12	4.01	3.61	0.77	0.081	0.62	1.65	4.133	2.674	1.458	0.95	0.84	1.44
5O/12	5.40	5.35	0.70	0.139	0.43	0.91	2.495	1.474	1.021	0.92	0.72	0.84
4MO/12	11.40	4.27	1.09	0.141	0.90	2.37	3.430	2.479	0.951	0.96	0.72	1.44
7O/13	61.04	3.75	1.04	0.154	0.77	1.83	3.501	2.133	1.368	0.97	0.73	0.90
6MO/13	10.95	6.51	1.94	0.242	0.73	2.17	3.328	2.249	1.079	0.95	0.73	1.47
5O/13	27.19	4.16	0.39	0.085	0.69	1.14	4.874	2.799	2.075	0.95	0.73	0.92
4MO/13	5.72	3.55	0.59	0.170	0.67	2.31	5.873	4.412	1.460	0.94	0.58	1.31
4M/14	19.03	1.49	3.89	0.084	1.18	5.90	2.618	1.918	0.700	0.79	0.40	1.22
2I/15	6.13	2.97	2.55	0.081	0.51	5.20	9.509	5.350	4.159	0.63	0.61	1.17
3K/15	13.29	3.83	0.96	0.299	1.05	1.21	4.527	2.362	2.165	0.97	0.84	1.56
2K/16	4.31	9.02	3.52	0.119	0.47	1.67	2.018	1.280	0.738	0.95	0.74	0.83
3I/16	7.90	1.19	1.59	0.067	0.56	3.42	9.025	4.921	3.184	0.72	0.72	0.58

Notes: REY defined as sum of REE and Y; LREE defined as sum of La, Ce, Pr, Nd, Sm, and Eu; HREE defined as sum of Gd, Tb, Dy, Ho, Er, Tm, Yb, Lu, and Y; Ce_n/Ce^* and Eu_n/Eu^*, with Ce* and Eu* equal to $0.5 \cdot La_n + 0.5 \cdot Pr_n$ and $0.67 \cdot Sm_n + 0.33 \cdot Tb_n$ (Mishra et al., 2019).

Appendix B. Detailed calculations used to determine mean gas content for Guasare coals

(1) A hypothetical coal "molecule" was assumed to contain 10000 atoms of carbon in the initial state of high-volatile bituminous rank (for which the starting H/C and O/C atomic ratios appear to be 0.85 and 0.13). Thus, the number of hydrogen and oxygen atoms present in the initial high-volatile bituminous coal "molecule" would be 8500 and 1300. The aim is to calculate how many molecules of methane would be released during the transition from the beginning of high-volatile bituminous rank to the average maturity level for Guasare coals.

(2) Let: X = the number of molecules of CH_4 generated; Y = the number of molecules of CO_2 generated, and Z = the number of molecules of H_2O generated. For example, each molecule of CO_2 evolved removes 2 oxygen atoms for every carbon atom removed from the coal "molecule". At the average maturity level for Guasare coals: the number of carbon atoms that remain equals to $10000 - X - Y$; the number of H atoms that remain equals to $8500 - 4X - 2Z$; and the number of O atoms that remain equals to $1300 - 2Y - Z$.

(3) The next step is to calculate how many molecules of CH_4, CO_2 and H_2O must be generated to reach the H/C and O/C atomic ratios (0.782 and 0.066) at the average maturity level for Guasare coals. The following equations can be used:

$$\text{H/C} = 0.782 = (8500 - 4X - 2Z)/(10000 - X - Y)$$
$$\text{O/C} = 0.066 = (1300 - 2Y - Z)/(10000 - X - Y).$$

(4) The above equations are solved in terms of Y and Z by fixing X at a constant number of molecules of CH_4 generated:

$$3.218X - 680 = 0.782Y - 2Z$$
$$0.066X + 640 = 1.934Y + Z.$$

(5) Both equations are solved for Y by standard methods:

$$Y = (3.35X + 600)/4.65$$

(6) A latter equation can be applied when considering the high-volatile bituminous A rank of Guasare coals:

$$Y = 2X$$

(7) The solution to the latter two equations is accomplished and the result is approximately 100 molecules of CH_4 generated per coal "molecule" containing 10000, 8500 and 1300, respectively, carbon, hydrogen and oxygen atoms.

(8) Assuming the International Standard Metric Conditions for natural gas (288.15 K and 1 atm) and applying the ideal gas low, a quantity of ~16 cm^3 per gram of raw coal is obtained. Then, if we also assumed a mass loss of around one third during the transition from lignite to high-volatile bituminous A coal, the amount of methane generated would be about 11 cm^3/g.

(9) Finally, considering the estimation of coal reserves for the study area (~1600 million tons), it can be preliminarily concluded that coalbed methane reserves in the Guasare Coalfield would be close to 17.6 billion cubic meters.

Declaration of interests

☒The authors declare that they have no known competing financial interests or personal relationships that could have appeared to influence the work reported in this paper.

☐The authors declare the following financial interests/personal relationships which may be considered as potential competing interests:

CRediT author statement

Gonzalo Márquez: Conceptualization, Writing - Original Draft, Investigation, Supervision; **Manuel Martínez**: Writing - Review & Editing, Formal analysis, Validation; **Gabriela Carruyo**: Visualization, Investigation; **Carlos Boente**: Writing - Review & Editing, Formal analysis; **Erika Lorenzo**: Investigation, Data curation; **Rafael Tocco**: Writing - Review & Editing, Resources.